



NORTHWEST TERRITORIES CANADA

Ontaratue H-34 well

**Reconstruction of thermal, burial and source rock
maturation histories using AFTA® and VR results**

GEOTRACK REPORT #813A

**A multi-client study by
Geotrack International Pty Ltd in association with Alconsult International**

Report prepared by:

I. R. Duddy

AFTA determinations by:

M.E. Moore

May 2002



NORTHWEST TERRITORIES CANADA

Ontaratue H-34 well

Reconstruction of thermal, burial and source rock maturation histories using AFTA® and VR results

GEOTRACK REPORT #813A

CONTENTS

	Page
Executive Summary	i-xi
Reconstructed thermal history - Figure i	vi
Evolution of maturity with time - Figure ii	vii
AFTA and new VR paleotemperature analysis summary - Table i	viii
Open-file VR paleotemperature analysis summary - Table ii	ix
Paleogeothermal gradient summary - Table iii	x
Removed section estimates - Table iv	xi

1. Thermal history reconstruction of the Ontaratue H-34 well Northwest Territories, Canada	
1.1 Introduction	1
1.2 Aims and Objectives	1
1.3 Data Quality	2
1.4 Report Structure	3
2. Interpretation strategy	
2.1 Thermal history interpretation of AFTA data	6
2.2 Thermal history interpretation of VR data	7
2.3 Comparison of paleotemperature estimates from AFTA and VR	8
2.4 Paleogeothermal gradients	9
2.5 Eroded section	10
3. Thermal history interpretation for the Ontaratue H-34 well	
3.1 Geological background	12
3.2 Thermal history interpretation of Ontaratue H-34 well from AFTA data	12
3.3 Thermal history interpretation of Ontaratue H-34 well from VR data	14
3.4 Paleogeothermal gradients: mechanisms of heating & cooling	17
3.5 Reconstructed thermal history in the Ontaratue H-34 well	18
3.6 Reconstructed maturation history in the Ontaratue H-34 well	19
3.7 Estimating section removed by erosion	20
3.8 Burial history reconstruction	21
3.9 Recommendations for further work	22
References	23



CONTENTS continued

Appendix A	- Sample Details and Geological Data	A.1 - A.9
Appendix B	- Sample Preparation, Analytical Details and Data Presentation	B.1 - B.20
Appendix C	- Principles of Interpretation of AFTA Data in Sedimentary Basins	C.1 - C.23
Appendix D	- Vitrinite Reflectance Measurements	D.1 - D.37

TABLES

	Page
Table i - AFTA and new VR paleotemperature analysis summary	viii
Table ii - Open-file VR paleotemperature analysis summary	ix
Table iii - Paleogeothermal gradient summary	x
Table iv - Removed section estimates	xi
Table 3.1 - Apatite Fission Track data summary; Ontaratue H-34 well	24
Table 3.2 - Thermal history interpretation summary; Ontaratue H-34 well	25
Table 3.3 - Estimates of timing and magnitude of elevated paleo-temperatures from AFTA; Ontaratue H-34 well	26-27
Table A.1 - Details of AFTA samples and apatite yields	A.5
Table A.2 - Summary of stratigraphy	A.6
Table A.3 - Summary of temperature data	A.7
Table A.4 - Lower limits of detection for apatite analyses	A.8
Table A.5 - Percent errors in chlorine content	A.8
Table B.1 - Apatite fission track analytical results	B.10
Table B.2 - Length distribution summary data	B.11
Table B.3 - AFTA data in compositional groups	B.12 - B.13
Glossary	B.16
Analytical data	B.17 - B.20
Table D.1 - Paleotemperature - vitrinite reflectance nomogram	D.7
Table D.2 - Vitrinite reflectance sample details and results supplied by Keiraville Konsultants	D.8-D.9
Table D.3 - Open-file Vitrinite reflectance sample details and results from Feinstein et al (1989)	D.10-D.12
VR maceral descriptions: Keiraville Konsultants	D.13 - D.14
VR maceral histograms: Keiraville Konsultants	D.15 - D.24
VR raw data sheets: Keiraville Konsultants	D.25 - D.37

FIGURES

	Page
Figure i - Reconstructed thermal history Ontaratue H-34 well	vi
Figure ii - Evolution of maturity with time Ontaratue H-34 well	vii



CONTENTS continued

FIGURES continued

Figure 1.1 - Location of the Ontaratue H-34 well	5
Figure 3.1 - AFTA parameters plotted against sample depth and present temperature; Ontaratue H-34 well	28
Figure 3.2 - Measured VR data and predicted maturity versus depth plot; Ontaratue H-34 well	29
Figure 3.3 - Default Burial history; Ontaratue H-34 well	30
Figure 3.4 - Paleotemperatures derived from AFTA and VR data; Ontaratue H-34 well	31
Figure 3.5 - Paleogeothermal gradient plot: Paleocene-Eocene episode from AFTA & VR; Ontaratue H-34 well	32
Figure 3.6 - Reconstructed thermal history Ontaratue H-34 well	33
Figure 3.7 - Maturity depth plot from reconstructed thermal history; Ontaratue H-34 well	34
Figure 3.8 - Removed section plot: Paleocene-Eocene episode AFTA & VR; Ontaratue H-34 well	35
Figure 3.9 - Cross plot of total section removed & paleogeothermal gradient Paleocene-Eocene episode; Ontaratue H-34	36
Figure 3.10 - Possible burial history reconstruction; Ontaratue H-34 well	37
Figure A.1 - Present-day temperature profile	A.9
Figure B.1 - Construction of a radial plot	B.14
Figure B.2 - Simplified structure of radial plots	B.15
Figure C.1a - Comparison of mean length in Otway Basin reference wells with predictions of Laslett et al. (1987) model	C.17
Figure C.1b - Comparison of mean length in apatites of the same Cl content as Durango from Otway Group samples with predictions of Laslett et al. (1987) model	C.17
Figure C.2 - Comparison of mean length in apatites of differing chlorine compositions	C.18
Figure C.3 - Comparison of mean length in Otway Basin reference wells with predictions of new multi-compositional annealing model	C.18
Figure C.4 - Histogram of Cl contents in typical samples	C.19
Figure C.5 - Comparison of mean length in Otway Basin reference wells with predictions of Crowley et al. (1991) model for F-apatite	C.20
Figure C.6 - Comparison of mean length in Otway Basin reference wells with predictions of Crowley et al. (1991) model for Durango apatite	C.20
Figure C.7 - Changes in radial plots of post-depositional annealing	C.21
Figure C.8 - Typical AFTA parameters: a. Maximum temperatures now b. Hotter in the past	C.22
Figure C.9 - Constraint of paleogeothermal gradient	C.23
Figure C.10 - Estimation of section removed	C.24

NORTHWEST TERRITORIES CANADA

Ontaratue H-34 well

Reconstruction of thermal, burial and source rock maturation histories using AFTA® and VR results

GEOTRACK REPORT #813A

EXECUTIVE SUMMARY

Introduction and Objectives

Apatite Fission Track Analysis (AFTA®) and Vitrinite Reflectance (VR) have been applied to samples from the **Ontaratue H-34 well**, Northwest Territories, to provide a thermal history framework for understanding the structural and hydrocarbon generation histories at this location.

AFTA and VR are used to *identify, characterise and quantify* any episodes of elevated paleotemperatures which have affected the well section, with particular emphasis on determining the timing of major paleo-thermal episodes, the magnitude of paleotemperatures in each episode, and the way in which paleotemperatures vary with depth. This information is used to infer the origins of the various episodes of heating and cooling, and provides rigorous constraints for modelling of the structural and source rock maturation histories.

Summary Conclusions

*Active hydrocarbon generation in the Cretaceous, Devonian and older sections drilled at **Ontaratue H-34** ceased when cooling commenced in the Paleocene - Eocene, between 60 and 40 Ma. Maximum maturity levels were reached at this time and range from early to late maturity for oil (VR ~0.65 to 1.3% R_{Omax}) in the Early Cretaceous section and the underlying Devonian section (Imperial, Canol and Hume Fms) to post-mature for dry gas (VR >2.0% R_{Omax}) in the Cambrian section near TD. Cooling from this thermal episode involved kilometre-scale uplift and erosion*

A Miocene thermal episode revealed by AFTA (25 to 5 Ma) had no effect on source rock maturation or active hydrocarbon generation within the preserved section, but associated kilometre-scale uplift and erosion at this time may have had a significant effect on hydrocarbon re-migration and preservation.

Thermal History Reconstruction

1. Synthesis of AFTA and VR results indicate that at least two major paleo-thermal episodes have affected the preserved Cretaceous to Cambrian section at the **Ontaratue H-34** well location, with cooling beginning at some time in the intervals:
 - 60 to 40 Ma (Paleocene - Eocene)
 - 25 to 5 Ma (Miocene - Pliocene)

AFTA clearly reveals that the preserved Cretaceous, Devonian and older sections cooled from maximum paleotemperatures beginning in the Paleocene-Eocene (between 60 and 40 Ma), with the sampled section also cooling from a lower peak in paleotemperatures beginning in the Miocene-Pliocene (25 to 5 Ma), as illustrated in Figure i.

Paleotemperature estimates from AFTA and the new VR results are summarised in Table i. Paleotemperatures estimates from open file maturity data are summarised in Table ii.

2. The AFTA and VR-derived paleotemperatures for the Paleocene - Eocene thermal episode, between 60 and 40 Ma, define a maximum likelihood paleogeothermal gradient of 44.5°C/km with an allowed range at $\pm 95\%$ confidence limits of 36.0 to 49.0°C/km. The allowed range encompasses the present-day gradient of 39.0°C/km, suggesting that heating in this episode due to deeper burial on the top-Early Cretaceous unconformity is a viable explanation of the results. Note however, that within the allowed range of values, slightly higher basal heat-flow *combined with* a lesser amount of deeper burial is also possible.
3. AFTA-derived paleotemperatures for the Miocene-Pliocene thermal episode, between 25 and 5 Ma, are available for only two samples and this is insufficient to define the paleogeothermal gradient at this time. Regional data suggest that heating in this episode is also likely to have resulted from deeper burial on the top-Early Cretaceous unconformity, with cooling due to uplift and erosion.

Paleogeothermal gradient estimates are summarised in Table iii.

Maturation History Reconstruction

4. The thermal history results indicate that there is no break in the maturity trend at the sub-Cretaceous unconformity in this well.

5. The VR analyst notes the presence of particular bitumens as evidence for oil previously reservoired in the Bear Rock Formation and possibly in the Cambrian section, as well.
6. The integrated AFTA and VR thermal history reconstruction for the **Ontaratue H-34 well**, illustrated in Figure ii, reveals that:
 - there is no evidence for active source rock maturation in any Cretaceous, Paleozoic or older stratigraphic unit (i.e. no active hydrocarbon generation) at the present-day;
 - the Cretaceous and shallow Devonian section (Imperial, Canol and Hume Fms) reached maximum maturity (early to late maturity for oil - ~0.65 to 1.3 % R_{Omax}) prior to cooling beginning in the Paleocene-Eocene, at some time between 60 and 40 Ma.
 - the Cambrian section near TD is interpreted to have reached peak maturity beyond dry gas ($>2\%$ R_{Omax}) prior to cooling at the same time, although the quality of the measured maturity data in the deeper section is poor, and it is not possible to rule out earlier thermal episodes involving higher maturity.

Burial History Reconstruction

7. Extrapolation of the paleogeothermal gradient results allows estimation of the magnitude of erosion that may have been associated with cooling from elevated paleotemperatures. Magnitudes of paleo-burial and erosion allowed by extrapolation of the thermal history results, as represented by the maximum likelihood estimates and $\pm 95\%$ confidence limits, are summarised in Table iv.
8. The well defined best fit-solution for cooling since the Paleocene-Eocene thermal episode requires a total of 2300 m of section removed for uplift and erosion commencing between 60 and 40 Ma, with between 2000 and 3000 m allowed at $\pm 95\%$ confidence limits. For a paleogeothermal gradient of $39.0^{\circ}\text{C}/\text{km}$ at this time (equal to the present-day gradient as allowed by the constrained gradient range), ~2900 m of additional burial is required in order to honour the AFTA and VR-derived paleotemperatures results.
9. No quantitative paleogeothermal gradient and hence additional burial constraints could be obtained on the magnitude of erosion associated with the Miocene-Pliocene thermal episode. Assuming a paleogeothermal gradient of $39.0^{\circ}\text{C}/\text{km}$ (equal to the present-day gradient) during this episode, indicates ~1150 to 1650 m of section removed beginning between 25 and 5 Ma are required to honour the paleotemperature constraints from AFTA data in sample GC813-3 (Table i).

10. A reconstructed burial history (based on a constant gradient of $39.0^{\circ}\text{C}/\text{km}$) has a total of 2900 m of additional Cretaceous to Paleocene burial prior to uplift and erosion beginning between 60 and 40 Ma, with 1500 m of this additional section eroded prior to 10 Ma and 1400 m eroded between 10 Ma and the present-day. A range of alternative burial histories are allowed within the bounds defined by the thermal history constraints, as detailed in Table iv and explained in the text.

Geological implications

11. The results imply that a major cooling event beginning at some time between 60 and 40 Ma was due in large measure to kilometre-scale uplift and erosion. Roughly 2.9 km of additional burial is required in the preferred reconstruction, but lower amounts are possible if a higher paleogeothermal gradient was acting during this interval. Even so, the minimum amount of additional section is 2 km for the maximum allowed paleogeothermal gradient of $49^{\circ}\text{C}/\text{km}$ (see Tables iii and iv). The thermal history results are consistent with around half of the additional burial removed since between the Paleocene-Eocene and the Pliocene, with the remainder removed since Miocene (assuming no intervening re-burial).
12. The Early Tertiary time at which erosion began is most likely associated with regional Laramide tectonism which is known to have affected preserved Paleocene sediments in the general region, with the additional section required ranging from Early Cretaceous to as young as Eocene in depositional age.
13. The Miocene-Pliocene timing on the most recent erosional episode may possibly reflect the final phases of this Laramide tectonism, or it may be a largely unrecognised and unrelated episode without a preserved stratigraphic record. The presence of such a major erosional event in the recent geological past has important implication on the migration and redistribution of earlier reservoired hydrocarbons and deserves further attention.

Recommendations for follow-up studies

14. Additional AFTA samples are not recommended in this well as the two thermal events identified are relatively well constrained by the available data, while the application of (U-TH)/He apatite dating noted below may significantly refine the timing of the most recent event (Miocene-Pliocene; 25 to 5 Ma).

15. Analysis of several samples by the new (U-TH)/He apatite dating techniques is suggested for a companion study to provide refinement of the timing and magnitude of the major Miocene-Pliocene thermal episode revealed by AFTA. Analysis of several samples should enable definition of the paleogeothermal gradient during this episode.
16. Analysis of outcrop samples from the region, using AFTA, VR and (U-TH)/He apatite dating is suggested as a viable strategy for tracking the extent and magnitude of the Tertiary thermal episodes identified in Ontaratie H-34. Special attention should be given to outcrops of Tertiary, Cretaceous and Devonian sediments in the region.

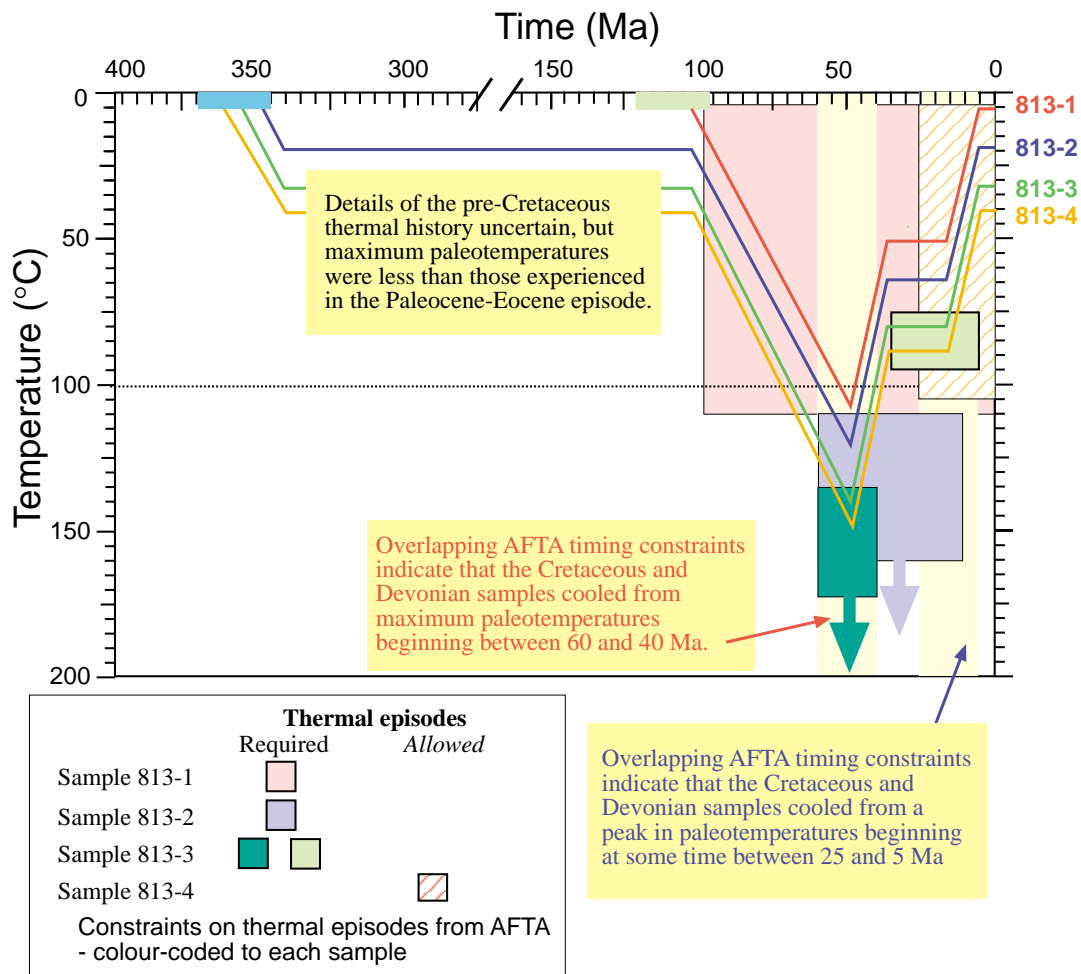


Figure i: Schematic illustration of the thermal histories derived from the AFTA results in individual samples (Table i) from the **Ontaratue H-34 well, Northwest Territories, Canada**.

The coloured-coded boxes indicate time and temperatures constraints obtained from AFTA in each sample and the yellow columns indicate the time of two major thermal episodes derived from the overlap in timing constraints obtained from all samples. This approach indicates that the Cretaceous and Devonian section cooled from maximum paleotemperatures beginning between 60 and 40 Ma (Paleocene-Eocene) and cooled from peak paleotemperatures beginning between 25 and 5 Ma (Miocene-Pliocene).

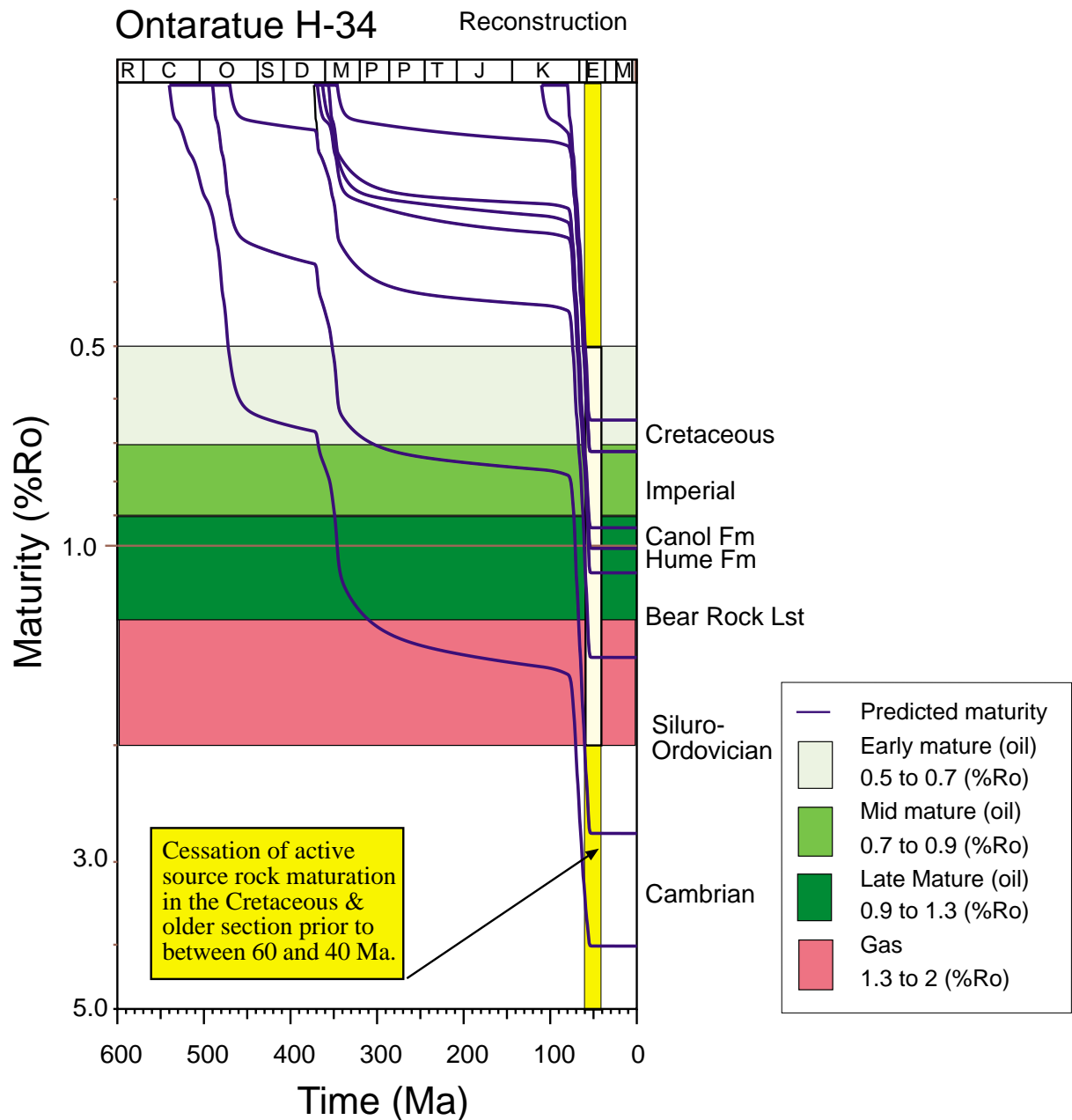


Figure ii: Maturation history reconstruction for the **Ontaratue H-34 well, North West Territories, Canada**, derived from the AFTA and VR results (Table i).

The yellow coloured column between 60 and 40 Ma represents the integrated AFTA and VR-derived timing constraint on the maximum paleotemperature episode, and also directly indicates the time at which active source rock maturation ceased in these stratigraphic units.



Table i: Paleotemperature analysis summary from AFTA and VR samples from the Ontaratue H-34 well, Northwest Territories, Canada (Geotrack Report #813A)

Sample number (GC-)	Mean depth (mKB)	Stratigraphic age (Ma)	Present temperature *1 (°C)	----- from AFTA and VR -----			
				Early episode(s) Maximum paleotemperature *2 (°C)	Onset of cooling (Ma)	Late episode Maximum paleotemperature *2 (°C)	Onset of cooling (Ma)
813-1 813-1	145	115 to 98	5	<110 109*3	Post-Deposition	No constraint	
813-2 813-2	465	356 to 346	18	>110 122*3	60 to 10	No constraint	
813-3.1 813-3	762 792	356 to 346 356 to 346	31	139*3 >135	60 to 40	75 - 95	35 to 5
813-4.1 813-4	935.7 995	373 to 356	39	149*3 >105	Depn to 25	<105	25 to 0
813-4.2	1054.6			152*3			
813-5	1379.2			No VR			
813-6.1	1594.1			>151*3, *4			
813-6.2	1693.2			No VR			
813-7	2407.9			<222*3, *5			
813-8	2892.4			No VR			
813-9	3063.2			No VR			
813-10	3052.1			<244*3, *6			
813-11	3236.1			No VR			

Overlap in timing constraints from AFTA:

60 to 40 Ma

25 to 5 Ma

N.B. Bracketed & italicised constraints indicate paleo-thermal episodes which are *allowed* by AFTA, but *not required*.

*1 Present temperature estimates for each sample are based on a mean annual surface temperature of 0°C and a corrected present-day geothermal gradient of 39.0°C/km as described in Appendix A.

*2 All AFTA and VR paleotemperature estimates are derived assuming a heating rate of 1°C/Ma and a cooling rate of 10°C/Ma (see Section 2).

*3 Maximum paleotemperatures estimated from the vitrinite reflectance data using Burnham and Sweeney (1989).

*4 Maximum estimate from vitrinite that may be caved – see maceral descriptions Appendix D.

*5 Maximum paleotemperatures estimated from the bitumen reflectance data using Burnham and Sweeney (1989).

*6 Maximum paleotemperatures estimated from the reflectance of vitrinite-like material using Burnham and Sweeney (1989). Considered to be a maximum VR value.



Table ii: Paleotemperature analysis summary from open-file VR samples from the Ontaratue H-34, NWT (Geotrack Report #813A)

Sample number (GC-)	Depth (m)	Stratigraphic unit	Stratigraphic age (Ma)	Measured VR ^{*1} (%)	Calculated Ro(max) ^{*2} (%)	Maximum Paleotemperature ^{*3} (°C)
Cretaceous						
813-OF.1	39.6	Cretaceous	115-98	0.59	0.62	101
813-OF.2	109.7	Cretaceous	115-98	0.55	0.57	94
813-OF.3	213.4	Cretaceous	115-98	0.65	0.69	114
Imperial Fm						
813-OF.4	304.8	Devonian	356-346	0.66	0.70	115
813-OF.5	396.2	Devonian	356-346	0.69	0.74	121
813-OF.6	487.7	Devonian	356-346	1.04	1.16	152
813-OF.7	597.4	Devonian	356-346	0.71	0.76	123
813-OF.8	755.9	Devonian	356-346	0.81	0.88	133
813-OF.9	841.2	Devonian	356-346	0.92	1.01	143
Canol/Hare Indian Fms						
813-OF.10	902.2	Devonian	363-356	0.98	1.09	152
813-OF.11	978.4	Devonian	363-356	1.17	1.32	161
Bear Rock Lst						
813-OF.12	1103.4	Devonian	369-363	1.11	1.24	157
813-OF.13	1158.2	Devonian	369-363	1.07	1.20	155
813-OF.14	1216.2	Devonian	369-363	1.18	1.33	161
Cambrian						
813-OF.15	3383.3	Cambrian	540-490	2.45-3.32 ^{*4}	2.86-3.92	219 - 259

^{*1} Mean Random reflectance; Open-file values from Feinstein et al. (1989) – see also Table D.3.

^{*2} Ro(max) calculated from Mean Random reflectance values – see text Section 3.3.

^{*3} Maximum paleotemperatures estimated from the vitrinite reflectance data using Burnham and Sweeney (1989). All VR paleotemperature estimates are derived assuming a heating rate of 1°C/Ma and a cooling rate of 10°C/Ma (see Section 2).

^{*4} Maximum paleotemperatures estimated from bitumen reflectance (higher value in range) and equivalent vitrinite reflectance data derived from bitumen reflectance values using Burnham and Sweeney (1989) – see text.



Table iii: Paleogeothermal gradient estimates for the Ontaratue H-34 well, Northwest Territories, Canada (Geotrack Report #813A)

	Paleocene-Eocene Episode 60 to 40 Ma^{*2}	Miocene Episode 25 to 5 Ma^{*2}
Present-day gradient ^{*1}	Paleogeothermal gradient ^{*3}	Paleogeothermal gradient ^{*4}
(°C/km)	(°C/km)	(°C/km)
39.0	44.5 (36.0 – 49.0)	No effective constraint

- *1 Present-day gradient is based on corrected BHT data and a surface temperature of 0°C (see Appendix A).
*2 Time of cooling from maximum paleotemperatures is constrained by AFTA (Table i).
*3 Maximum likelihood value derived from AFTA and VR results with 95% confidence interval range in brackets.
*4 Maximum likelihood value derived from AFTA results alone with 95% confidence interval range in brackets.



Table iv: Removed section estimates for the Ontaratue H-34 well, Northwest Territories, Canada (Geotrack Report #813A)

	Paleocene-Eocene Episode 60 to 40 Ma^{*2}	Miocene Episode 25 to 5 Ma^{*2}
Present-day gradient ^{*1}	Section removed ^{*3}	Section removed ^{*3}
(°C/km)	(m)	(m)
	2300 (2000 - 3000)	No formal constraint
<i>39.0</i>	<i>(2900)^{*4}</i>	<i>(1130-1640)^{*4}</i>

- ^{*1} Present-day gradient is based on corrected BHT data and a surface temperature of 0°C (see Appendix A).
^{*2} Maximum likelihood value with the 95% confidence interval range in brackets underneath. A paleo-surface temperature of 0°C is assumed at the time of each paleothermal episode
^{*3} Total section removed with respect to the top of the preserved Cretaceous section.
^{*4} Values italicised in brackets are amounts of removed section based on paleogeothermal gradients in each episode equal to the present-day level of 39°C/km as allowed by the thermal history results – see Table iii.

Notes: Details of maximum likelihood estimation of paleogeothermal gradient and section removed are provided in Section 2 and Appendix C (Section C.9). The allowed ranges of values of paleogeothermal gradient and section removed (within ±95% confidence limits) are highly correlated. Estimation of section removed depends on the assumption that the paleogeothermal gradient is linear and can be extrapolated through the removed section to the paleo-surface temperature. If this assumption is not valid (e.g., if the paleo-thermal effects were due to fluid flow, with a higher paleogeothermal gradient in the shallower [removed] section), the estimated section removed will not be accurate.

The paleotemperature constraints (Tables i & ii) and the estimated paleogeothermal gradient through the preserved section (Table iii) are not affected by any of the assumptions required in order to estimate the amount of section removed, and can be regarded as reliable.

The amount of section removed has been estimated for an assumed paleo-surface temperature of 0°C. The resulting estimate can be adjusted to refer to other values of paleo-surface temperature simply by adding or subtracting the depth interval corresponding to the difference between the preferred value and 0°C, as appropriate, for the maximum likelihood value of paleogeothermal gradient



Ontaratue H-34 well Northwest Territories, Canada

Reconstruction of thermal, burial and source rock maturation histories using AFTA® and VR results

GEOTRACK REPORT #813A

1. Thermal history reconstruction

1.1 Introduction

This non-exclusive report carried on by Geotrack International Pty Ltd in conjunction with Alconsult International Ltd (Calgary) presents the results of a thermal history reconstruction study based on AFTA® apatite fission track analysis of four samples (of seven samples processed for analysis) and vitrinite reflectance (VR) results on 13 new samples and 15 open-file samples from the **Ontaratue H-34 well, Northwest Territories, Canada** (Figure 1.1).

Stratigraphic details of the four AFTA samples are summarised in Table A.1 (Appendix A), with AFTA results summarised in Tables B.1 and B.2 (Appendix B). Details of the new VR results are summarised in Table D.2 (Appendix D). Fifteen open-file VR results together with some Rock-Eval Tmax data are also available for this well from Feinstein et al. (1989), as listed in Table D.3 (Appendix D).

1.2 Aims and objectives

The principle objective of this study was to determine the thermal history in the drilled section of the **Ontaratue H-34 well** and discuss the implications of the thermal history for the burial, tectonic and source rock maturation histories at this location.

More specifically, key objectives of this study are:

- 1) To use AFTA to determine the timing and magnitude of the maximum paleotemperature of key stratigraphic units;
- 2) To estimate the maximum paleotemperature from each VR value;
- 3) To integrate the maximum paleotemperatures estimated from AFTA and VR to provide a coherent thermal history assessment for the well;

- 4) To identify the mechanism controlling heating and cooling in each paleo-thermal episode and to quantify the paleogeothermal gradient in each episode;
- 5) To derive a hydrocarbon source rock maturation history from the reconstructed thermal history;
- 6) To quantify the magnitude of uplift and erosion, if any, associated with each of the identified thermal episodes.

1.3 Data quality

AFTA data

Stratigraphic sections targeted in the Mackenzie Valley Region to optimise apatite yields provided apatite suitable for analysis from four of the seven samples processed.

The new AFTA data generated from two Devonian samples (813-3 and -4) for this report are of high quality based on good yields of detrital apatite (see Table A.1, Appendix A). Lesser yields of apatite were obtained from the Cretaceous sample (GC813-1) and another Devonian sample (GC813-2), but the fission track age and length data obtained still provide good constraints on the thermal history owing to the significant post-depositional heating experienced by these samples. Three samples from the Bear Rock Formation and the Siluro-Ordovician were also processed (GC813-5, -6 & -7), but these provided insufficient apatite for analysis.

Despite the lack of apatite from the deeper samples, the results obtained from the Cretaceous and Devonian sections provide excellent constraints on key aspects of the post-Cretaceous thermal history, the true levels of source rock maturity and the timing of peak maturation in the Devonian and Cretaceous sections in the **Ontaratue H-34 well**.

VR data

The quality of the vitrinite reflectance data obtained from most samples is less than ideal with the majority of samples providing less than 10 measurements on in-situ vitrinite (25 being the target for a complete determination). A mean value based on 10 or more measurements is considered very reliable because of the way in which the VR data are gathered, with primary in-situ vitrinite identified on petrographic grounds within polished sections (see Appendix D).

Key samples from the Devonian Imperial Formation (GC813-2) and Hume-Canol-Hare Indian Formation (GC813-4.1) gave more than 10 measurements while the single sample from the Cretaceous Arctic Red Formation gave 8 measurements

(Table D.2). More limited data from in-situ vitrinite were obtained from the other Devonian samples, with Imperial Formation sample GC813-3.1 providing 5 measurements, and two Bear Rock Formation samples GC813-4.2 and -6.1 giving 9 and 3 measurements, respectively.

Overall, despite the low numbers of measurements in these samples, the results provide a coherent maturity profile through the drilled section, and are also consistent with the open-file results from the section.

No organic reflectance measurements were obtained from one of the three Devonian Bear Rock Formation samples (GC813-5), two of the four Cambrian samples (GC813-8 & -11) and both Siluro-Ordovician samples (GC813-6.2 & -7) analysed (Table D.2, Appendix D).

Reflectance measurements in some of the new samples were also made on other macerals including inertinite, bitumen and possible graphitic carbon, and these data also provide information on the general level of maturity in the section consistent with the trends derived from the true vitrinite data. In particular, bitumen reflectance data have been used to provide constraints on the thermal history in the deeper part of the section.

Open-file organic reflectance data (from Feinstein et al., 1989) were available from fifteen samples representing all major stratigraphic units encountered in the well from the Cretaceous Arctic Red Formation to the Cambrian (Table D.3, Appendix D). Results are available on true vitrinite and pyrobitumen. The values listed for pyrobitumen in Table D.3 are equivalent VR values as listed in Feinstein et al. (1989) and not the measured bitumen reflectance values, which can also be found in Feinstein et al. (1989). The quality of the organic reflectance data obtained from the open-file data is unknown, but the results are very similar to those obtained from the new samples and are also based on generally low numbers of measurements in individual samples. One major difference between the new and open file data sets is the measurement methodology; Ro(max) for the new data set and Ro(random) for the open-file data set, which means that the measured values cannot be compared directly. This difference is addressed in Section 3 where an attempt is made to calculate equivalent Ro(max) values for the open-file data.

1.4 Report structure

The main conclusions of this report are provided in the Executive Summary. A summary of the paleotemperature estimates from individual AFTA and VR samples is provided in Table i with paleotemperature estimates from open-file VR results in Table ii. Table iii provides estimates (maximum likelihood and $\pm 95\%$ confidence

limits) of paleogeothermal gradient in each thermal episode revealed by AFTA and Table iv provides estimates of uplift and erosion associated with each episode derived from extrapolation of the paleogeothermal gradients.

A schematic illustration of key features of the thermal history reconstruction derived from the AFTA and VR results is presented in Figure i. Figure ii illustrates the reconstructed variation of maturity with time derived from the reconstructed thermal history in Figure i.

Section 2 briefly explains the principles of interpretation of AFTA and VR data (also see Appendix C). Section 3 deals with a detailed interpretation of the AFTA and VR results in the **Ontaratue H-34** well in terms of thermal, maturation and burial histories, including comprehensive presentation of results in Tables and Figures. Supporting information and data are provided in four Appendices (A, B, C and D). Details of all AFTA samples are presented in Table A.1 (Appendix A), together with the yields and quality of detrital apatite obtained after mineral separation. Sample preparation and analytical procedures for AFTA are described in Appendix B, followed by the presentation of all AFTA data, including raw track counts, fission track ages and the chlorine contents of dated grains. Appendix C outlines the principles employed in interpreting the AFTA data in terms of thermal history. Appendix D discusses the principles involved in integrating AFTA and VR data to provide a rigorous thermal history reconstruction.

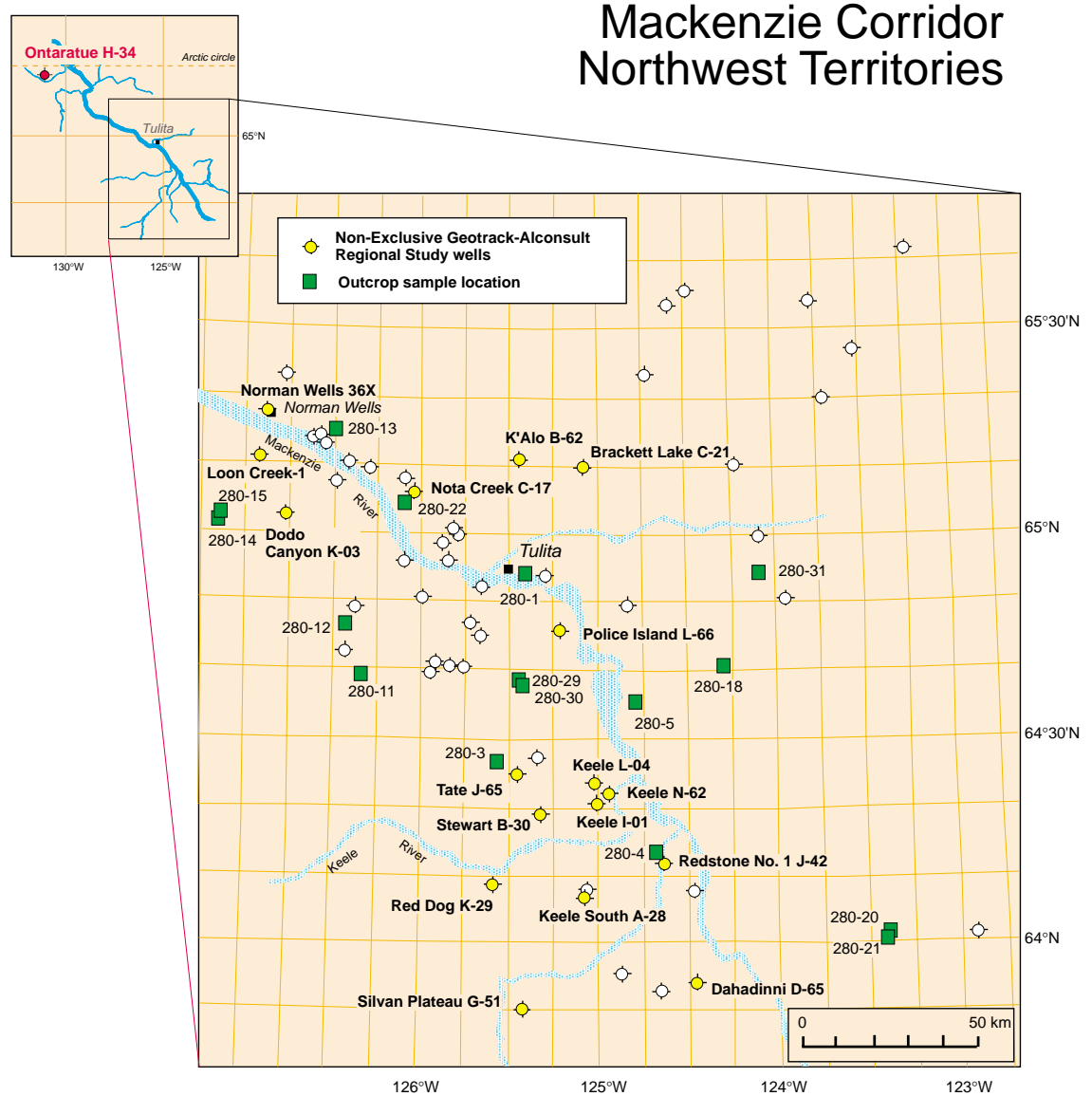


Figure 1.1: Location of the Ontaratue H-34 well in relation to other wells and outcrops in the Geotrack-Alconsult Northwest Territories Thermal History Reconstruction study package. New AFTA and vitrinite reflectance data have been obtained for thermal history reconstruction studies in all named wells, with AFTA obtained from the outcrop samples.

2. Interpretation strategy

2.1 Thermal history interpretation of AFTA data

Basic principles

Interpretation of AFTA data in this report begins by assessing whether the fission track age and track length data in each sample could have been produced if the sample has never been hotter than its present temperature at any time since deposition. To this end, we consider a "Default Thermal History" for each sample, which forms the basis of interpretation. Default Thermal Histories throughout a well are derived from the stratigraphy of the preserved sedimentary section, combined with constant values for paleogeothermal gradient and paleo-surface temperature which are adopted from present-day values.

Using this history, AFTA parameters are predicted for each sample. If the measured data show a greater degree of fission track annealing (in terms of either fission track age reduction or track length reduction) than expected on the basis of this history, the sample must have been hotter at some time in the past. In this case, the AFTA data are analysed to provide estimates of the magnitude of the maximum paleotemperature in that sample, and the timing of cooling from the thermal maximum.

Because of the possible presence of tracks inherited from sediment source terrains, it is possible that track length data might show definite evidence that the sample has been hotter in the past (since deposition) while fission track ages are still greater than predicted from the Default Thermal History (which only refers to tracks formed after deposition). Similarly in samples in which all or most fission tracks were totally annealed in a paleo-thermal episode, and which have subsequently been cooled and then reburied, fission track age data might show clear evidence of exposure to higher temperatures in the past while track length data may be dominated by the present-day thermal regime and will not directly reveal the paleo-thermal effects. In circumstances such as these, evidence from either track length or fission track age data alone is sufficient to establish that a sample has been hotter in the past.

As AFTA data provide no information on the *approach* to a thermal maximum, they cannot independently constrain the heating rate and a value must therefore be assumed in order to interpret the data. The resulting paleotemperature estimates are therefore conditional on this assumed value. AFTA data do provide some control on the history after cooling from maximum paleotemperatures, through the lengths of tracks formed during this period.

Wherever possible, data from each sample are normally interpreted in terms of two episodes of heating and cooling, using assumed heating and cooling rates during each episode. The maximum paleotemperature is assumed to be reached during the earlier episode. The timing of the onset of cooling and the peak paleotemperatures during the two episodes are varied systematically, and by comparing predicted and measured parameters the range of conditions which are compatible with the data can be defined. One additional episode during the cooling history is the limit of resolution from typical AFTA data. Alternatively, if the data can be explained by a single episode of heating and cooling, then a heating rate is assumed and the range of values of maximum paleotemperature and the time of cooling is defined as before.

If AFTA data show a lower degree of fission track annealing (age and/or length reduction) than expected on the basis of the Default Thermal History, this either suggests present temperatures may be overestimated or temperatures have increased very recently. In such cases, the data may allow a more realistic estimate of the present temperature, or an estimate of the time over which temperatures have increased.

AFTA data are predicted using a multi-compositional kinetic model for fission track annealing in apatite developed by Geotrack, described in more detail in Appendix C.

Specific to this report

For all samples analysed for this report, chlorine content has been determined in every apatite grain analysed (i.e., for both fission track age and track length measurement), as explained in more detail in Appendix A. For rigorous thermal history interpretation the age and length data have been grouped into 0.1 wt% Cl divisions (see Table B.3, Appendix B).

In this report, AFTA (and VR data) in all samples were interpreted using a heating rate of 1°C/Ma and a cooling rate of 10°C/Ma. All paleotemperature estimates are conditional on the assumed rates. However, it should be borne in mind that for the kinetics characterising both AFTA and VR, each order of magnitude change in heating rate has a systematic effect on the paleotemperature estimate of only ~10°C.

2.2 Thermal history interpretation of VR data

Basic principles

Interpretation of VR data follows similar principles to those used in interpreting the AFTA data (Section 2.1). If a measured VR value is higher than the value predicted from the Default Thermal History (making due allowance for analytical uncertainty), the sample must have been hotter at some time in the past. In this case, VR data

provide an independent estimate of maximum paleotemperature, which can be calculated using an assumed heating rate and timing information provided from AFTA data, if available (assumed, otherwise). Cooling rates do not significantly affect VR data, which are dominated by the maximum paleotemperature provided that cooling occurs immediately after reaching the thermal maximum. If both AFTA and VR data are available from the same sample or well, then an identical heating rate must be used to obtain consistent paleotemperature estimates.

If a measured VR value is lower than expected on the basis of the Default Thermal History, either present temperatures may have been overestimated or temperatures have increased very recently. In such cases, the measured VR value may allow an estimate of the true present-day temperature. Alternatively the measured VR value may underestimate the true maturity for some other reason, e.g., suppression of reflectance in certain organic macerals, misidentification of true "in-situ" vitrinite, presence of caved material etc. Comparison of AFTA and VR data usually allows such factors to be identified, and where applicable they are discussed in the relevant section of text.

Vitrinite reflectance data (specifically $R_{o\max}$ values) are predicted using the distributed activation energy model describing the evolution of VR, with temperature and time developed by Burnham and Sweeney (1989) (see also Sweeney and Burnham, 1990).

Values of VR less than ~0.3% and greater than 5% cannot be assigned to a specific maximum paleotemperature with confidence, and such values are given maximum and minimum limits, respectively, appropriate to the particular heating rate used (see Appendix D). Further discussion of the methodology employed in interpreting VR data are given in Appendix D, which also briefly discusses the benefits of integrating AFTA and VR data.

Specific to this report

For this report, all VR values were interpreted using a heating rate of 1°C/Ma and a cooling rate of 10°C/Ma. These rates were used for consistency with the interpretation of the AFTA data, as specified in Section 2.1.

2.3 Comparison of paleotemperature estimates from AFTA and VR

Maximum paleotemperatures derived from AFTA and VR ($R_{o\max}$) using the strategies outlined above are usually highly consistent. Estimates of maximum paleotemperature from AFTA (Table i) are often quoted in terms of a range of paleotemperatures, as the data can often be explained by a variety of scenarios.

Paleotemperature estimates from VR (Tables i and ii) are usually quoted to the nearest degree Celsius, as the value which predicts the exact measured reflectance. This is not meant to imply VR data can be used to estimate paleotemperatures to this degree of precision. VR data from individual samples typically show a scatter equivalent to a range of between ± 5 and $\pm 10^\circ\text{C}$. Estimates from a series of samples are normally used to define a paleotemperature profile in samples from a well, or a regional trend in paleotemperatures from outcrop samples.

2.4 Paleogeothermal gradients

Basic principles

A series of paleotemperature estimates from AFTA and/or VR over a range of depths can be used to reconstruct a paleotemperature profile through the preserved section. The slope of this profile defines the paleogeothermal gradient. As explained by Bray et al. (1992), the shape of the paleotemperature profile and the magnitude of the paleogeothermal gradient provides unique insights into the origin and nature of the heating and cooling episodes expressed in the observed paleotemperatures.

Linear paleotemperature profiles with paleogeothermal gradients close to the present-day geothermal gradient provide strong evidence that heating was caused by greater depth of burial with no significant increase in basal heat flow, implying in turn that cooling was due to uplift and erosion. Paleogeothermal gradients significantly higher than the present-day geothermal gradient suggest that heating was due, at least in part, to increased basal heat flow, while a component of deeper burial may also be important as discussed in the next section. Paleogeothermal gradients significantly lower than the present-day geothermal gradient suggest that a simple conductive model is inappropriate, and more complex mechanisms must be sought for the observed heating. One common cause of low paleogeothermal gradients is transport of hot fluids shallow in the section. However, the presence of large thicknesses of sediment with uniform lithology dominated by high thermal conductivities can produce similar paleotemperature profiles and each case has to be considered individually.

A paleotemperature profile can only be characterised by a single value of paleogeothermal gradient when the profile is linear. Departures from linearity may occur where strong contrasts in thermal conductivities occur within the section, or where hot fluid movement or intrusive bodies has produced localised heating effects. In such cases a single value of paleogeothermal gradient cannot be calculated. However, it is important to recognise that the validity of the paleotemperatures determined from AFTA and/or VR are independent of these considerations, and can still be used to control possible thermal history models.

Estimation of paleogeothermal gradients in this report

Paleogeothermal gradients for this report have been estimated from paleotemperature estimates over a range of depths using methods outlined in Appendix C. These methods provide a best estimate of the gradient ("maximum likelihood value") and upper and lower 95% confidence limits on this estimate (analogous to $\pm 2\sigma$ limits). The "goodness of fit" is displayed in the form of a log-likelihood profile, which is expected to show good quadratic behaviour for a dataset which agrees with a linear profile. This analysis depends on the assumption that the paleogeothermal gradient through the preserved section is linear. Visual inspection is usually sufficient to confirm or reject this assumption.

2.5 Eroded section

Basic principles

Subject to a number of important assumptions, extrapolation of a linear paleotemperature profile to a paleo-surface temperature allows estimation of the amount of eroded section represented by an unconformity, as explained in more detail in Section C.9 (Appendix C).

Specifically, this analysis assumes:

- The paleotemperature profile through the preserved section is linear;
- The paleogeothermal gradient through the preserved section can be extrapolated linearly through the missing section;
- The paleo-surface temperature is known; and,
- The heating rate used to estimate the paleotemperatures defining the paleogeothermal gradient is correct.

It is important to realise that any method of determining the amount of eroded section based on thermal methods is subject to these and/or additional assumptions. For example methods based on heat-flow modelling must assume values of thermal conductivities in the eroded section, which can never be known with confidence. Such models also require some initial assumption of the amount of eroded section to allow for the effect of compaction on thermal conductivity. Methods based on geothermal gradients, as used in this study, are unaffected by this consideration, and can therefore provide independent estimates of the amount of eroded section. But these estimates are always subject to the assumptions set out above, and should be considered with this in mind.

The analysis used to estimate paleogeothermal gradients is easily extended to provide maximum likelihood values of eroded section, for an assumed paleo-surface

temperature, together with $\pm 95\%$ confidence limits. These parameters are quoted for the specific paleo-thermal episodes in which the paleotemperature profiles suggest that past heating may have been due, at least in part, to deeper burial. However, it is emphasised that such interpretations are not unique, and alternative interpretations are always possible. For instance, where the eroded section was dominated by units with high thermal conductivities the paleogeothermal gradient through the missing section may have been much higher than in the preserved section, and extrapolation of a linear gradient will lead to overestimation of the eroded section.

Estimation of eroded section in this report

The analysis used to estimate paleogeothermal gradients is easily extended to provide maximum likelihood values of eroded section for an assumed paleo-surface temperature, together with $\pm 95\%$ confidence limits.

However, it is emphasised that such interpretations are not unique and alternative interpretations are always possible. For instance, the paleogeothermal gradient through the missing section may have been much higher than in the preserved section where the eroded section was dominated by units with high thermal conductivities, and extrapolation of a linear gradient will lead to overestimation of the eroded section.

For the well analysed in this report, the estimates of eroded section are conditional on:

- Heating rates of $1^{\circ}\text{C}/\text{Ma}$ and cooling rates of $10^{\circ}\text{C}/\text{Ma}$ in each episode, and
- A paleo-surface temperature of 0°C , equivalent to the present-day value,

as well as the other assumptions outlined above. The effects of higher paleo-surface temperatures can be simply allowed for by subtracting the depth increment corresponding to the increase in temperature, for the appropriate value of paleogeothermal gradient. For instance, if the paleogeothermal gradient was $45^{\circ}\text{C}/\text{km}$ and the paleo-surface temperature was 10°C higher than the value assumed in this report, the estimated eroded section should be *reduced by 222 metres*. Different heating rates can be allowed for in similar fashion, with an order of magnitude change in heating rate equivalent to a 10°C change in paleotemperature (paleotemperatures increase for higher heating rates, and decrease for lower heating rates). For typical values, the assumed value of heating rate will not affect the shape or slope of the paleotemperature profile significantly.

3. Thermal history interpretation for the Ontaratue H-34 well

3.1 Geological background

Formation top information compiled from GSC sources for the **Ontaratue H-34 well** (Figure 1.1) indicates that the well intersected Early Cretaceous sediments (Arctic Red and Martin House Formations) unconformably overlying Devonian (Imperial to Bear Rock Formations), Silurian-Ordovician and Cambrian sections. An unconformity separates the Devonian and the Silurian-Ordovician sections. The detailed stratigraphic succession is summarised in Table A.2.

Eleven samples (seven cuttings and four core sample) from clastic intervals in the well were originally collected for AFTA, but only the shallower seven samples were subjected to mineral separation due to the presently high temperatures ($>110^{\circ}\text{C}$) for the four deeper samples (Table A.1). Of these seven samples, four samples provided sufficient apatite for full AFTA analysis as summarised in Table A.1. Splits of eight AFTA samples plus five additional samples, were subjected to VR analysis (Table D.2, Appendix D).

Apatite yields varied from Good to None (Table A.1) and sufficient data were obtained from four of the samples for a reliable assessment of the thermal history to be obtained.

3.2 Thermal history interpretation of Ontaratue H-34 AFTA data

Introduction

Fission track age and mean track length data in samples analysed from this well are summarised in Table 3.1 and plotted as a function of depth and present temperature (derived from the present-day geothermal gradient of $39.0^{\circ}\text{C}/\text{km}$, Appendix A) in Figure 3.1, where the fission track age data are contrasted with the variation of stratigraphic age through the section.

Interpretation of the AFTA data in terms of evidence that the samples may have been hotter in the past is summarised in Table 3.2. Following the strategy outlined in Section 2.1, estimates of the magnitude and timing of maximum paleotemperatures derived from the AFTA data in each sample are summarised in Table 3.3.

Evidence for elevated paleotemperatures from AFTA

As explained in Table 3.2, in three of the four samples that provided apatite, the AFTA data can be explained only by the effects of additional post-depositional heating, and thus provide clear evidence that these samples must have been hotter

than their respective present-day temperatures at some time after deposition. AFTA data in the Cretaceous sample (GC813-1) are limited by a lack of track length data but provide a constraint on the maximum possible post-depositional temperature.

Timing and magnitude of maximum paleotemperatures from AFTA

Estimates of the magnitude and timing of maximum paleotemperatures have been obtained by modelling the AFTA parameters for each sample through likely thermal history scenarios to determine the range of conditions giving predictions which are consistent with the measured data. The approach is described in more detail in Appendix C. Thermal history solutions for each sample and further detailed comments are provided in Table 3.3.

Sample GC813-1 is attributed to the Early Cretaceous Arctic Red and Martin House Formations based on the Formation top information compiled by Alconsult from GSC information (Table A.2, Appendix A), with the AFTA data restricting the maximum post-depositional temperature to less than 110°C as detailed in Table 3.3.

Data in sample GC813-3 from the Devonian Imperial Formation requires at least two post-Early Cretaceous thermal episodes with cooling from >135°C beginning at some time between 60 and 40 Ma and with cooling from 75 to 95°C beginning at some time between 35 and 5 Ma (Table 3.3). Data in Imperial Formation sample GC813-2 is less comprehensive, but provides clear evidence for at least one thermal episode, indicating cooling from >110°C began at some time between 60 and 10 Ma. A lack of track length data preclude resolution of any more recent thermal episodes in this sample.

Similar results have been obtained from Devonian Bear Rock-Canol/Hare Indian Formation sample GC813-4, with cooling from >105°C beginning at some time between deposition and 25 Ma and with paleotemperatures in the last 25 Ma restricted to less than 105°C (Table 3.3).

Reconciliation of the AFTA timing constraints obtained from individual samples, plus integration with the VR results (discussed below) suggests at least two thermal episodes are likely to have affected the section drilled in the well, with cooling beginning at some time within the following intervals:

- **60 to 40 Ma (Paleocene-Eocene)**
- **25 to 5 Ma (Miocene)**

Thermal history constraints derived from AFTA data in individual samples are summarised in Table i (Executive Summary).

Equivalent $R_o(\max)$ VR levels estimated from the AFTA data

Estimates of maximum paleotemperature from AFTA data in each sample have been converted to equivalent vitrinite reflectance values (using the Burnham and Sweeney, 1989, algorithm) which are also provided in Table 3.3.

3.3 Thermal history interpretation of Ontaratue H-34 VR data

Introduction

Mean VR values (including reflectance measurements on other macerals) from new analyses by Keiraville Konsultants are summarised in Table D.2 (Appendix D) with open-file results from Feinstein et al (1989) summarised in Table D.3 (Appendix D).

As noted in Section 1.3, the new and open-file data sets have been measured using different methodologies - random reflectance, **$R_o(\text{random})$** , for the open file data and **$R_o(\text{max})$** for the new data. At increasing levels of maturity these differing methodologies will result in an increasing difference between mean levels from the same sample due to reflectance anisotropy, whereby A.C. Cook (pers. comm.) has calculated:

$$R_o(\max) = (1.2089 \times R_o(\text{random})) - 0.0977: \quad [\text{for up to } \sim 5\% R_o(\max)]$$

Cook's relationship is remarkably similar to that derived from measurement of $R_o(\max)$ and $R_o(\text{random})$ on Appalachian coals over a range of 0.6 to 1.6% $R_o(\max)$ by Zhang and Davis (1993),

$$R_o(\max) = (1.2005 \times R_o(\text{random})) - 0.0903$$

Thus, for a measured $R_o(\text{random})$ of 1.17% (978 m, Table D.3), the calculated $R_o(\max)$ value is $\sim 1.32\%$. Feinstein et al (1989) also provide equivalent $R_o(\text{random})$ measurements derived from pyrobitumen reflectance and these have also been converted to $R_o(\max)$ using the same calculation. Thus, the equivalent VR of 2.45% estimated by Feinstein et al (1989) from an $R_o(\text{random})$ measurement on pyrobitumen at 3383 m (Table D.3) is equivalent to an VR $R_o(\max)$ level of 2.86% using the Cook equation above. Calculated $R_o(\max)$ for all open-file $R_o(\text{random})$ measurements are provided in Table ii (Executive Summary). Note that an equivalent $R_o(\max)$ level of 3.92% has also been calculated from the measured pyrobitumen reflectance of 3.32%, using this equation as A.C. Cook (pers comm.) believes that the at this level, measured pyrobitumen reflectance is close to the true VR level without correction to a lower value as carried out by Feinstein et al (1989). Despite this uncertainty, it is reasonable

to conclude that the actual VR level in this sample lies between ~2.86 and 3.92% $R_o(\text{max})$.

Finally, it should be noted that these calculated $R_o(\text{max})$ values have an additional uncertainty in that the $R_o(\text{random})$ measuring methodology has an inherent problem of establishing sample flatness that can lead to incorrect VR measurements. Establishing sample flatness is integral to the $R_o(\text{max})$ methodology and this results in a more robust estimate of the mean reflectance and a smaller uncertainty (see Appendix D).

$R_o(\text{max})$ values from both data sets are plotted against depth (with respect to KB) in Figure 3.2 together with the VR profile calculated on the basis of the Default Thermal History (explained in Section 2.1), which is derived from the preserved stratigraphy in the **Ontaratue H-34 well** (Figure 3.3) and a present-day geothermal gradient of 39.0°C/km. VR values from each data set are quite consistent throughout the drilled section, varying from ~0.6% in the Cretaceous section near the present-day ground surface to around 1.3% near the top of the Bear River Formation, with values (from pyrobitumen reflectance) in the Cambrian section interpreted to be ~2.9 to 3.9% $R_o(\text{max})$ equivalent. Other equivalent VR values for samples from the Devonian to Cambrian section are shown as lower or upper limits in Figure 3.2 based on maturity assessments discussed by the VR analyst in the detailed maceral descriptions presented in Appendix D (pages D.13 - D.14). Thus, a measured $R_o(\text{max})$ level in sample GC813-6.1 is considered to be cavings, and this has been plotted in Figure 3.2 as a minimum VR level for this depth. Similarly, bitumen reflectance of 2.95% and 3.57% in samples GC813-7 and -10 are considered to indicate a maximum likely maturity levels at these depths. The analyst considers that VR-like material in sample GC813-9 with an extremely high reflectance of 10.53% and that of 6.93% on possible graphic carbon in sample GC813-10 may indicate very high temperatures, but the rarity of organic matter in this part of the section does not allow firm conclusions to be drawn.

Also shown in Figure 3.2 are equivalent vitrinite reflectance values (using the Burnham and Sweeney, 1989, algorithm) determined from the AFTA-derived maximum paleotemperature estimates in each (Table 3.3).

Evidence that samples have been hotter in the past for the VR data

All VR values plotted in Figure 3.2 fall well above the profile predicted from the Default Thermal History, clearly indicating that the sampled section has cooled from maximum paleotemperatures higher than present temperatures at some time after deposition. Furthermore, there is no obvious break in the VR profile at the unconformity between the Cretaceous and Devonian sections suggesting that maximum paleotemperatures throughout the drilled section were reached at some

time after deposition of the Cretaceous section. This aspect of the data is discussed further below in terms of the quantitative thermal history reconstruction (THR).

Magnitude of paleotemperatures from VR and integration with AFTA

Maximum paleotemperatures derived from both the new and open-file VR data in this well, using the strategy outlined in Section 2.2, are summarised in Tables i and ii (Executive Summary). Paleotemperature constraints from AFTA and VR are plotted against depth in Figure 3.4.

Inspection of the paleotemperature depth plot indicates:

1. Maximum paleotemperatures vary from ~100 to 120°C in the Cretaceous section near surface to between ~220 and 260°C in the Cambrian section at ~3400 m.
2. Maximum paleotemperatures derived from the VR values throughout the section are highly consistent with those derived from the AFTA results in the same parts of the section for the Paleocene-Eocene thermal episode (60 to 40 Ma; Figure 3.4).
3. The AFTA and VR-derived maximum paleotemperature estimates define a well-constrained linear profile throughout the drilled section, from the Cretaceous section near surface to the Cambrian section near TD. The slope of the Paleocene-Eocene paleotemperature profile is similar to the present-day geothermal gradient, suggesting that simple deeper burial of the entire preserved section is a viable explanation of the observed paleo-heating effects.
4. There is no break in the paleotemperature profile at the sub-Cretaceous unconformity confirming the qualitative conclusion from inspection of the VR-depth plot in Figure 3.2. This indicates that maximum paleotemperatures throughout the Cretaceous and Devonian sections, at least, were reached immediately prior to cooling that commenced at some time between 60 and 40 Ma. The paleotemperature profile through the Siluro-Ordovician and Cambrian sections is more speculative given the lack of true vitrinite (see VR discussion above), however the estimates from pyrobitumen are highly consistent with the shallower results and on this basis a single linear gradient is considered to provide a viable explanation for the results (Figure 3.4).
5. The two AFTA-derived paleotemperature estimates constraining the Miocene episode (25 to 5 Ma), are insufficient to define a paleotemperature profile, but would also be consistent with a linear trend parallel to the present-day geothermal gradient.

In summary, reconciliation of the AFTA timing constraints obtained from individual samples, plus integration with the VR results indicates that two thermal episodes have affected the section drilled in the well, with cooling beginning at some time within the following intervals:

- **60 to 40 Ma (Paleocene-Eocene)**
- **25 to 5 Ma (Miocene)**

Thermal history constraints derived from the AFTA and VR results in individual samples are summarised in Tables i and ii (Executive Summary).

3.4 Paleogeothermal gradients and mechanisms of heating and cooling

Introduction

The synthesis of thermal history results presented in Section 3.3 concludes that the drilled section in the **Ontaratue H-34 well** was subjected to two distinct thermal episodes. Inspection of the paleotemperature constraints in Figure 3.4 suggests it would be possible to construct a coherent linear, paleogeothermal gradient profile for the Paleocene-Eocene (60 to 40 Ma) thermal episode from the AFTA and VR results. On the other hand, the two AFTA-derived paleotemperature estimates available for the Miocene episode are insufficient to provide any rigorous constraint on the geothermal gradient at this time.

Quantitative estimation of the paleogeothermal gradient in the Paleocene-Eocene thermal episode is discussed in the following sections.

Episode 1: 60 to 40 Ma (Paleocene-Eocene)

The AFTA and VR-derived maximum paleotemperatures reached by the entire drilled Cretaceous to Cambrian section prior to cooling beginning between 60 and 40 Ma are consistent with a linear profile as shown in Figure 3.4. Using the approach outlined in Section 2.5 and methods explained in Appendix C (Section C.9), the paleogeothermal gradient and its limits have been determined for this thermal episode revealed by AFTA.

Fitting a line to the profile of maximum paleotemperature estimates from the AFTA and VR data for this event (60 to 40 Ma) gives a maximum likelihood estimate of 44.5°C/km and well constrained allowed range of paleogeothermal gradients from 36.0 to 49.0°C/km, at 95% confidence limits (Figure 3.5). The allowed range of paleogeothermal gradient at 95% confidence limits encompasses the present-day gradient of 39.0°C/km. On this basis, heating throughout the drilled section between

60 and 40 Ma due to deeper burial on the top-Cretaceous unconformity is a viable explanation of the results. While a slightly higher paleogeothermal gradient (higher basal heat flow) is allowed during this episode (i.e. up to 49°C/km), any explanation for heating still requires additional kilometre-scale burial on the top-Cretaceous unconformity. This is discussed in more detail in Section 3.6.

Episode 2: 25 to 5 Ma: (Miocene)

No formal estimation of paleogeothermal gradient is possible for the 25 to 5 Ma thermal episode due to a lack of data over a sufficiently broad depth range, as discussed in previous Sections.

Paleogeothermal gradient estimates for the **Ontaratue H-34 well** are summarised in Table iii (Executive Summary).

3.5 Reconstructed thermal history in the Ontaratue H-34 well

A schematic illustration of the thermal history for the AFTA results from individual samples in the **Ontaratue H-34 well** is presented in Figure i. Integration of the AFTA and VR results and incorporation of the constrained paleogeothermal gradient results allows a generalized thermal history to be reconstructed for the whole well section as presented in Figure 3.6. This history incorporates a constant paleogeothermal gradient of 39.0°C/km for the entire history. This value (equal to the present-day value) is allowed within the $\pm 95\%$ confidence limits for the constrained gradient determined for the Paleocene-Eocene thermal episode (Figure 3.5) and is consistent with the limited results for the Miocene thermal episode constrained by the paleotemperature results discussed in Section 3.4.

Two end-member scenarios for the cooling history between the Paleocene and the present-day are illustrated in Figure 3.6, both of which are consistent with the AFTA and VR results. One scenario shows a “stepped” cooling history without intervening heating between the Paleocene-Eocene and Miocene episodes. The second scenario (dashed paths) involves a major heating event between the Paleocene-Eocene and Miocene cooling episodes, implying original burial by an Eocene-Miocene section now totally removed. While both of these end-member scenarios are possible, an intermediate situation with some lesser degree of intervening burial heating is considered to be the most geologically reasonable scenario, although this cannot be resolved using AFTA results alone.

Note that other periods of elevated geothermal gradient would be allowed by the AFTA results, but only within the limits as discussed in Section 3.4 and listed in

Table iii (Executive Summary) such that maximum paleotemperatures throughout the section were experienced between 60 and 40 Ma.

3.6 Reconstructed maturation history in the Ontaratue H-34 well

Predicted maturity-depth profile

Figure 3.7 shows the maturity-depth profile in **Ontaratue H-34 well** predicted (using Burnham and Sweeney, 1989) from the reconstructed thermal history shown in Figure i, together with the measured VR data and AFTA-equivalent VR levels (Table 3.3). The profile is in excellent agreement with the AFTA-equivalent levels and the organic results from the throughout the drilled section.

Predicted maturity levels within the Cretaceous section in **Ontaratue H-34** compare closely with the measured levels, reaching about 0.7% $R_o(\max)$ (mid-mature for oil) at the base of the Cretaceous section (Figure 3.7).

Maturity levels within the preserved Devonian section are predicted to vary from ~0.7% $R_o(\max)$ at the sub-Cretaceous unconformity to ~1.5% at the base of Bear Rock Limestone. That is, from mid-mature for oil to mature for dry gas. Maturity levels deeper than ~2000 m, within the Siluro-Ordovician section, exceeds 2% and reaches ~4% at TD, this section being post-mature for dry gas.

Predicted variation of maturity with time

Figure ii (Executive Summary) shows the variation of maturity with time for the **Ontaratue H-34 well** (using the maturation algorithm of Burnham and Sweeney, 1989) derived from the reconstructed thermal history shown in Figure 3.6. Maximum maturity throughout the section is shown as being reached immediately prior to cooling at 55 Ma, with anytime between 60 and 40 Ma allowed by the AFTA results for this well. Therefore, at the **Ontaratue H-34 well** site, there has been no *active* hydrocarbon generation from any potential Early Cretaceous, Devonian or Cambrian source rocks (should they exist at this location) since the onset of cooling at 55 Ma (within the 60 to 40 Ma time range allowed by AFTA).

The final cooling episode that commenced between 25 and 5 Ma has no effect on the maturation history of any of the preserved stratigraphic section, as paleotemperatures in this episode were lower than experienced in the previous episode. However, uplift and erosion associated with this episode (see Section 3.7) may have had a significant effect on re-migration of any reservoired hydrocarbons. Further discussion of this aspect of petroleum system is beyond the scope of this report, but should be borne in mind when integrating the results of this study with other geological information.

3.7 Estimating section removed by erosion

Introduction

The data presented in the previous sections provide good constraints on the main aspects of the thermal history for the **Ontaratue H-34 well**, as illustrated by the schematic thermal history results from AFTA shown in Figure i (Executive Summary) and the generalised thermal history shown in Figure 3.7. Reconstruction of the burial history is more speculative as it depends on the various assumptions described in Section 2.5. The principal difficulty lies with definition of the paleogeothermal gradient through the removed section which must be assumed. For the estimates described above and listed in Table iii, the paleogeothermal gradients through the removed section are assumed to be the same as those measured in the preserved section (or the same as the present-day value) and this assumption may be invalid if the elevated paleotemperatures are caused by processes involving lateral or local introduction of heat, such as by confined fluid flow or igneous intrusions (for example). There are no compelling indications in the results for significant lateral heat transfer in the **Ontaratue H-34 well** and this possibility will not be considered further.

Nevertheless, the burial history reconstruction presented below remains, to a certain extent, speculative and would benefit from independent estimates of section removed (e.g., sonic velocity studies etc.) in the region.

Paleo-burial on the top-Cretaceous unconformity beginning between 60 and 40 Ma (Paleocene-Eocene)

The thermal history reconstruction provides a good constraint on the time of cooling from maximum paleotemperatures beginning between 60 and 40 Ma (Paleocene-Eocene). On the basis of the preserved stratigraphy, this AFTA-derived timing is completely within the time range represented by the unconformity at the top of the Albian Arctic Red Formation at the present ground surface, viz. ~98 to 0 Ma (Table A.2). Therefore, the analysis of removed section in this cooling episode has been carried out in terms of depth with respect to this unconformity.

Linear extrapolation of the paleogeothermal gradient in Figure 3.5 to a paleo-surface temperature of 0°C gives a maximum likelihood estimate of 2300 metres for the total amount of section removed (paleo-burial) from the top-Cretaceous unconformity, with lower and upper 95% confidence limits of 2000 and 3000 metres, respectively (Figure 3.8). Note that higher or lower paleo-surface temperatures would require correspondingly less or more section removed as explained in Section 2.5.

Figure 3.9 illustrates the correlation between values of Paleocene-Eocene paleogeothermal gradient and section removed (equivalent to paleo-burial) allowed by the AFTA and VR data, within $\pm 95\%$ confidence limits. That is, any set of paired values inside the contoured region are compatible with the data at 95% confidence limits. For example, for a paleo-gradient equal to the present-day gradient of $39.0^\circ\text{C}/\text{km}$, ~ 2900 m of additional post-Arctic Red Formation burial is required to honour the AFTA and VR paleotemperature constraints.

Section-removed on the top-Cretaceous unconformity beginning between 25 and 5 Ma (Miocene)

The AFTA results also clearly require a period of cooling beginning between 20 and 5 Ma, but the limited depth spread of the paleotemperature estimates means that no useful constraints can be placed on paleogeothermal gradient during this episode, although a gradient similar to the present-day gradient of $39^\circ\text{C}/\text{km}$ is *allowed*.

Assuming that the paleogeothermal gradient between 25 and 5 Ma was the same as the present day gradient, between ~ 1130 and 1640 m of uplift and erosion is required since this time in order to explain the allowed range of AFTA paleotemperature estimates in sample GC813-3 (Table i).

Removed section estimates determined by these methods are summarised in Table iv (Executive Summary).

3.8 Burial history reconstruction

Figure 3.10 shows a reconstructed burial and uplift history for the section preserved in the **Ontaratue H-34 well**, based on the new AFTA and VR results. The construction of this history adopts a constant paleogeothermal gradient of $39.0^\circ\text{C}/\text{km}$ (equal to the present-day value) for the whole history, as this value is within the 95% confidence limits for the Paleocene-Eocene thermal episode constrained by the paleogeothermal gradient results discussed in Section 3.4 and is *allowed* by the limited results for the Miocene thermal episode.

Thus, heating prior to the Paleocene-Eocene episode beginning at 55 Ma (any time between 60 and 40 Ma is allowed by AFTA) is attributed to 2900 m of additional burial (Table iv) on the top-Cretaceous unconformity, with cooling due to simple uplift and erosion. The preservation of the Albian Arctic Red Formation at ground surface implies that the removed section can only have been composed of section of Albian to Eocene depositional age (as young as 40 Ma).

Miocene cooling is shown as beginning at 10 Ma (although any value within the range 25 to 5 Ma is allowed by AFTA) and involves uplift and erosion of 1400 m of the total 2900 m of additional burial (within the allowed range 1130 to 1640 m, as summarised in Table iv).

The appropriate amounts of missing section in each event are drawn from the crossplot in Figures 3.9, for the paleogeothermal gradients specified above, as listed in Table iii. Other magnitudes for erosion would be allowed during each episode within specified limits corresponding to other values of paleogeothermal gradient. However, for alternative reconstructions these allowable variations have no effect on the maturity analysis presented in Section 3.6, as the paleotemperature and timing constraints are independent of any arguments about the magnitude of erosion, and the allowed combination of values of paleogeothermal gradient and erosion give similar thermal history scenarios.

Note also, that as discussed in Section 3.6, the exact nature of the cooling history, whether “stepped” or with intervening burial heating, is unconstrained by the results as illustrated in Figure 3.6. This range of possible styles of cooling also applies to the reconstructed burial history. The history illustrated in Figure 3.10 has no intervening burial between the Paleocene-Eocene and Miocene cooling episodes, but such re-burial by Eocene and Miocene sediments would be allowed up to the total magnitude eroded since 10 Ma (i.e. up to 1400 m in the case illustrated in Figure 3.10). The most likely geologically reasonable scenario probably involves some degree of re-burial during this interval, but this cannot be constrained.

3.9 Recommendations for further work

- The results obtained in this study have provided robust constraints on key aspects of the thermal and maturation histories at **Ontaratue H-34**. Additional VR samples with high quality maceral descriptions, in the Silurian, Ordovician and Cambrian sections would be useful in confirming the Paleocene-Eocene paleogeothermal gradient through this section. Unfortunately, the general paucity of suitable organic matter in the samples examined in this and other wells in the regional study does not suggest that this will be easily achieved.
- Additional AFTA samples are not recommended as the two thermal events identified are relatively well constrained in this well by current data, however, tighter constraints on the timing of the Miocene thermal episode and the Miocene paleogeothermal gradient might be obtained by application of the emerging (U-Th)/He apatite dating technology which allows precise timing constraints to be placed on samples exposed to Miocene paleotemperatures in

the range ~60 to 80°C. Geotrack intends to investigate application of this technique in the NWT and will seek interest from exploring companies.

- Analysis of outcrop samples from the region, using AFTA, VR and (U-TH)/He apatite dating is suggested as a viable strategy for tracking the extent and magnitude of the Tertiary thermal episodes identified in Ontaratie H-34. Special attention should be given to outcrops of Tertiary, Cretaceous and Devonian sediments in the region.

References

- Bray, R.J., Green, P.F. and Duddy, I.R., (1992). Thermal History Reconstruction using apatite fission track analysis and vitrinite reflectance: a case study from the UK East Midlands and the Southern North Sea. In: Hardman, R.F.P. (ed.), *Exploration Britain: Into the next decade. Geological Society Special Publication*, 67, 3-25.
- Burnham, A.K. and Sweeney, J.J., (1989). A chemical kinetic model of vitrinite reflectance maturation. *Geochimica et Cosmochimica Acta.*, 53, 2649-2657.
- Feinstein, S., Brooks, P.W., Gentzis, T., Goodarzi, F., Snowden, L.R. and Williams, G.K. (1989). Thermal maturity in the Mackenzie Corridor, Northwest Territories and Yukon Territories, Canada. *GSC Open File 1994*.
- Sweeney, J.J. and Burnham, A.K., (1990). Evaluation of a simple model of vitrinite reflectance based on chemical kinetics. *AAPG Bulletin*, 74, 1559-1570.
- Zhang, E. and Davis, A. (1993). Coalification Patterns of the Pennsylvanian Coal Measures in the Appalachian Foreland Basin, Western and South-Central Pennsylvania. *Bull. Geol. Soc. Am.*, 105, 162-174.

Table 3.1: Summary of AFTA data in samples from the Ontaratue H-34 well, Northwest Territories, Canada (Geotrack Report #813A)

Sample number	Average depth ^{*1}	Present temperature ^{*2}	Stratigraphic Age	Measured mean track length	Default mean track length ^{*3}	Measured apatite fission track age ^{*4}	Default fission track age ^{*3}
GC	(m)	(°C)	(Ma)	(µm)	(µm)	(Ma)	(Ma)
813-1	144	5	110 - 65	No lengths	14.3	<i>174.5 ± 85.0</i>	91
813-2	465	18	356 - 346	No lengths	14.4	57.0 ± 10.8	345
813-3	792	31	356 - 346	12.94 ± 0.67	14.3	42.3 ± 5.2	340
813-4	995	39	373 - 356	12.85	13.6	<i>14.7 ± 4.9</i>	334
813-5	1379	54	373-369	No apatite	-	No apatite	-
813-6	1699	66	490-369	No apatite	-	No apatite	-
813-7	2408	94	490-470	No apatite	-	No apatite	-
813-8	2893	113	540-490	Not processed	-	Not processed	-
813-9	3064	119	540-490	Not processed	-	Not processed	-
813-10	3052	119	540-490	Not processed	-	Not processed	-
813-11	3236	126	540-490	Not processed	-	Not processed	-

*1 All depths quoted are true vertical depth (TVD) with respect to KB.

*2 See Appendix A for a discussion of present temperature estimation.

*3 AFTA values predicted from the "Default Thermal History" (Section 2.1); i.e., assuming that each sample is now at its maximum temperature since deposition. The values refer only to tracks formed after deposition. Samples may also contain tracks inherited from sediment provenance areas. Calculation of the Default values refer to actual measured compositions of apatites analysed within a particular sample, which is discussed in Appendix A.

*4 Central fission track age quoted (in italics) where $P(\chi^2) < 5\%$

Table 3.2: Summary of thermal history interpretation of AFTA data in samples from the Ontaratue H-34 well, Northwest Territories, Canada (Geotrack Report #813A)

Sample number	Do AFTA data require revision of present temperature?	Evidence of higher temperatures in the past from length data?	Evidence of higher temperatures in the past from fission track age data?	Conclusion
GC813-1 145 m Cretaceous	No 5°C	No confined track lengths.	Yes, Equivocal [Poor data. Only 4 grains measured that do not allow rigorous interpretation. Central fission track age is similar to, but a single grain is significantly younger than expected from the Default Thermal History].	Sample has probably been hotter than present temperatures since deposition as suggested by the single grain age data.
GC813-2 465 m Devonian Imperial Fm	No 18°C	No confined track lengths.	Yes [Pooled fission track age is significantly younger than expected on the basis of the Default Thermal History.]	Sample has been hotter than present temperatures since deposition as shown by the fission track age data.
GC813-3 792 m Devonian Imperial Fm	No 31°C	Yes [Mean track length is at least 1.0 µm shorter than expected on the basis of the Default Thermal History. Modelling the AFTA parameters through likely thermal history scenarios shows that measured lengths can be explained <i>only</i> by higher paleotemperatures after deposition and not by inheritance of short tracks from the sediment source terrain.]	Yes [Pooled fission track age is significantly younger than expected on the basis of the Default Thermal History.]	Sample has been hotter than present temperatures since deposition as shown by both the fission track age and length data.
GC813-4 995 m Devonian Hume Fm	No 39°C	Insufficient data for rigorous interpretation [Only one track length measured].	Yes [Central fission track age and all single grain ages are significantly younger than expected on the basis of the Default Thermal History.]	Sample has been hotter than present temperatures since deposition.

Note: Interpretation of AFTA data is based on comparison of measured AFTA parameters with values predicted from "Default Thermal History" (Section 2.1); i.e., assuming that each sample is now at its maximum temperature since deposition. The predicted values for each sample are summarised in Table 3.1, and refer only to tracks formed after deposition. Samples may also contain tracks inherited from sediment provenance areas, which must be allowed for in interpreting the data. Calculations refer to apatites with the compositional range measured in each sample, as explained in Appendix A.



Table 3.3: Estimates of timing and magnitude of elevated paleotemperatures from AFTA data in samples from the Ontaratué H-34 well, Northwest Territories, Canada (Geotrack Report #813A)

Sample number	Stratigraphic age	Present temperature ^{*1}	Maximum paleo-temperature	Onset of cooling	Maximum paleo-temperature	Onset of cooling	Comments
Average depth	(Ma)	(°C)	(°C)	(Ma)	(°C)	(Ma)	
GC813-1	110 to 65 Cretaceous	5	<110	Post-depn	No	constraint	Poor data derived from 4 age measurements and no track lengths. At face value the AFTA results indicate that maximum post-depositional temperatures did not exceed 110°C. The lack of track length data precludes constraints on any more recent thermal episodes.
GC813-2	356 to 346	18	>110	60 to 10	No	constraint	The AFTA-derived maximum paleotemperature predicts an equivalent VR level less than 0.66%, consistent with the new measured VR level of 0.66% in the same sample (Table D.2 Appendix D).
465 m	U. Devonian Imperial Fm						Relatively low quality data derived from 8 age measurements and no track lengths. Nevertheless the AFTA age data clearly indicate at least one paleo-thermal episode after deposition, with cooling from greater than 110°C occurring at some time between 60 and 10 Ma. The lack of track length data precludes constraints on any more recent thermal episodes.
							The AFTA-derived maximum paleotemperature predicts an equivalent VR level greater than 0.66%, consistent with the new measured VR level of 0.75% in the same sample (Table D.2 Appendix D).

^{*1} Present temperature estimates were based on a surface temperature of 0°C and linear gradient of 39.0°C/km. (See Appendix A.)



Table 3.3 (cont.): Ontaratie H-34 well, Northwest Territories, Canada (Geotrack Report #813A)

Sample number	Stratigraphic age	Present temperature ^{*1}	Maximum paleo-temperature	Onset of cooling	Maximum paleo-temperature	Onset of cooling	Comments
Average depth	(Ma)	(°C)	(°C)	(Ma)	(°C)	(Ma)	
GC813-3	356 to 346	31	>135	60 to 40	75 - 95	35 to 5	Key sample with high quality AFTA data which requires at least two paleo-thermal episodes, with cooling from paleotemperatures of at least 135°C occurring between 60 and 40 Ma, and with cooling from 75 to 95°C beginning between 35 and 5 Ma.
792 m	U. Devonian Imperial Fm						
							The AFTA-required paleotemperature of >135°C, predicts an equivalent VR level >0.95%, consistent with the new measured VR level of 0.95% in a split of the same sample (sample GC813-3.1, Table D.2 Appendix D).
GC813-4	373 to 356	39	>105	Depn to 25	<105	25 to 0	AFTA requires at least one paleo-thermal episode, with cooling from >105°C beginning at some time between deposition and 25 Ma. AFTA also constrains paleotemperatures within the last 25 Ma to less than 105°C.
995 m	U. Devonian Hume Fm						
							The AFTA-required paleotemperature of >105°C, predicts an equivalent VR level of >0.64%, consistent with the new measured VR level of 1.11 to 1.15% in splits of the same sample (GC813-4.1 and -4.2, Table D.2 Appendix D).

^{*1} Present temperature estimates were based on a surface temperature of 0°C and linear gradient of 39.0°C/km. (See Appendix A.)

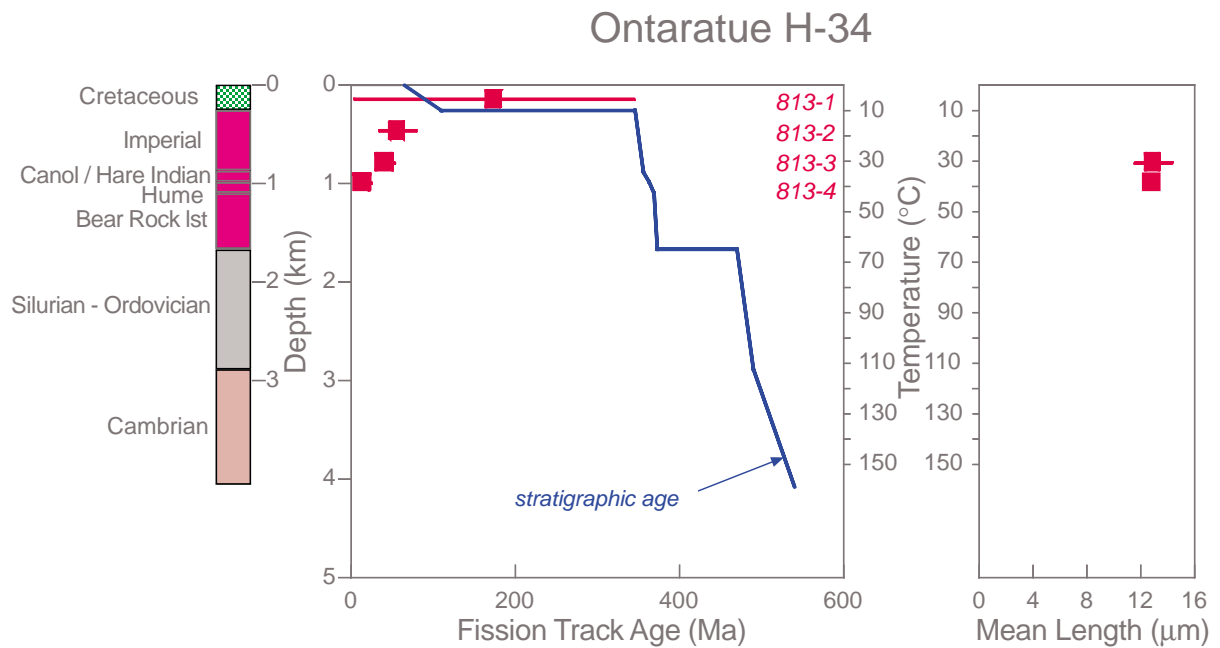


Figure 3.1: AFTA parameters plotted against sample depth and present temperature for samples from the **Ontaratie H-34 well, Northwest Territories, Canada**. The variation of stratigraphic age with depth is also shown, as the solid line in the central panel. The present-day geothermal gradient of 39.0°C/km is used for the temperature scale.

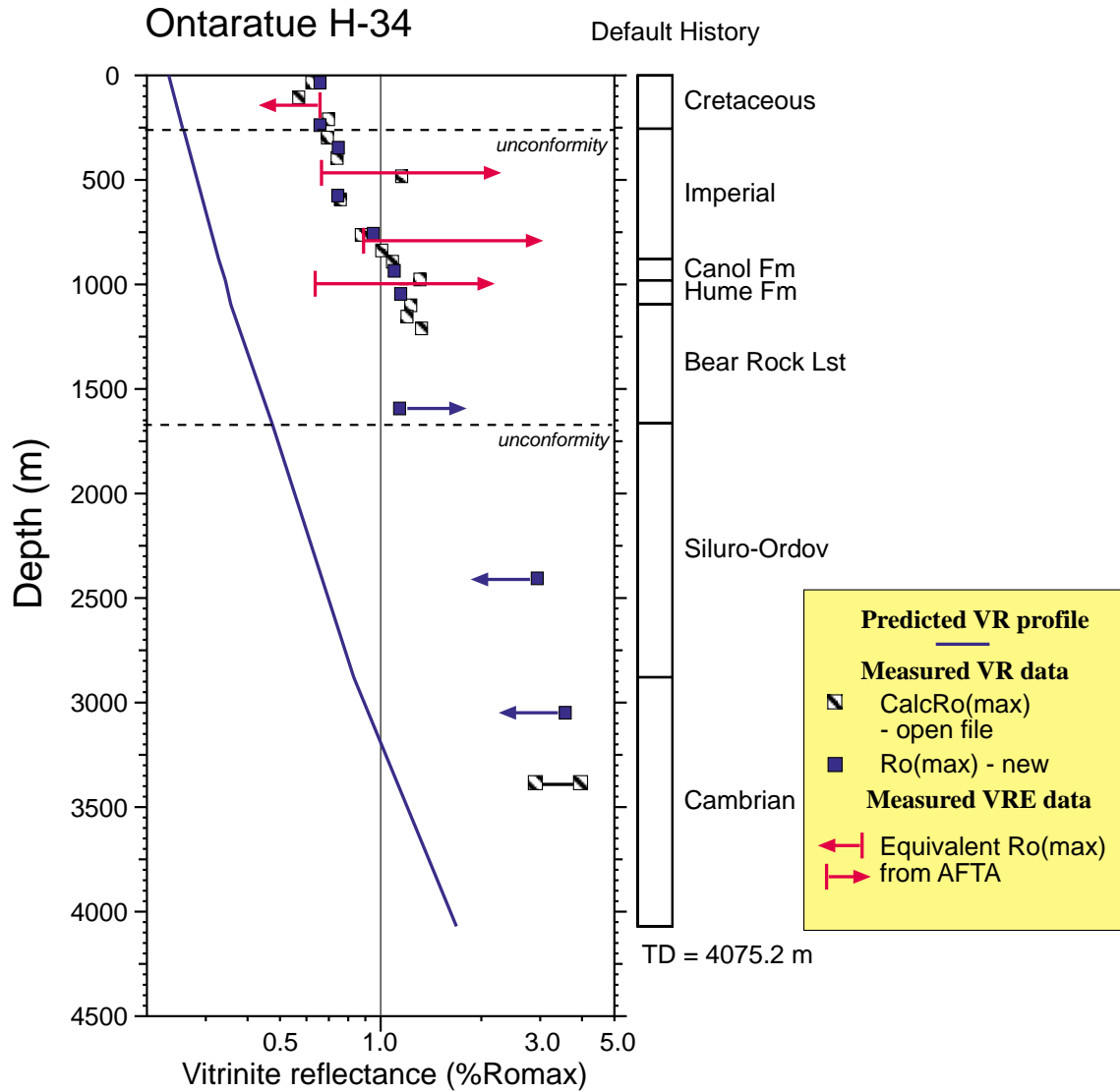


Figure 3.2: Measured and predicted maturity with respect to depth. The solid square symbols denote high quality $R_0(\text{max})$ VR data and the cross-hatched symbols denote equivalent $R_0(\text{max})$ levels calculated from open-file $R_0(\text{random})$ measurements (Table D.3, Appendix D). Equivalent $R_0(\text{max})$ levels from AFTA (Table 3.3) shows as left or right pointing arrows. The solid line shows the VR profile calculated on the basis of the Default Thermal History (explained in Section 2.1), which is derived from the preserved stratigraphy in the **Ontaratue H-34 well** (Figure 3.3) and a present-day geothermal gradient of $39.0^\circ\text{C}/\text{km}$. All values lie above the predicted profile, indicating the sampled sequence was exposed to maximum paleotemperatures higher than present temperatures at some time after deposition.

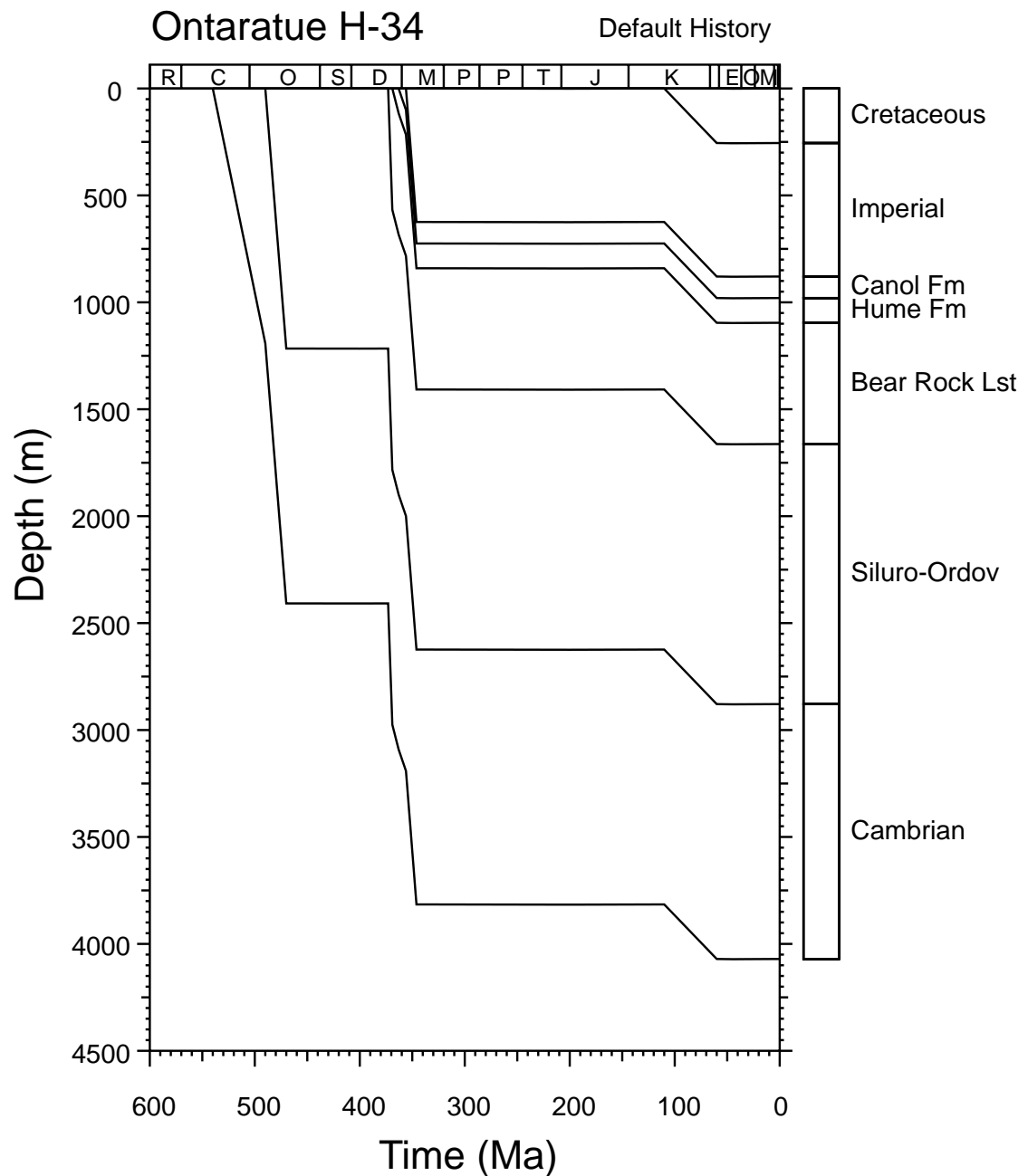


Figure 3.3: Default Burial History showing the history derived from the preserved stratigraphy in the **Ontaratue H-34 well**. This history, together with the present-day geothermal gradient (39.0°C/km) and a surface temperature of 0°C, has been used to calculate the Default Thermal Histories for each sample from which default parameters are calculated (see Table 3.1). Default parameters are compared with observed AFTA parameters and measured VR data to evaluate the degree of heating which is attributable to the present thermal regime and hence to determine whether samples have been hotter in the past.

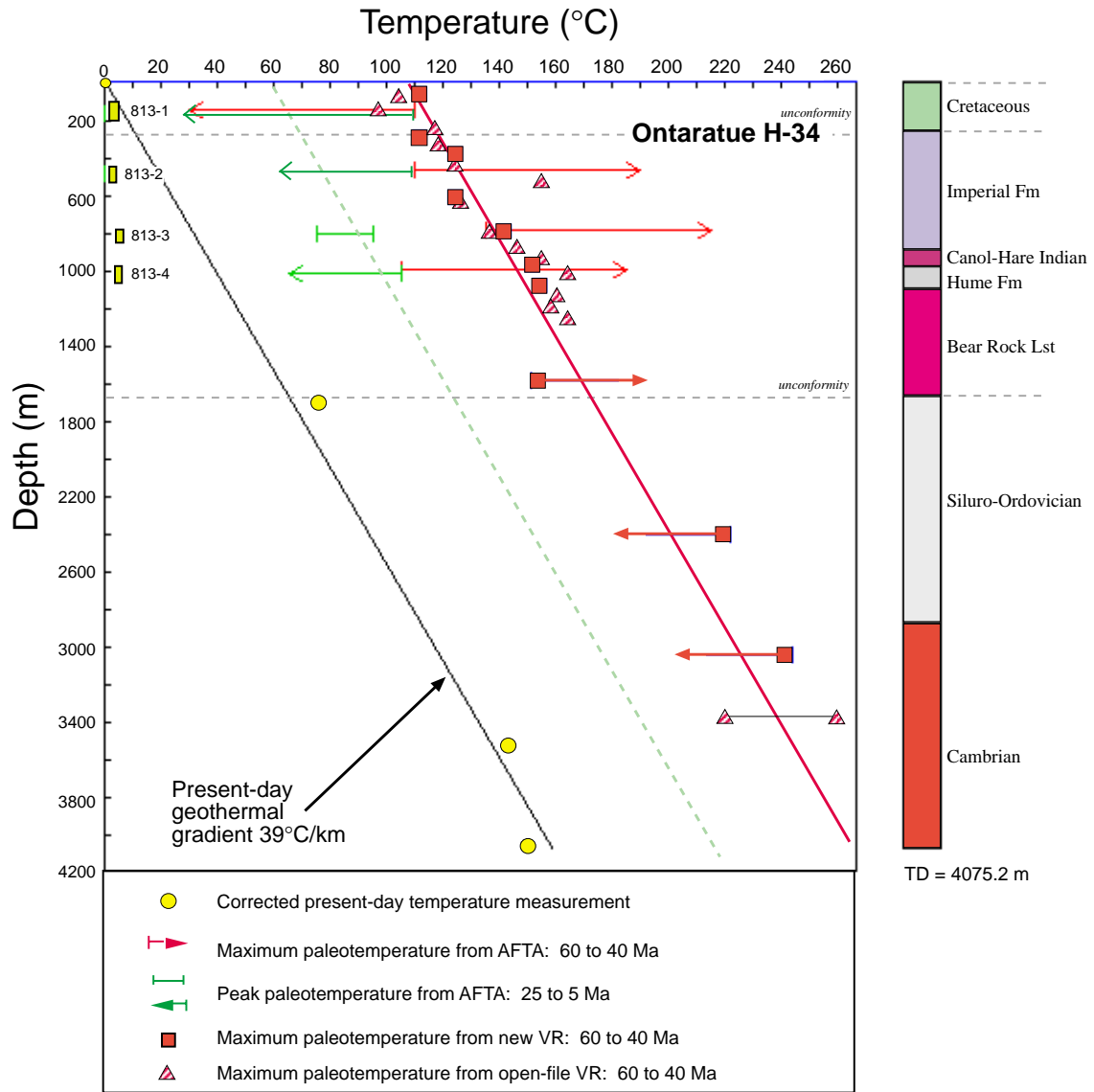


Figure 3.4: Plot of paleotemperatures derived from AFTA and VR data in the **Ontaratue H-34 well**, Northwest Territories, Canada, against depth and the estimated present temperature profile for this well (Appendix A). Integration of AFTA and new VR results indicate at least two thermal episodes have effected the drilled section in **Ontaratue H-34**:

1. The entire drilled section of Cretaceous to Cambrian age is interpreted to have cooled from maximum paleotemperatures beginning at some time between 60 and 40 Ma (Paleocene-Eocene).
2. The entire drilled section also cooled from a peak in paleotemperatures beginning between 25 and 5 Ma (Miocene).

Quantitative estimates of paleogeothermal gradient (represented schematically by the colour-coded lines) for the two thermal episodes identified are provided in Table ii (Executive Summary).

Ontaratie-H34 Early Tertiary Episode

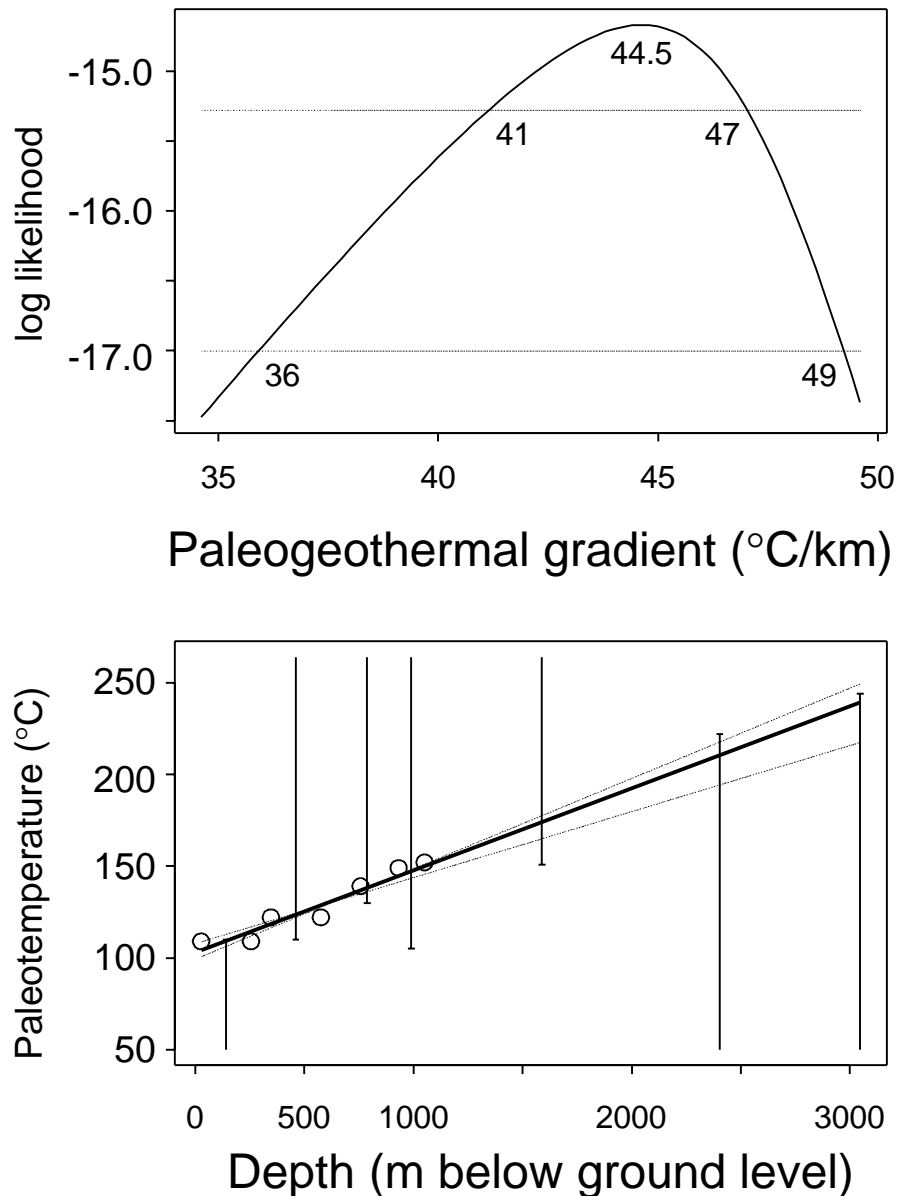


Figure 3.5: Upper: Maximum likelihood profile of linear paleogeothermal gradient for the **Paleocene-Eocene thermal episode (60 to 40 Ma)** fitted to the maximum paleotemperature estimates from AFTA and VR data in the **Ontaratie H-34 well**. The profile shows good quadratic behaviour with upper and lower confidence limits of 49.0 and 36°C/km, respectively, and a best-fit value of 44.5°C/km. The methodology employed in deriving this profile is outlined in Appendix C.

Lower: Maximum paleotemperature estimates from AFTA and VR data plotted against depth below the top-Cretaceous unconformity, with the fitted profile (solid line) and lines (dashed) representing upper and lower 95% confidence limits.

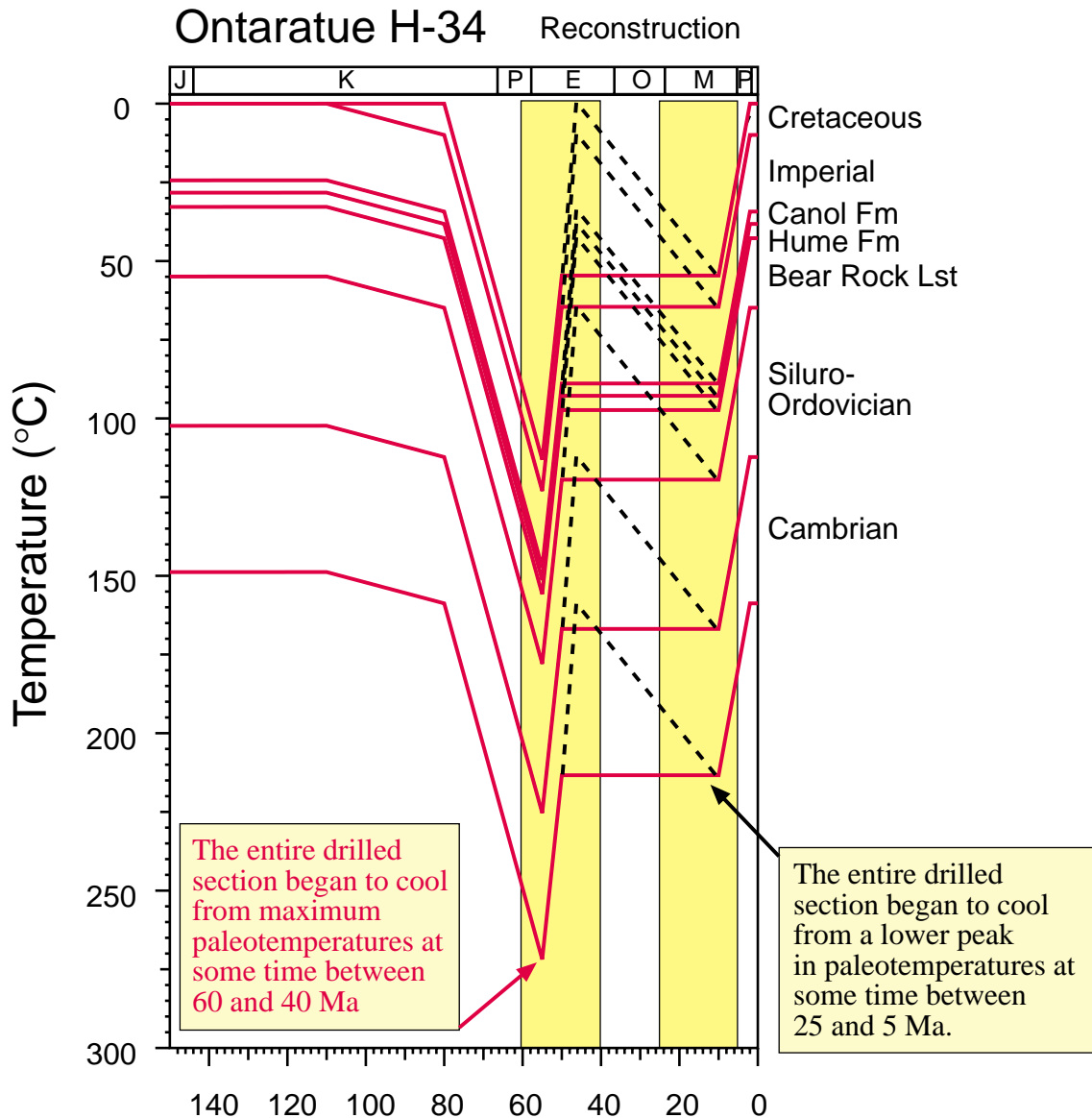


Figure 3.6: Reconstructed thermal history for the **Ontaratue H-34 well**, Northwest Territories, Canada, based on AFTA plus new and open-file VR results (only the last 150 Ma shown for clarity).

AFTA indicates that cooling from maximum paleotemperatures began in the Paleocene-Eocene, between 60 and 40 Ma, with a subsequent cooling episode beginning between 25 and 5 Ma (Miocene).

The solid path represents one end-member for the cooling history defined by the AFTA results between the Paleocene and the present-day involving cooling in two cooling phases without any intervening heating. The dashed paths show an alternative end-member (perhaps more geologically reasonable) with an intervening period of heating (due to burial). Intermediate scenarios are also possible and in all cases the peak paleotemperatures in each episode are the same, but AFTA alone cannot distinguish between these scenarios.

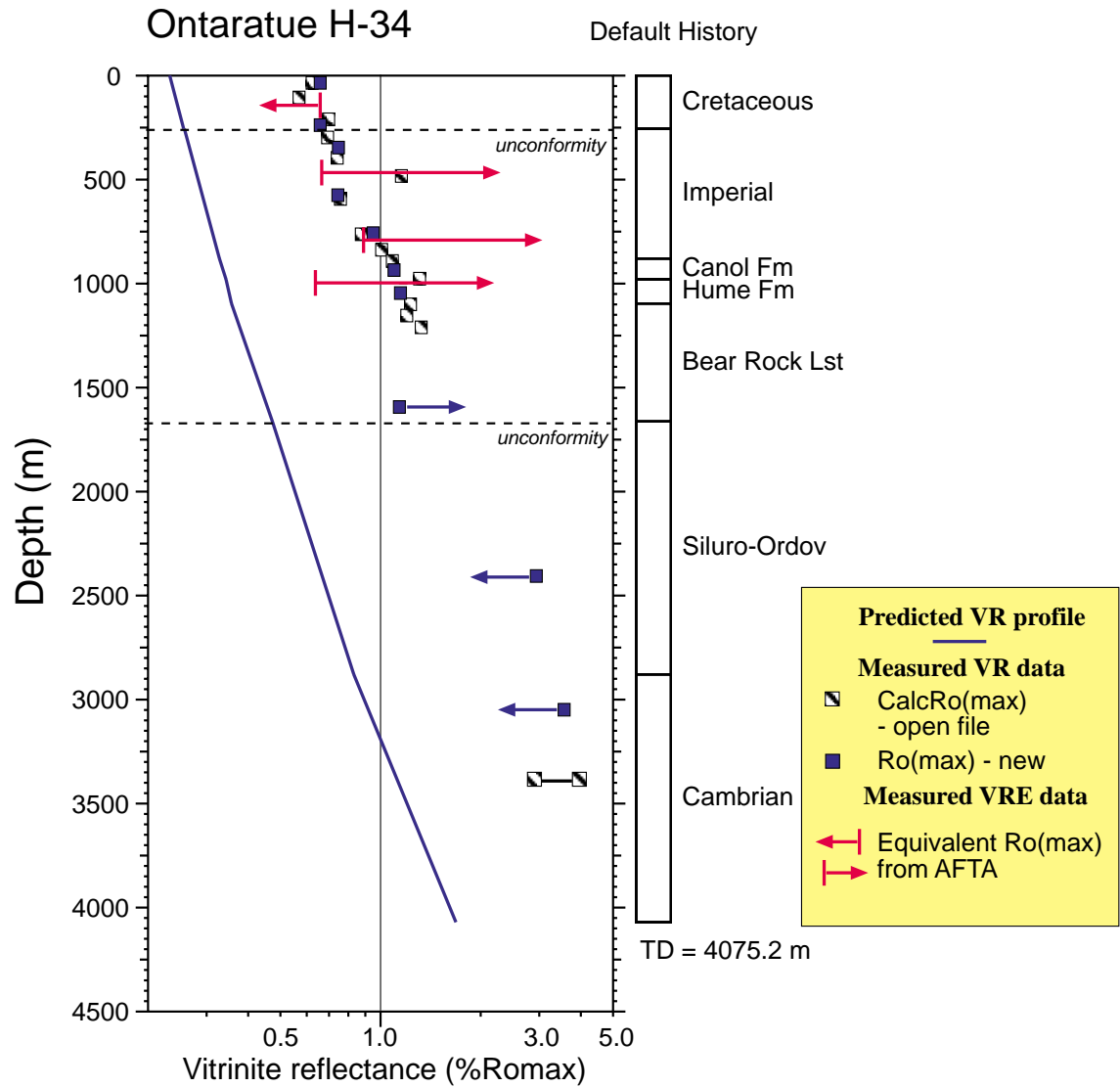


Figure 3.7: Maturity-depth plot for the **Ontaratue H-34 well** derived from the reconstructed thermal history derived only from the AFTA and new VR data as illustrated in Figure 3.6. The predicted profile shows an excellent fit to both the new VR data (Table D.2, Appendix D), as expected, and the $R_o(\text{max})$ data calculated from the $R_o(\text{random})$ open-file VR data (Table D.3, Appendix D). Dashed profile derived from the Default Thermal History for comparison (see Figure 3.2).

Ontaratue-H34 Early Tertiary Episode

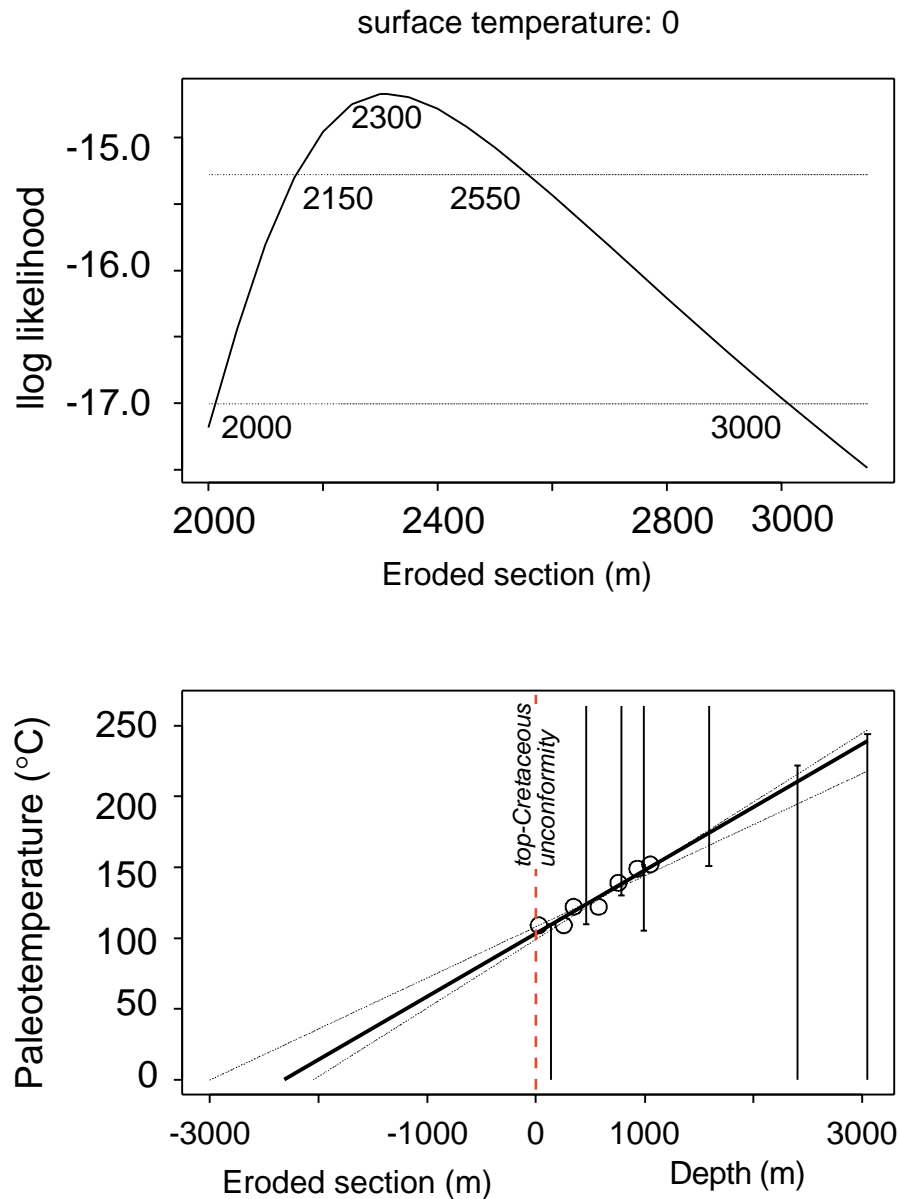


Figure 3.8:

Upper: Maximum likelihood profile of estimated total section removed by uplift and erosion at the level of the top-Cretaceous unconformity at the present-day surface (4.6 m bKB) in the **Ontaratue H34 well** beginning between **60 and 40 Ma**. The profile is derived from AFTA and new VR data and the constrained paleogeothermal gradient shown in Figure 3.5, assuming a paleo-surface temperature of 0°C. The profile gives lower and upper confidence limits of 2000 and 3000 m, and a well constrained best-fit value of 2300 m. The methodology employed in deriving this profile is outlined in Appendix C.

Lower: Maximum paleotemperature estimates from AFTA and VR data plotted against depth below the top-Cretaceous unconformity, with the fitted profile (solid line) and lines (dashed) representing upper and lower 95% confidence limits, extrapolated to the assumed paleo-surface temperature of 0°C.

Ontaratue-H34 Early Tertiary Episode

surface temperature: 0

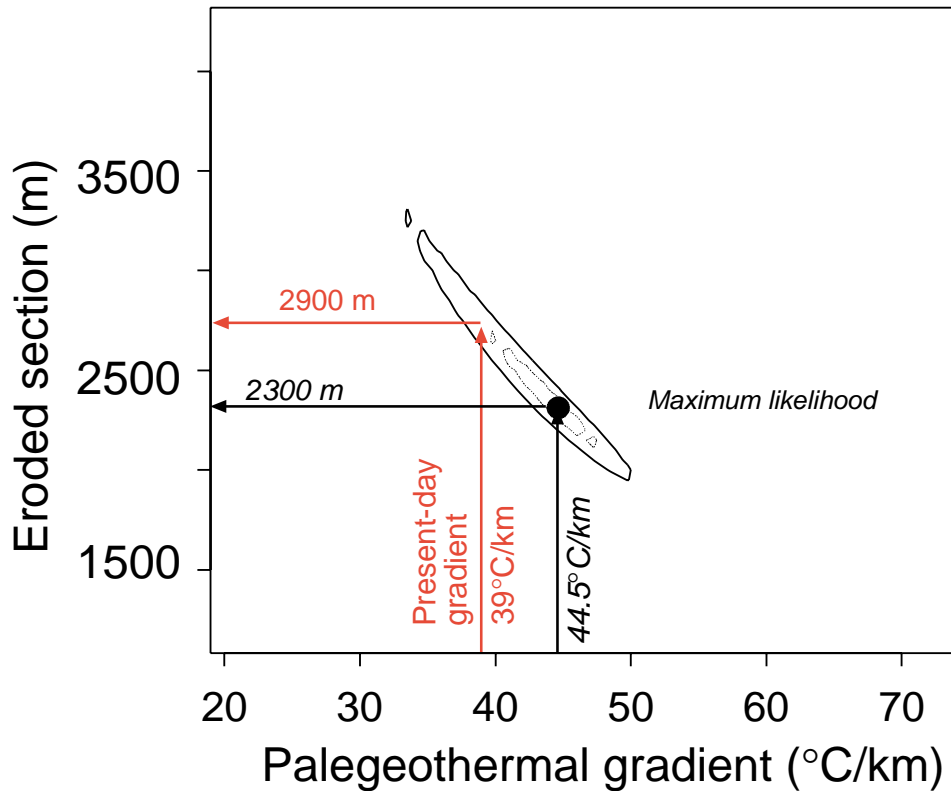


Figure 3.9:

Crossplot of total section removed from the unconformity at the top of the Cretaceous section at the present-day surface (4.6 m bKB) in the **Ontaratue H34 well** since the Paleocene-Eocene (60 to 40 Ma) against paleogeothermal gradient. The plot shows the range of values (paired within the contoured region) compatible with the maximum paleotemperatures derived from AFTA and VR data at the 95% confidence level. The values printed within the plot are amounts of removed section corresponding to $\pm 2\sigma$ limits at various values of paleogeothermal gradient. For example, for a paleogeothermal gradient of 39.0°C/km, equal to the present day value, ~2900 m of additional burial is required on the top-Cretaceous unconformity in order to honour the paleotemperature constraints.

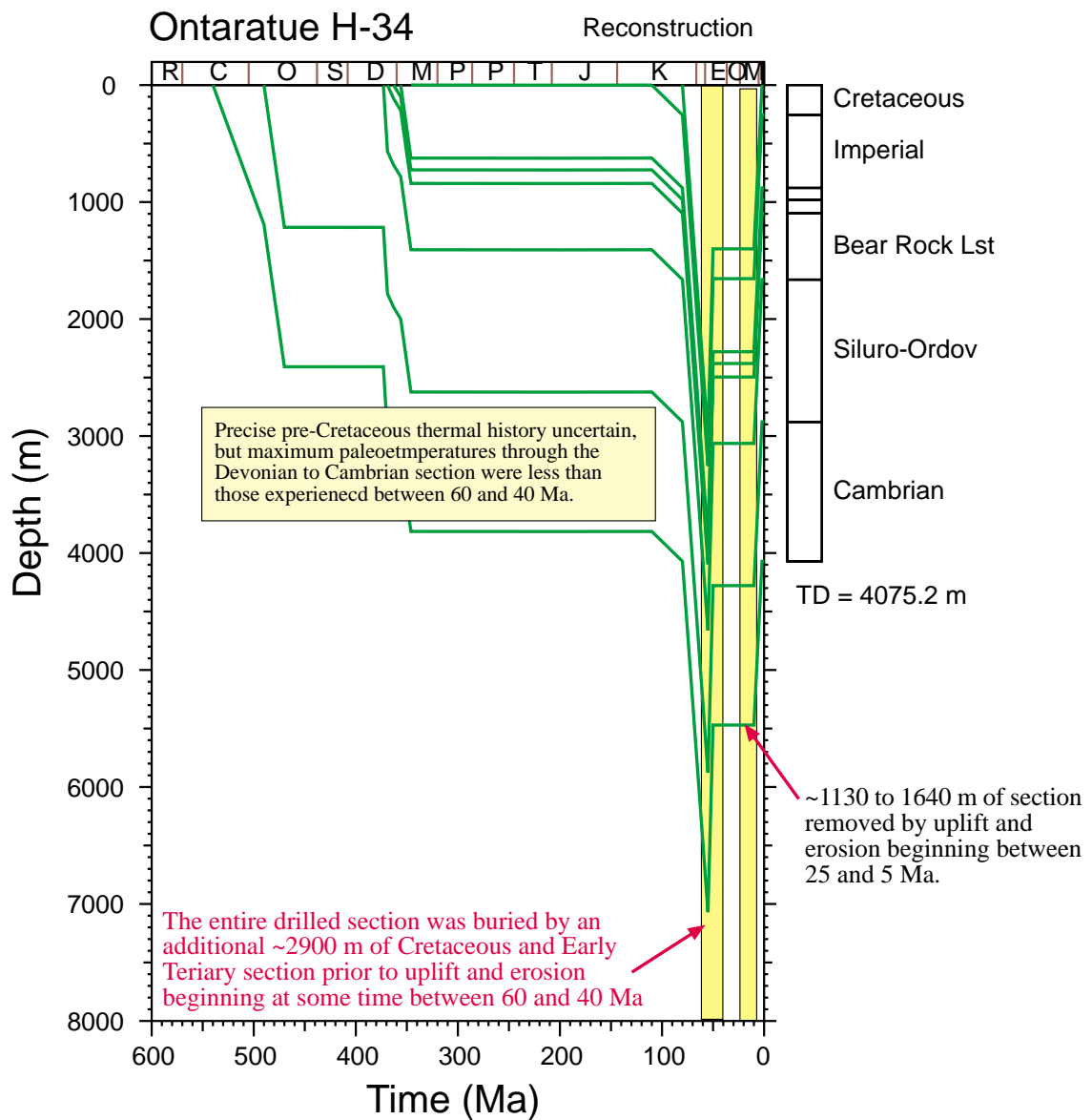


Figure 3.10: Burial History constructed on the basis of the preferred thermal history reconstruction in the **Ontaratue H-34 well**, with 2900 m of uplift and erosion on the top-Cretaceous unconformity beginning at 55 Ma (any time between 60 and 40 Ma allowed) and 1400 m of erosion on the top-Cretaceous unconformity beginning at 10 Ma (between 25 and 5 Ma allowed). Note that maximum burial in this reconstruction occurs immediately prior to cooling beginning between 60 and 40 Ma. Other burial histories are also allowed within bounds defined by the thermal history constraints. Further details are provided in the text (Section 3.8).



NORTHWEST TERRITORIES CANADA

Ontaratue H-34 well

**Reconstruction of thermal, burial and source rock
maturation histories using AFTA® and VR results**

APPENDICES A to D.

GEOTRACK REPORT #813A

**A multi-client study by
Geotrack International Pty Ltd in association with Alconsult International**

Report prepared by:

I. R. Duddy

AFTA determinations by:

M.E. Moore

May 2002

Geotrack International Pty Ltd ABN 16 006 821 209

37 Melville Road, Brunswick West, Victoria 3055, Australia Ph +613 9380 1077 facsimile +61 3 9380 1477
email mail@geotrack.com.au



APPENDIX A

Sample Details, Geological Data and Apatite Compositions

A.1 Sample locations

Eleven samples from the **Ontaratue H-34 well**, ~300 km north-west of Tulita, Northwest Territories, Canada (Figure 1.1), were originally collected for AFTA, and of these, the seven shallower samples (at present temperature less than 100°C) were processed through the mineral separation procedures. Splits of eight of these AFTA samples plus five additional samples were also analysed for vitrinite reflectance as detailed in Appendix D (Table D.2).

Details of all AFTA samples, including sample depths, stratigraphic ages and estimates of present temperature for each sample, are summarised in Table A.1. Details of present temperature estimation are summarised in Section A.3 (below). Yields of apatite obtained from each AFTA sample are also summarised in Table A.1, with four of the seven samples processed yielding sufficient apatite suitable for analysis.

Details of all samples collected for VR are summarised in Table D.2, together with summary results. Full details of the results of these analyses are presented in Appendix D, where aspects such as vitrinite abundance and maceral types are also discussed. VR data quality is discussed in Section 1.3.

A.2 Stratigraphic details

Details of the stratigraphic breakdown of the preserved section in the **Ontaratue H-34 well** are derived from information compiled by Alconsult International Ltd from various sources at the Geological Survey of Canada. Formation tops were assigned chronostratic ages using the time scale of the GSC. The resulting information is summarised in Table A.2, in the form of depths and ages of major units in the well. The stratigraphic age of each AFTA sample, derived from this information, is summarised in Table A.1, while similar information for VR samples is summarised in Table D.2 (Appendix D).

Any slight errors in the estimated chronometric ages of each sample are not expected to affect the thermal history interpretation of either the AFTA or VR data to any significant degree, because of the profound effects of elevated paleotemperatures after deposition in all samples.



A.3 Present temperatures

In application of any technique involving estimation of paleotemperatures, it is critical to control the present temperature profile, since estimation of maximum paleotemperatures proceeds from trying to determine how much of the observed effect can be explained by the magnitude of present temperatures.

Recorded temperature data are often not reported in sufficient detail to allow rigorous analysis (typically consisting of single BHT measurements at a given depth for a single time since circulation). In order to have a consistent methodology for this well and wells included in our associated regional study, all BHT data are treated in the same way. BHT data obtained from log headers of the **Ontaratue H-34 well** were adjusted by a simplified correction procedure adapted from the literature (Oxburgh and Andrews-Speed, 1981; Andrews-Speed et al., 1984). While no doubt simplistic, this procedure has the advantage of allowing a common approach in all wells, and appears to give roughly consistent results. Furthermore, the thermal history tools applied in this study are calibrated in studies using this same approach, and therefore use of this correction method provides a high degree of internal consistency.

Assuming a surface temperature of 0°C, quoted BHT data were corrected by increasing the difference between the surface temperature and the uncorrected BHT by 20% for uncorrected temperatures below 150°F (66°C), and by 25% above 150°F. Where multiple temperature measurements were available at a given depth, the earliest recorded BHT value is used. (Corrected BHT data derived from the above method are usually in good agreement with uncorrected DST data if these data are available). Where appropriate, a linear geothermal gradient, constrained to the surface temperature, is fitted to the BHT data corrected in this way.

The raw and BHT corrected values and the resulting geothermal gradient derived from the above procedure are listed in Table A.3 and are plotted against depth in Figure A.1. The linear profile has a gradient of **39.0°C/km**. Present-day temperature values used for interpreting the thermal history results in each AFTA and VR sample have been interpolated from this linear gradient.



A.4 Apatite Grain morphologies

The majority of grains analysed from all samples from Ontaratue H-34 were sub-rounded euhedral and euhedral in shape. Some grains showed evidence of surface dissolution but there are no obvious trends that can be related to the stratigraphy or possible provenance differences.

A.5 Apatite compositions

The annealing kinetics of fission tracks in apatite are affected by chemical composition, specifically the Cl content, as explained in more detail in Appendix C. In all samples collected for this study, Cl contents were measured in all apatite grains analysed (i.e. for both fission track age determination and track length measurement), and the measured compositions in individual grains have been employed in interpreting the AFTA data, using methods outlined in Appendix C.

Chlorine contents were measured using a fully automated Jeol JXA-5A electron microprobe equipped with a computer controlled X-Y-Z stage and three computer controlled wavelength dispersive crystal spectrometers, with an accelerating voltage of 15kV and beam current of 25nA. The beam was defocussed to 20 μm diameter to avoid problems associated with apatite decomposition, which occur under a fully focussed 1 μm - 2 μm beam. The X-Y co-ordinates of dated grains within the grain mount were transferred from the Autoscan Fission Track Stage to a file suitable for direct input into the electron microprobe. The identification of each grain was verified optically prior to analysis. Cl count rates from the analysed grains were converted to wt% Cl by reference to those from a Durango apatite standard (Melbourne University Standard APT151), analysed at regular intervals. This approach implicitly takes into account atomic number absorption and fluorescence matrix effects, which are normally calculated explicitly when analysing for all elements. A value of 0.43 wt% Cl was used for the Durango standard, based on repeated measurements on the same single fragment using pure rock salt (NaCl) as a standard for chlorine. This approach gives essentially identical results to Cl contents determined from full compositional measurements, but has the advantage of reducing analytical time by a factor of ten or more.

Cl contents in individual grains are listed in the fission track Age Data Sheets in Appendix B, together with histograms of Cl contents in individual samples and plots of fission track age against Cl content. Table B.3 (Appendix B) contains fission track age and length data grouped into 0.1 wt% Cl intervals on the basis of chlorine contents of the grains from which the data are derived.

The Cretaceous sample (GC813-1) and the Devonian Bear Rock – Canol - Hume Fm sample (GC813-4) analysed from **Ontaratie H-34** have apatites with Cl content between 0 and 0.5wt%, which are similar to the “normal sandstone” type (e.g. quartzose and arkosic sandstones) derived from mixed “granitic basement” terrains, as illustrated in Figure C.4b, Appendix C.

On the other hand apatite in the two Devonian Imperial Formation samples (GC813-2 &-3) have a much broader spread of chlorine, ranging from 0 to 1.7 Wt%, patterns which are typical of the presence of volcanogenic detritus in these samples, as illustrated by the typical histograms shown in Figure C.4c, Appendix C.

Lower limits of detection for chlorine content have been calculated for typical analytical conditions (beam current, counting time, etc.) and are listed in Table A.4. Errors in wt% composition are given as a percentage and quoted at 1σ for chlorine determinations. A generalised summary of errors for various wt% chlorine values is presented in Table A.5.

References

Andrews-Speed, C.P., Oxburgh, E.R. and

**Table A.1: Details of fission track samples and apatite yields - samples from North West Territories (Geotrack Report #813A)**

Sample number	Depth (m)	Sample type	Stratigraphic Subdivision	Stratigraphic age (Ma)	Present temperature *1 (°C)	Raw weight (g)	Washed weight (g)	Apatite yield *2
Ontaratie H-34								
GC813-1	30-259 (100-850')	cuttings	Martin House Fm - Arctic Red Fm	115-98	5	410	220	very poor
GC813-2	351-579 (1150-1900')	cuttings	Imperial	356-346	18	480	260	poor
GC813-3	701-884 (2300-2900')	cuttings	Imperial	356-346	31	360	190	good
GC813-4	887-1103 (2910-3620')	cuttings	Bear Rock Ist - Canol / Hare Indian	373-356	39	660	420	good
GC813-5	1370-1388 (4495-4555')	core	Bear Rock Ist	373-369	54	440	250	none
GC813-6	1554-1844 (5100-6050')	cuttings	Bear Rock Ist (Silurian - Ordovician -)	490-369	66	620	340	none
GC813-7	2347-2469 (7700-8100')	cuttings	Silurian - Ordovician	490-470	94	350	260	none
GC813-8	2890-2895 (9480-9499')	core	Cambrian	540-490	113	-	Not	Processed
GC813-10	3049-3055 (10004-10023')	core	Cambrian	540-490	119	-	Not	Processed
GC813-9	3018-3109 (9900-10200')	cuttings	Cambrian	540-490	119	-	Not	Processed
GC813-11	3231-3241 (10602-10632')	core	Cambrian	540-490	126	-	Not	Processed

*1 See Appendix A for discussion of present temperature data.

*2 Yield based on quantity of mineral suitable for age determination. Excellent: >20 grains; Good: 15-19 grains; Fair: 10-14 grains; Poor: 5-9 grains; Very Poor: <5 grains.



**Table A.2: Summary of stratigraphy - North West Territories
(Geotrack Report #813A)**

KB elevation (mAMSL)	Ground level (m)	Stratigraphic Interval	Depth of Top TVD rKB (m)	Age of Top (Ma)
Ontaratue H-34 141.7	137.2	<i>Unconformity</i>	4.6	0
		Arctic Red Fm	4.6	98
		Martin House Fm	253	110
		<i>Unconformity</i>	259.7	115
		Imperial	259.7	346
		Canol / Hare Indian	886.1	356
		Hume	984.2	363
		Bear Rock Ist	1100.3	369
		<i>Unconformity</i>	1667.9	373
		Silurian - Ordovician	1667.9	470
		Cambrian	2884	490
		TD	4075.2	540

All depths quoted are with respect to KB, except where otherwise stated.



**Table A.3: Summary of temperature data - North West Territories
(Geotrack Report #813A)**

KB elevation (mAMSL)	Ground level (m)	Depth (ft)	BHT (°F)	BHT (°C)	T.S.C (hrs)	Depth (m)	Corrected BHT (°C)	Geothermal gradient (°C/km)
Ontaratue H-34								
141.7	137.2							39.0
		5625	146.0	63.3	-	1714.5	76.0	
		11599	238.0	114.4	-	3535.4	143.1	
		13353	248.0	120.0	-	4070.0	150.0	

Quoted BHT values have been corrected by increasing the difference between surface temperature and measured BHT by 20% for measured temperatures <150°F (<66°C) and by 25% for temperatures >150°F (>66°C). A surface temperature of 0°C has been assumed.

All depths quoted are with respect to KB, except where otherwise stated.

*Measurements not used in calculation of geothermal gradient.

**Table A.4: Lower Limits of Detection for Apatite Analyses (Geotrack Report #813A)**

Element	LLD (95% c.l.)		LLD (99% c.l.)	
	(wt%)	(ppm)	(wt%)	(ppm)
Cl	0.01	126	0.02	182

Table A.5: Per cent errors in chlorine content (Geotrack Report #813A)

Chlorine content (wt%)	Error (%)
0.01	9.3
0.02	8.7
0.05	7.3
0.10	6.1
0.20	4.7
0.50	3.2
1.00	2.3
1.50	1.9
2.00	1.7
2.50	1.5
3.00	1.4

Errors quoted are at 1σ . See Appendix A for more details.

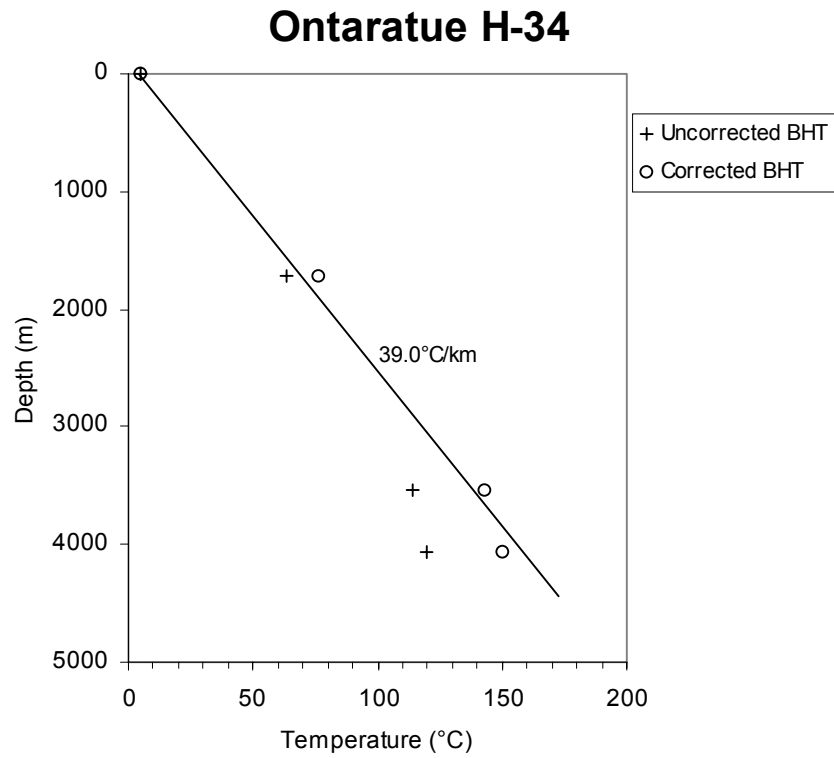


Figure A.1: Present temperature profile calculated for **North West Territories well Ontaratue H-34**. See Table A.3 and Appendix A for more detail.



APPENDIX B

Sample Preparation, Analytical Details and Data Presentation

B.1 Sample Preparation

Core and outcrop samples are crushed in a jaw crusher and then ground to sand grade in a rotary disc mill. Cuttings samples are washed and dried before grinding to sand grade. The ground material is then washed to remove dust, dried and processed by conventional heavy liquid and magnetic separation techniques to recover heavy minerals. Apatite grains are mounted in epoxy resin on glass slides, polished and etched for 20 sec in 5M HNO₃ at 20°C to reveal the fossil fission tracks.

After etching, all mounts are cut down to 1.5 X 1 cm, and cleaned in detergent, alcohol and distilled water. The mounts are then sealed in intimate contact with low-uranium muscovite detectors within heat-shrink plastic film. Each batch of mounts is stacked between two pieces of uranium standard glass, which has been prepared in similar fashion. The stack is then inserted into an aluminium can for irradiation.

After irradiation, the mica detectors are removed from the grain mounts and standard glasses and etched in hydrofluoric acid to reveal the fission tracks produced by induced fission of ²³⁵U in the apatite and standard glass.

B.2 Analytical Details

Fission track ages

Fission track ages are calculated using the standard fission track age equation using the zeta calibration method (equation five of Hurford and Green, 1983), viz:

$$\text{F.T. AGE} = \frac{1}{\lambda_D} \ln \left[1 + \left(\frac{\zeta \lambda_D \rho_s g \rho_D}{\rho_i} \right) \right] \quad \text{B.1}$$

where: λ_D = Total decay constant of ²³⁸U (= 1.55125 x 10⁻¹⁰)
 ζ = Zeta calibration factor
 ρ_s = Spontaneous track density
 ρ_i = Induced track density
 ρ_D = Track density from uranium standard glass
 g = A geometry factor (= 0.5)



Fission track ages are determined by the external detector method or EDM (Gleadow, 1981). The EDM has the advantage of allowing fission track ages to be determined on single grains. In apatite, tracks are counted in 20 grains from each mount wherever possible. In those samples where the desired number is not present, all available grains are counted, the actual number depending on the availability of suitably etched and oriented grains. Only grains oriented with surfaces parallel to the crystallographic c-axis are analysed. Such grains can be identified on the basis of the etching characteristics, as well as from morphological evidence in euhedral grains. The grain mount is scanned sequentially, and the first 20 suitably oriented grains identified are analysed.

Tracks are counted within an eyepiece graticule divided into 100 grid squares. In each grain, the number of spontaneous tracks (N_s) within a certain number of grid squares (N_a) is recorded. The number of induced tracks (N_i) in the corresponding location within the mica external detector is then counted. Spontaneous and induced track densities (ρ_s and ρ_i , respectively) are calculated by dividing the track counts by the total area counted, given by the product of N_a and the area of each grid square (determined by calibration against a ruled stage graticule or diffraction grating). Fission track ages may be calculated by substituting track counts (N_s and N_i) for track densities (ρ_s and ρ_i) in equation B.1, since the areas cancel in the ratio.

Translation between apatite grains in the grain mount and external detector locations corresponding to each grain is carried out using AutoscanTM microcomputer-controlled automatic stages (Smith and Leigh Jones, 1985). This system allows repeated movement between grain and detector, and all grain locations are stored for later reference if required.

Neutron irradiations are carried out in a well-thermalised flux (X-7 facility; Cd ratio for Au ~ 98) in the Australian Atomic Energy Commission's HIFAR research reactor. Total neutron fluence is monitored by counting tracks in mica external detectors attached to two pieces of Corning Glass Works standard glass CN5 (containing ~ 11 ppm Uranium) included in the irradiation canister at each end of the sample stack. In determining track densities in external detectors irradiated adjacent to uranium standard glasses, 25 fields are normally counted in each detector. The total track count (N_D) is divided by the total area counted to obtain the track density (ρ_D). The positions of the counted fields are arranged in a 5 X 5 grid covering the whole area of the detector. For typical track densities of between $\sim 5 \times 10^5$ and 5×10^6 , this is a convenient arrangement to sample across the detector while gathering sufficient counts to achieve a precision of $\sim \pm 2\%$ in a reasonable time.



A small flux gradient is often present in the irradiation facility over the length of the sample package. If a detectable gradient is present, the track count in the external detector adjacent to each standard glass is converted to a track density (ρ_D) and a value for each mount in the stack is calculated by linear interpolation. When no detectable gradient is present, the track counts in the two external detectors are pooled to give a single value of ρ_D , which is used to calculate fission track ages for each sample.

A Zeta calibration factor (ζ) has been determined empirically for each observer by analysing a set of carefully chosen age standards with independently known K-Ar ages, following the methods outlined by Hurford and Green (1983) and Green (1985).

All track counting is carried out using Zeiss^(R) Axioplan microscopes, with an overall linear magnification of 1068 x using dry objectives.

For further details and background information on practical aspects of fission track age determination, see e.g. Fleischer, Price and Walker (1975), Naeser (1979) and Hurford (1986).

Track length measurements

For track length studies in apatite, the full lengths of "confined" fission tracks are measured. Confined tracks are those which do not intersect the polished surface but have been etched from other tracks or fractures, so that the whole length of the track is etched. Confined track lengths are measured using a digitising tablet connected to a microcomputer, superimposed on the microscope field of view via a projection tube. With this system, calibrated against a stage graticule ruled in 2 μm divisions, individual tracks can be measured to a precision of $\pm 0.2 \mu\text{m}$. Tracks are measured only in prismatic grains, characterised by sharp polishing scratches with well-etched tracks of narrow cone angle in all orientations, because of the anisotropy of annealing of fission tracks in apatite (as discussed by Green et al. 1986). Tracks are also measured following the recommendations of Laslett et al. (1982), the most important of which is that only horizontal tracks should be measured. One hundred tracks are measured whenever possible. In apatite samples with low track density, or in those samples in which only a small number of apatite grains are obtained, fewer confined tracks may be available. In such cases, the whole mount is scanned to measure as many confined tracks as possible.

Integrated fission track age and length measurement

Fission track age determination and length measurement are now made in a single pass of the grain mount, in an integrated approach. The location of each grain in which



tracks are either counted or measured is recorded for future reference. Thus, track length measurements can be tied to age determination in individual grains. As a routine procedure we do not measure the age of every grain in which lengths are determined, as this would be much too time-consuming. Likewise we do not only measure ages in grain in which lengths are measured, as this would bias the age data against low track density grains. Nevertheless, the ability to determine the fission track age of certain grains from which length data originate can be a particularly useful aid to interpretation in some cases. Grain location data are not provided in this report, but are available on request.

B.3 Data Presentation

Fission track age data

Data sheets summarising the apatite fission track age data, including full details of fission track age data for individual apatite grains in each sample, together with the primary counting results and statistical data, are given in the following pages. Individual grain fission track ages are calculated from the ratio of spontaneous to induced fission track counts for each grain using equation B.1, and errors in the single grain ages are calculated using Poissonian statistics, as explained in more detail by Galbraith (1981) and Green (1981). All errors are quoted as $\pm 1\sigma$ throughout this report, unless otherwise stated.

The variability of fission track ages between individual apatite grains within each sample can be assessed using a chi-squared (χ^2) statistic (Galbraith, 1981), the results of which are summarised for each sample in the data sheets. If all the grains counted belong to a single age population, the probability of obtaining the observed χ^2 value, for ν degrees of freedom (where ν = number of crystals - 1), is listed in the data sheets as $P(\chi^2)$ or $P(\text{chi squared})$.

A $P(\chi^2)$ value greater than 5% can be taken as evidence that all grains are consistent with a single population of fission track age. In this case, the best estimate of the fission track age of the sample is given by the "pooled age", calculated from the ratio of the total spontaneous and induced track counts in all grains analysed. Errors for the pooled age are calculated using the "conventional" technique outlined by Green (1981), based on the total number of tracks counted for each track density measurement (see also Galbraith, 1981).

A $P(\chi^2)$ value of less than 5% denotes a significant spread of single grain ages, suggesting real differences exist between the fission track ages of individual apatite



grains. A significant spread in grain ages can result either from inheritance of detrital grains from mixed source areas (in sedimentary rocks), or from differential annealing in apatite grains of different composition, within a narrow range of temperature.

Calculation of the pooled age inherently assumes that only a single population of ages is present, and is thus not appropriate to samples containing a significant spread of fission track ages. In such cases Galbraith, has recently devised a means of estimating the modal age of a distribution of single grain fission track ages which is referred to as the "central age". Calculation of the central age assumes that all single grain ages belong to a Normal distribution of ages, with a standard deviation (σ) known as the "age dispersion". An iterative algorithm (Galbraith and Laslett, 1993) is used to provide estimates of the central age with its associated error, and the age dispersion, which are all quoted in the data sheets. Note that this treatment replaces use of the "mean age", which has been used in the past for those samples in which $P(\chi^2) < 5\%$. For samples in which $P(\chi^2) > 5\%$, the central age and the pooled age should be equal, and the age dispersion should be less than $\sim 10\%$.

Table B.1 summarises the fission track age data in apatite from each sample analysed.

Construction of radial plots of single grain age data

Single grain age data are best represented in the form of radial plot diagrams (Galbraith, 1988, 1990). As illustrated in Figure B.1, these plots display the variation of individual grain ages in a plot of y against x , where:

$$y = (z_j - z_0) / \sigma_j \quad x = 1/\sigma_j \quad \text{B.2}$$

and;

z_j	=	Fission track age of grain j
z_0	=	A reference age
σ_j	=	Error in age for grain j

In this plot, all points on a straight line from the origin define a single value of fission track age, and, at any point, the value of x is a measure of the precision of each individual grain age. Therefore, precise individual grain ages fall to the right of the plot (small error, high x), which is useful, for example, in enabling precise, young grains to be identified. The age scale is shown radially around the perimeter of the plot (in Ma). If all grains belong to a single age population, all data should scatter between $y = +2$ and $y = -2$, equivalent to scatter within $\pm 2\sigma$. Scatter outside these boundaries shows a significant spread of individual grain ages, as also reflected in the values of $P(\chi^2)$ and age dispersion.



In detail, rather than using the fission track age for each grain as in equation B.2, we use:

$$z_j = \frac{N_{sj}}{N_{ij}} \quad \sigma_j = \{1/N_{sj} + 1/N_{ij}\} \quad \text{B.3}$$

as we are interested in displaying the scatter within the data from each sample in comparison with that allowed by the Poissonian uncertainty in track counts, without the additional terms which are involved in determination of the fission track age (ρ_D , ζ , etc).

Zero ages cannot be displayed in such a plot. This can be achieved using a modified plot, (Galbraith, 1990) with:

$$z_j = \arcsin \sqrt{\left\{ \frac{N_{sj} + 3/8}{N_{sj} + N_{ij} + 3/4} \right\}} \quad \sigma_j = \frac{1}{2} \sqrt{\left\{ \frac{1}{N_{sj} + N_{ij}} \right\}} \quad \text{B.4}$$

Note that the numerical terms in the equation for z_j are standard terms, introduced for statistical reasons. Using this arc-sin transformation, zero ages plot on a diagonal line which slopes from upper left to lower right. Note that this line does not go through the origin. Figure B.2 illustrates this difference between conventional and arc-sin radial plots, and also provides a simple guide to the structure of radial plots.

Use of arc-sin radial plots is particularly useful in assessing the relative importance of zero ages. For instance, grains with $N_s = 0$, $N_i = 1$ are compatible with ages up to ~900 Ma (at the 95% confidence level), whereas grains with $N_s = 0$, $N_i = 50$ are only compatible with ages up to ~14 Ma. The two data would readily be distinguishable on the radial plot as the 0,50 datum would plot well to the right (high x) compared to the 0,1 datum.

In this report the value of z corresponding to the stratigraphic age of each sample (or the midpoint of the range where appropriate) is adopted as the reference value, z_0 . This allows rapid assessment of the fission track age of individual grains in relation to the stratigraphic age, which is a key component in the interpretation of AFTA data, as explained in more detail in Appendix C.

Note that the x axis of the radial plot is normally not labelled, as this would obscure the age scale around the plot. In general labelling is not considered necessary, as we are concerned only with relative variation within the data, rather than absolute values of precision.



Radial plots of the single grain age data in apatite from each sample analysed in this report are shown on the fission track age data summary sheets at the end of this Appendix. Use of radial plots to provide thermal history information is explained in Appendix C and Figure C.7.

Track length data

Distributions of confined track lengths in apatite from each sample are shown as simple histograms on the fission track age data summary sheets at the end of this Appendix. For every track length measurement, the length is recorded to the nearest 0.1 μm , but the measurements have been grouped into 1 μm intervals for construction of these histograms. Each distribution has been normalised to 100 tracks for each sample to facilitate comparison. A summary of the length distribution in each sample is presented in Table B.2, which also shows the mean track length in each sample and its associated error, the standard deviation of each distribution and the number of tracks (N) measured in each sample. The angle which each confined track makes with the crystallographic c-axis is also routinely recorded, as is the width of each fracture within which tracks are revealed. These data are not provided in this report, but can be supplied on request.

Breakdown of data into compositional groups

In Table B.3, AFTA data are grouped into compositional intervals of 0.1 wt% Cl width. Parameters for each interval represent the data from all grains with Cl contents within each interval. Also shown are the parameters for each compositional interval predicted from the Default Thermal History (see Section 2.1). These data form the basis of interpretation of the AFTA data, which takes full account of the influence of Cl content on annealing kinetics, as described in Appendix C. Distributions of Cl contents in all apatites analysed from each sample (i.e. for both age and length determinations) are shown on the fission track age data summary sheets at the end of this Appendix.

Plots of fission track age against Cl content for individual apatite grains

Fission track ages of single apatite grains within individual samples are plotted against the Cl content of each grain on the fission track age data summary sheets at the end of this Appendix. These plots are useful in assessing the degree of annealing, as expressed by the fission track age data. For example, if grains with a range of Cl contents from zero to some upper limit all give similar fission track ages which are significantly less than the stratigraphic age, then grains with these compositions must have been totally annealed. Alternatively, if fission track age falls rapidly with decreasing Cl content, the sample displays a high degree of partial annealing.



B.4 A note on terminology

Note that throughout this report, the term "fission track age" is understood to denote the parameter calculated from the fission track age equation, using the observed spontaneous and induced track counts (either pooled for all grains or for individual grains). The resulting number (with units of Ma) should not be taken as possessing any significance in terms of events taking place at the time indicated by the measured fission track age, but should rather be regarded as a measure of the integrated thermal history of the sample, and should be interpreted in that light using the principles outlined in Appendix C. Use of the term "apparent age" is not considered to be useful in this regard, as almost every fission track age should be regarded as an apparent age, in the classic sense, and repeated use becomes cumbersome.



References

- Fleischer, R. L., Price, P. B., and Walker, R. M. (1975) Nuclear tracks in solids, University of California Press, Berkeley.
- Galbraith, R. F. (1981) On statistical models for fission-track counts. *Mathematical Geology*, 13, 471-488.
- Galbraith, R. F. (1988) Graphical display of estimates having differing standard errors. *Technometrics*, 30, 271-281.
- Galbraith, R. F. (1990) The radial plot: graphical assessment of spread in ages. *Nuclear Tracks*, 17, 207-214.
- Galbraith R.F. & Laslett G.M. (1993) Statistical methods for mixed fission track ages. *Nuclear Tracks* 21, 459-470.
- Gleadow, A. J. W. (1981) Fission track dating methods; what are the real alternatives? *Nuclear Tracks*, 5, 3-14.
- Green, P. F. (1981) A new look at statistics in fission track dating. *Nuclear Tracks* 5, 77-86.
- Green, P. F. (1985) A comparison of zeta calibration baselines in zircon, sphene and apatite. *Chem. Geol. (Isot. Geol. Sect.)*, 58, 1-22.
- Green, P. F., Duddy, I. R., Gleadow, A. J. W., Tingate, P. R. and Laslett, G. M. (1986) Thermal annealing of fission tracks in apatite 1. A qualitative description. *Chem. Geol. (Isot. Geosci. Sect.)*, 59, 237-253.
- Hurford, A. J. (1986) Application of the fission track dating method to young sediments: Principles, methodology and Examples. In: Hurford, A. J., Jäger, E. and Ten Cate, J. A. M. (eds), Dating young sediments, CCOP Technical Publication 16, CCOP Technical Secretariat, Bangkok, Thailand.
- Hurford, A. J. and Green, P. F. (1982) A user's guide to fission track dating calibration. *Earth. Planet. Sci. Lett.* 59, 343-354.
- Hurford, A. J. and Green, P. F. (1983) The zeta age calibration of fission track dating. *Isotope Geoscience* 1, 285-317.
- Laslett, G. M., Kendall, W. S., Gleadow, A. J. W. and Duddy, I. R. (1982) Bias in measurement of fission track length distributions. *Nuclear Tracks*, 6, 79-85.
- Naeser, C. W. (1979) Fission track dating and geologic annealing of fission tracks. In: Jäger, E. and Hunziker, J. C. (eds), Lectures in Isotope Geology, Springer Verlag, Berlin.
- Smith, M. J. and Leigh-Jones, P. (1985) An automated microscope scanning stage for fission-track dating. *Nuclear Tracks*, 10, 395-400.



Table B.1: Apatite fission track analytical results - samples from North West Territories (Geotrack Report #813A)

Sample number	Number of grains	ρ_D (N _D) x10 ⁶ /cm ²	ρ_s (N _s) x10 ⁶ /cm ²	ρ_i (N _i) x10 ⁶ /cm ²	Uranium content (ppm)	P(χ^2) (%)	Age dispersion (%)	Fission track age (Ma)
Ontaratue H-34								
GC813-1	4	1.312 (2017)	1.169 (78)	1.034 (69)	9	<1	86	285.0 ± 47.8 174.5 ± 85.0*
GC813-2	8	1.307 (2017)	0.329 (35)	1.476 (157)	13	7	57	57.0 ± 10.8
GC813-3	17	1.303 (2017)	0.341 (81)	2.056 (489)	18	31	25	42.3 ± 5.2
GC813-4	15	1.298 (2017)	0.089 (18)	1.589 (320)	14	2	83	14.3 ± 3.5 14.7 ± 4.9*

ρ_s = spontaneous track density; ρ_i = induced track density; ρ_D = track density in glass standard external detector. Brackets show number of tracks counted. ρ_D and ρ_i measured in mica external detectors; ρ_s measured in internal surfaces.

*Central age, used where sample contains a significant spread of single grain ages ($P(\chi^2) < 5\%$). Errors quoted at 1σ .

Ages calculated using dosimeter glass CN5, with a zeta of 392.9 ± 7.4 (Analyst: M. Moore) for samples; 1 - 4

**Table B.2: Length distribution summary data - samples from North West Territories (Geotrack Report #813A)**

Sample number	Mean track length (μm)	Standard deviation (μm)	Number of tracks (N)	Number of tracks in Length Intervals (μm)																			
				1	2	3	4	5	6	7	8	9	10	11	12	13	14	15	16	17	18	19	20
Ontaratue H-34																							
GC813-1	No confined	tracks	-	-	-	-	-	-	-	-	-	-	-	-	-	-	-	-	-	-	-	-	-
GC813-2	No confined	tracks	-	-	-	-	-	-	-	-	-	-	-	-	-	-	-	-	-	-	-	-	-
GC813-3	12.94 ± 0.67	1.78	7	-	-	-	-	-	-	-	-	-	-	1	1	2	1	-	2	-	-	-	-
GC813-4	12.85	-	1	-	-	-	-	-	-	-	-	-	-	-	-	1	-	-	-	-	-	-	-

Track length measurements by: M. Moore for samples; 1 - 4



Table B.3: AFTA Data in Compositional Groups - (Geotrack Report #813A)

Cl	Default fission track age* (Ma)					Measured fission track age (Ma)					Error in age (Ma)	P (χ^2)	Number of grains	Default fission track length* (μm)	Mean track length (μm)	Error in length (μm)	Std deviation (μm)	Number of lengths	Number of grains	Number of tracks in length interval (μm)																			
	1	2	3	4	5	6	7	8	9	10										11	12	13	14	15	16	17	18	19	20										
Ontaratuue H-34																																							
813-1† 0.0-0.1 0.1-0.2 0.2-0.3	91.2	174.5	84.8	0.0	4	15.0	0.0	0.0	0.0	0.0	0.0	0.0	0	0	0	0	0	0	0	0	0	0	0	0	0	0	0	0	0	0	0	0	0	0					
	91.0	271.7	104.8	11.0	2	15.0	0.0	0.0	0.0	0.0	0.0	0.0	0	0	0	0	0	0	0	0	0	0	0	0	0	0	0	0	0	0	0	0	0	0					
	91.3	30.3	22.6	100.0	1	15.0	0.0	0.0	0.0	0.0	0.0	0.0	0	0	0	0	0	0	0	0	0	0	0	0	0	0	0	0	0	0	0	0	0	0					
	91.4	397.2	81.7	100.0	1	15.0	0.0	0.0	0.0	0.0	0.0	0.0	0	0	0	0	0	0	0	0	0	0	0	0	0	0	0	0	0	0	0	0	0	0					
813-2† 0.0-0.1 0.1-0.2 0.2-0.3 0.3-0.4 0.4-0.5 0.5-0.6 0.6-0.7 0.7-0.8 0.8-0.9 0.9-1.0	345.3	57.0	10.7	7.0	8	14.5	0.0	0.0	0.0	0.0	0.0	0.0	0	0	0	0	0	0	0	0	0	0	0	0	0	0	0	0	0	0	0	0	0	0					
	342.5	30.1	11.3	22.0	2	14.5	0.0	0.0	0.0	0.0	0.0	0.0	0	0	0	0	0	0	0	0	0	0	0	0	0	0	0	0	0	0	0	0	0	0					
	-	-	-	-	-	-	-	-	-	-	-	-	0	0	0	0	0	0	0	0	0	0	0	0	0	0	0	0	0	0	0	0	0						
	344.6	0.0	0.0	110.0	1	14.6	0.0	0.0	0.0	0.0	0.0	0.0	0	0	0	0	0	0	0	0	0	0	0	0	0	0	0	0	0	0	0	0	0	0					
	345.6	90.6	20.4	52.0	3	14.6	0.0	0.0	0.0	0.0	0.0	0.0	0	0	0	0	0	0	0	0	0	0	0	0	0	0	0	0	0	0	0	0	0	0					
	346.5	0.0	0.0	110.0	1	14.6	0.0	0.0	0.0	0.0	0.0	0.0	0	0	0	0	0	0	0	0	0	0	0	0	0	0	0	0	0	0	0	0	0	0					
	-	-	-	-	-	-	-	-	-	-	-	-	0	0	0	0	0	0	0	0	0	0	0	0	0	0	0	0	0	0	0	0	0						
	-	-	-	-	-	-	-	-	-	-	-	-	0	0	0	0	0	0	0	0	0	0	0	0	0	0	0	0	0	0	0	0	0	0					
	-	-	-	-	-	-	-	-	-	-	-	-	0	0	0	0	0	0	0	0	0	0	0	0	0	0	0	0	0	0	0	0	0	0					
	-	-	-	-	-	-	-	-	-	-	-	-	0	0	0	0	0	0	0	0	0	0	0	0	0	0	0	0	0	0	0	0	0	0					
-	-	-	-	-	-	-	-	-	-	-	-	0	0	0	0	0	0	0	0	0	0	0	0	0	0	0	0	0	0	0	0	0	0						
-	-	-	-	-	-	-	-	-	-	-	-	0	0	0	0	0	0	0	0	0	0	0	0	0	0	0	0	0	0	0	0	0	0						
-	-	-	-	-	-	-	-	-	-	-	-	0	0	0	0	0	0	0	0	0	0	0	0	0	0	0	0	0	0	0	0	0	0						
-	-	-	-	-	-	-	-	-	-	-	-	0	0	0	0	0	0	0	0	0	0	0	0	0	0	0	0	0	0	0	0	0	0						
-	-	-	-	-	-	-	-	-	-	-	-	0	0	0	0	0	0	0	0	0	0	0	0	0	0	0	0	0	0	0	0	0	0						
-	-	-	-	-	-	-	-	-	-	-	-	0	0	0	0	0	0	0	0	0	0	0	0	0	0	0	0	0	0	0	0	0	0						
-	-	-	-	-	-	-	-	-	-	-	-	0	0	0	0	0	0	0	0	0	0	0	0	0	0	0	0	0	0	0	0	0	0						
-	-	-	-	-	-	-	-	-	-	-	-	0	0	0	0	0	0	0	0	0	0	0	0	0	0	0	0	0	0	0	0	0	0						
-	-	-	-	-	-	-	-	-	-	-	-	0	0	0	0	0	0	0	0	0	0	0	0	0	0	0	0	0	0	0	0	0	0						
-	-	-	-	-	-	-	-	-	-	-	-	0	0	0	0	0	0	0	0	0	0	0	0	0	0	0	0	0	0	0	0	0	0						
-	-	-	-	-	-	-	-	-	-	-	-	0	0	0	0	0	0	0	0	0	0	0	0	0	0	0	0	0	0	0	0	0	0						
-	-	-	-	-	-	-	-	-	-	-	-	0	0	0	0	0	0	0	0	0	0	0	0	0	0	0	0	0	0	0	0	0	0						
-	-	-	-	-	-	-	-	-	-	-	-	0	0	0	0	0	0	0	0	0	0	0	0	0	0	0	0	0	0	0	0	0	0						
-	-	-	-	-	-	-	-	-	-	-	-	0	0	0	0	0	0	0	0	0	0	0	0	0	0	0	0	0	0	0	0	0	0						
-	-	-	-	-	-	-	-	-	-	-	-	0	0	0	0	0	0	0	0	0	0	0	0	0	0	0	0	0	0	0	0	0	0						
-	-	-	-	-	-	-	-	-	-	-	-	0	0	0	0	0	0	0	0	0	0	0	0	0	0	0	0	0	0	0	0	0	0						
-	-	-	-	-	-	-	-	-	-	-	-	0	0	0	0	0	0	0	0	0	0	0	0	0	0	0	0	0	0	0	0	0	0						
-	-	-	-	-	-	-	-	-	-	-	-	0	0	0	0	0	0	0	0	0	0	0	0	0	0	0	0	0	0	0	0	0	0						
-	-	-	-	-	-	-	-	-	-	-	-	0	0	0	0	0	0	0	0	0	0	0	0	0	0	0	0	0	0	0	0	0	0						
-	-	-	-	-	-	-	-	-	-	-	-	0	0	0	0	0	0	0	0	0	0	0	0	0	0	0	0												

* Fission Track Age and Mean Track Length predicted from the Default Thermal History (i.e. if the sample has not been hotter in the past)
† Combined data for all compositional groups



Table B.3: Continued - (Geotrack Report #813A)

Cl	Default fission track age*					Measured fission track age					P (χ2)	Number of grains	Default fission track length*	Mean track length (μm)	Error in length (μm)	Std deviation (μm)	Number of lengths	Number of grains	Number of tracks in length interval																																																																																																																																																																																																																																																																																																																																																																																																																																																																																																																																																																																																																																																																																																																																																																																																																																																																																																																																																																																																				
	(Ma)	(Ma)	(Ma)	Error in age (Ma)	(Ma)	(Ma)	(Ma)	(μm)	(μm)	(μm)									(μm)	(μm)	(μm)	(μm)	(μm)	(μm)	(μm)	(μm)	(μm)	(μm)	(μm)	(μm)	(μm)	(μm)	(μm)	(μm)	(μm)	(μm)	(μm)	(μm)	(μm)	(μm)	(μm)	(μm)	(μm)	(μm)	(μm)	(μm)	(μm)	(μm)	(μm)	(μm)	(μm)	(μm)	(μm)	(μm)	(μm)	(μm)	(μm)	(μm)	(μm)	(μm)	(μm)	(μm)	(μm)	(μm)	(μm)	(μm)	(μm)	(μm)	(μm)	(μm)	(μm)	(μm)	(μm)	(μm)	(μm)	(μm)	(μm)	(μm)	(μm)	(μm)	(μm)	(μm)	(μm)	(μm)	(μm)	(μm)	(μm)	(μm)	(μm)	(μm)	(μm)	(μm)	(μm)	(μm)	(μm)	(μm)	(μm)	(μm)	(μm)	(μm)	(μm)	(μm)	(μm)	(μm)	(μm)	(μm)	(μm)	(μm)	(μm)	(μm)	(μm)	(μm)	(μm)	(μm)	(μm)	(μm)	(μm)	(μm)	(μm)	(μm)	(μm)	(μm)	(μm)	(μm)	(μm)	(μm)	(μm)	(μm)	(μm)	(μm)	(μm)	(μm)	(μm)	(μm)	(μm)	(μm)	(μm)	(μm)	(μm)	(μm)	(μm)	(μm)	(μm)	(μm)	(μm)	(μm)	(μm)	(μm)	(μm)	(μm)	(μm)	(μm)	(μm)	(μm)	(μm)	(μm)	(μm)	(μm)	(μm)	(μm)	(μm)	(μm)	(μm)	(μm)	(μm)	(μm)	(μm)	(μm)	(μm)	(μm)	(μm)	(μm)	(μm)	(μm)	(μm)	(μm)	(μm)	(μm)	(μm)	(μm)	(μm)	(μm)	(μm)	(μm)	(μm)	(μm)	(μm)	(μm)	(μm)	(μm)	(μm)	(μm)	(μm)	(μm)	(μm)	(μm)	(μm)	(μm)	(μm)	(μm)	(μm)	(μm)	(μm)	(μm)	(μm)	(μm)	(μm)	(μm)	(μm)	(μm)	(μm)	(μm)	(μm)	(μm)	(μm)	(μm)	(μm)	(μm)	(μm)	(μm)	(μm)	(μm)	(μm)	(μm)	(μm)	(μm)	(μm)	(μm)	(μm)	(μm)	(μm)	(μm)	(μm)	(μm)	(μm)	(μm)	(μm)	(μm)	(μm)	(μm)	(μm)	(μm)	(μm)	(μm)	(μm)	(μm)	(μm)	(μm)	(μm)	(μm)	(μm)	(μm)	(μm)	(μm)	(μm)	(μm)	(μm)	(μm)	(μm)	(μm)	(μm)	(μm)	(μm)	(μm)	(μm)	(μm)	(μm)	(μm)	(μm)	(μm)	(μm)	(μm)	(μm)	(μm)	(μm)	(μm)	(μm)	(μm)	(μm)	(μm)	(μm)	(μm)	(μm)	(μm)	(μm)	(μm)	(μm)	(μm)	(μm)	(μm)	(μm)	(μm)	(μm)	(μm)	(μm)	(μm)	(μm)	(μm)	(μm)	(μm)	(μm)	(μm)	(μm)	(μm)	(μm)	(μm)	(μm)	(μm)	(μm)	(μm)	(μm)	(μm)	(μm)	(μm)	(μm)	(μm)	(μm)	(μm)	(μm)	(μm)	(μm)	(μm)	(μm)	(μm)	(μm)	(μm)	(μm)	(μm)	(μm)	(μm)	(μm)	(μm)	(μm)	(μm)	(μm)	(μm)	(μm)	(μm)	(μm)	(μm)	(μm)	(μm)	(μm)	(μm)	(μm)	(μm)	(μm)	(μm)	(μm)	(μm)	(μm)	(μm)	(μm)	(μm)	(μm)	(μm)	(μm)	(μm)	(μm)	(μm)	(μm)	(μm)	(μm)	(μm)	(μm)	(μm)	(μm)	(μm)	(μm)	(μm)	(μm)	(μm)	(μm)	(μm)	(μm)	(μm)	(μm)	(μm)	(μm)	(μm)	(μm)	(μm)	(μm)	(μm)	(μm)	(μm)	(μm)	(μm)	(μm)	(μm)	(μm)	(μm)	(μm)	(μm)	(μm)	(μm)	(μm)	(μm)	(μm)	(μm)	(μm)	(μm)	(μm)	(μm)	(μm)	(μm)	(μm)	(μm)	(μm)	(μm)	(μm)	(μm)	(μm)	(μm)	(μm)	(μm)	(μm)	(μm)	(μm)	(μm)	(μm)	(μm)	(μm)	(μm)	(μm)	(μm)	(μm)	(μm)	(μm)	(μm)	(μm)	(μm)	(μm)	(μm)	(μm)	(μm)	(μm)	(μm)	(μm)	(μm)	(μm)	(μm)	(μm)	(μm)	(μm)	(μm)	(μm)	(μm)	(μm)	(μm)	(μm)	(μm)	(μm)	(μm)	(μm)	(μm)	(μm)	(μm)	(μm)	(μm)	(μm)	(μm)	(μm)	(μm)	(μm)	(μm)	(μm)	(μm)	(μm)	(μm)	(μm)	(μm)	(μm)	(μm)	(μm)	(μm)	(μm)	(μm)	(μm)	(μm)	(μm)	(μm)	(μm)	(μm)	(μm)	(μm)	(μm)	(μm)	(μm)	(μm)	(μm)	(μm)	(μm)	(μm)	(μm)	(μm)	(μm)	(μm)	(μm)	(μm)	(μm)	(μm)	(μm)	(μm)	(μm)	(μm)	(μm)	(μm)	(μm)	(μm)	(μm)	(μm)	(μm)	(μm)	(μm)	(μm)	(μm)	(μm)	(μm)	(μm)	(μm)	(μm)	(μm)	(μm)	(μm)	(μm)	(μm)	(μm)	(μm)	(μm)	(μm)	(μm)	(μm)	(μm)	(μm)	(μm)	(μm)	(μm)	(μm)	(μm)	(μm)	(μm)	(μm)	(μm)	(μm)	(μm)	(μm)	(μm)	(μm)	(μm)	(μm)	(μm)	(μm)	(μm)	(μm)	(μm)	(μm)	(μm)	(μm)	(μm)	(μm)	(μm)	(μm)	(μm)	(μm)	(μm)	(μm)	(μm)	(μm)	(μm)	(μm)	(μm)	(μm)	(μm)	(μm)	(μm)	(μm)	(μm)	(μm)	(μm)	(μm)	(μm)	(μm)	(μm)	(μm)	(μm)	(μm)	(μm)	(μm)	(μm)	(μm)	(μm)	(μm)	(μm)	(μm)	(μm)	(μm)	(μm)	(μm)	(μm)	(μm)	(μm)	(μm)	(μm)	(μm)	(μm)	(μm)	(μm)	(μm)	(μm)	(μm)	(μm)	(μm)	(μm)	(μm)	(μm)	(μm)	(μm)	(μm)	(μm)	(μm)	(μm)	(μm)	(μm)	(μm)	(μm)	(μm)	(μm)	(μm)	(μm)	(μm)	(μm)	(μm)	(μm)	(μm)	(μm)	(μm)	(μm)	(μm)	(μm)	(μm)	(μm)	(μm)	(μm)	(μm)	(μm)	(μm)	(μm)	(μm)	(μm)	(μm)	(μm)	(μm)	(μm)	(μm)	(μm)	(μm)	(μm)	(μm)	(μm)	(μm)	(μm)	(μm)	(μm)	(μm)	(μm)	(μm)	(μm)	(μm)	(μm)	(μm)	(μm)	(μm)	(μm)	(μm)	(μm)	(μm)	(μm)	(μm)	(μm)	(μm)	(μm)	(μm)	(μm)	(μm)	(μm)	(μm)	(μm)	(μm)	(μm)	(μm)	(μm)	(μm)	(μm)	(μm)	(μm)	(μm)	(μm)	(μm)	(μm)	(μm)	(μm)	(μm)	(μm)	(μm)	(μm)	(μm)	(μm)	(μm)	(μm)	(μm)	(μm)	(μm)	(μm)	(μm)	(μm)	(μm)	(μm)	(μm)	(μm)	(μm)	(μm)	(μm)	(μm)	(μm)	(μm)	(μm)	(μm)	(μm)	(μm)	(μm)	(μm)	(μm)	(μm)	(μm)	(μm)	(μm)	(μm)	(μm)	(μm)	(μm)	(μm)	(μm)	(μm)	(μm)	(μm)	(μm)	(μm)	(μm)	(μm)	(μm)	(μm)	(μm)	(μm)	(μm)	(μm)	(μm)	(μm)	(μm)	(μm)	(μm)	(μm)	(μm)	(μm)	(μm)	(μm)	(μm)	(μm)	(μm)	(μm)	(μm)	(μm)	(μm)	(μm)	(μm)	(μm)	(μm)	(μm)	(μm)	(μm)	(μm)	(μm)	(μm)	(μm)	(μm)	(μm)	(μm)	(μm)	(μm)	(μm)	(μm)	(μm)	(μm)	(μm)	(μm)	(μm)	(μm)	(μm)	(μm)	(μm)	(μm)	(μm)	(μm)	(μm)	(μm)	(μm)	(μm)	(μm)	(μm)	(μm)	(μm)	(μm)	(μm)	(μm)	(μm)	(μm)	(μm)	(μm)	(μm)	(μm)	(μm)	(μm)	(μm)	(μm)	(μm)	(μm)	(μm)	(μm)	(μm)	(μm)	(μm)	(μm)	(μm)	(μm)	(μm)	(μm)	(μm)	(μm)	(μm)	(μm)	(μm)	(μm)	(μm)	(μm)	(μm)	(μm)	(μm)	(μm)	(μm)	(μm)	(μm)	(μm)	(μm)	(μm)	(μm)	(μm)	(μm)	(μm)	(μm)	(μm)	(μm)	(μm)	(μm)	(μm)	(μm)	(μm)	(μm)	(μm)	(μm)	(μm)	(μm)	(μm)	(μm)	(μm)	(μm)	(μm)	(μm)	(μm)	(μm)	(μm)	(μm)	(μm)	(μm)	(μm)	(μm)	(μm)	(μm)	(μm)	(μm)	(μm)	(μm)	(μm)	(μm)	(μm)	(μm)	(μm)	(μm)	(μm)	(μm)	(μm)	(μm)	(μm)	(μm)	(μm)	(μm)	(μm)	(μm)	(μm)	(μm)	(μm)	(μm)	(μm)	(μm)	(μm)	(μm)	(μm)	(μm)	(μm)	(μm)	(μm)	(μm)	(μm)	(μm)	(μm)	(μm)	(μm)	(μm)	(μm)	(μm)	(μm)	(μm)	(μm)	(μm)	(μm)	(μm)	(μm)	(μm)	(μm)	(μm)	(μm)	(μm)	(μm)	(μm)	(μm)	(μm)	(μm)	(μm)	(μm)	(μm)	(μm)	(μm)	(μm)	(μm)	(μm)	(μm)	(μm)	(μm)	(μm)	(μm)	(μm)	(μm)	(μm)	(μm)	(μm)	(μm)	(μm)	(μm)	(μm)	(μm)	(μm)	(μm)	(μm)	(μm)	(μm)	(μm)	(μm)	(μm)	(μm)	(μm)	(μm)	(μm)	(μm)	(μm)

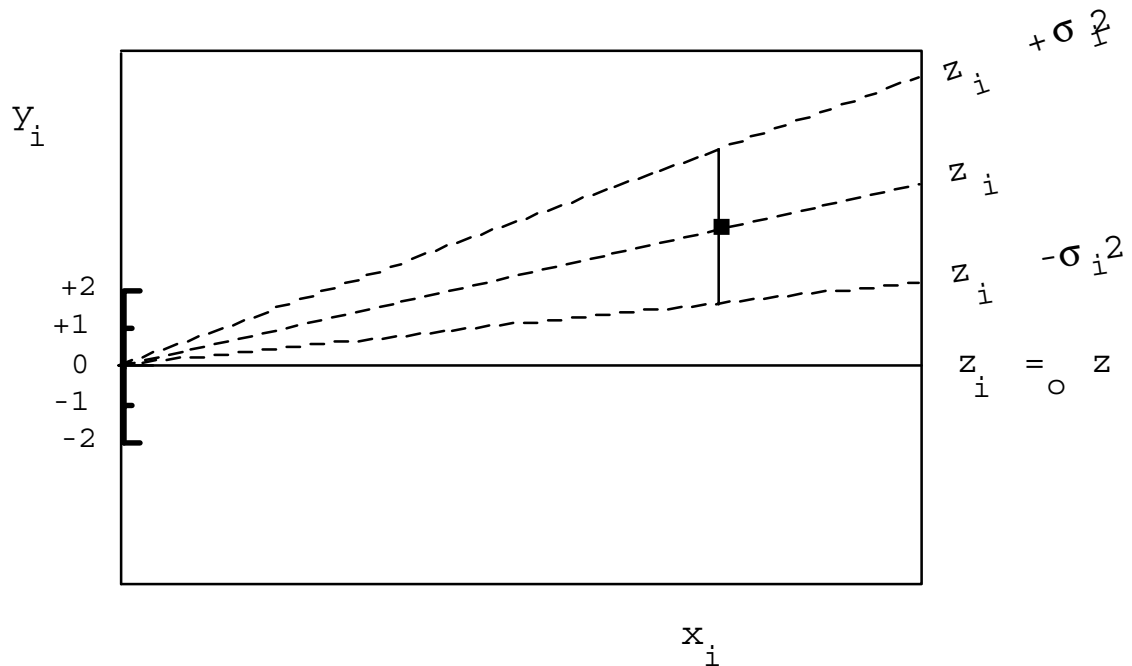
* Fission Track Age and Mean Track Length predicted from the Default Thermal History (i.e. if the sample has not been hotter in the past)

† Combined data for all compositional groups



Estimates	z_i
Standard errors	σ_i
Reference value	z_o
Standardised estimates	$y_i = (z_i - z_o) / \sigma_i$
Precision	$x_i = 1 / \sigma_i$

PLOT y_i against x_i



Slope of line from origin through data point

$$= y_i / x_i$$

$$= \{(z_i - z_o) / \sigma_i\} / \{1 / \sigma_i\}$$

$$= z_i - z_o$$

Key Points:

Radial lines emanating from the origin correspond to fixed values of z

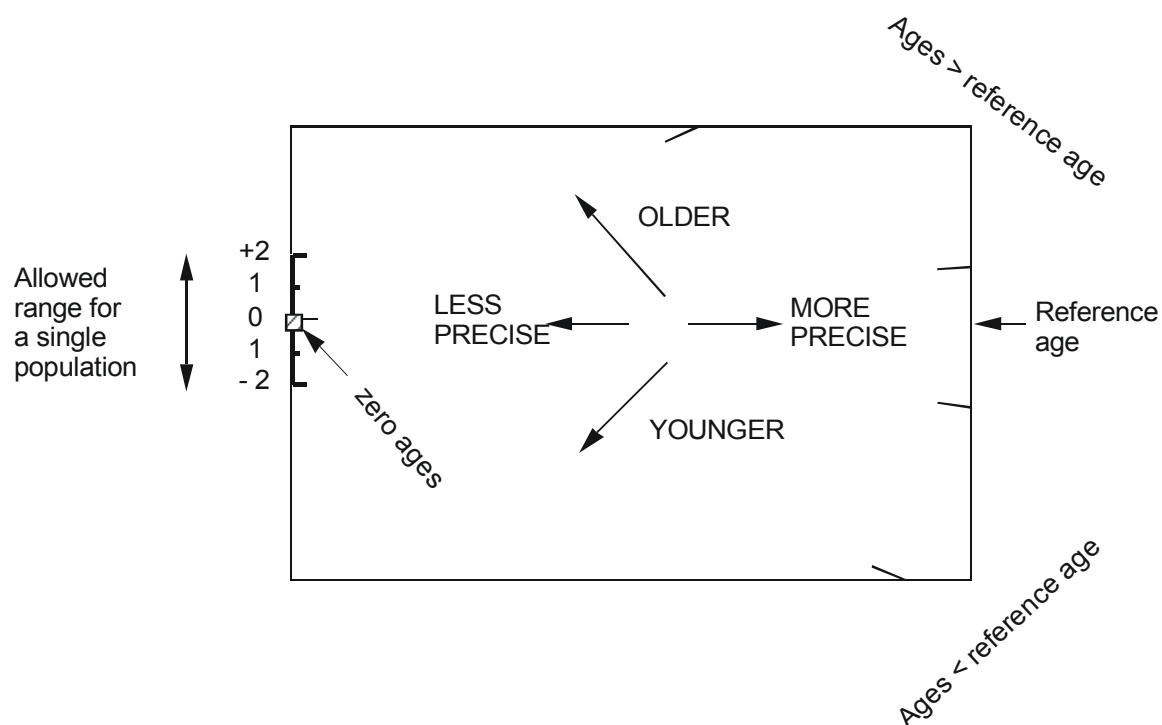
Data points with higher values of x_i have greater precision.

Error bars on all points are the same size in this plot.

Figure B.1 Basic construction of a radial plot. In AFTA, the estimates z_i correspond to the fission track age values for individual apatite grains. Any convenient value of age can be chosen as the reference value corresponding to the horizontal in the radial plot. Radial lines emanating from the origin with positive slopes correspond to fission track ages greater than the reference value. Lines with negative slopes correspond to fission track ages less than the reference value.



Normal radial plot (equations B.2 and B.3)



Arc-sin radial plot (equations B.2 and B.4)

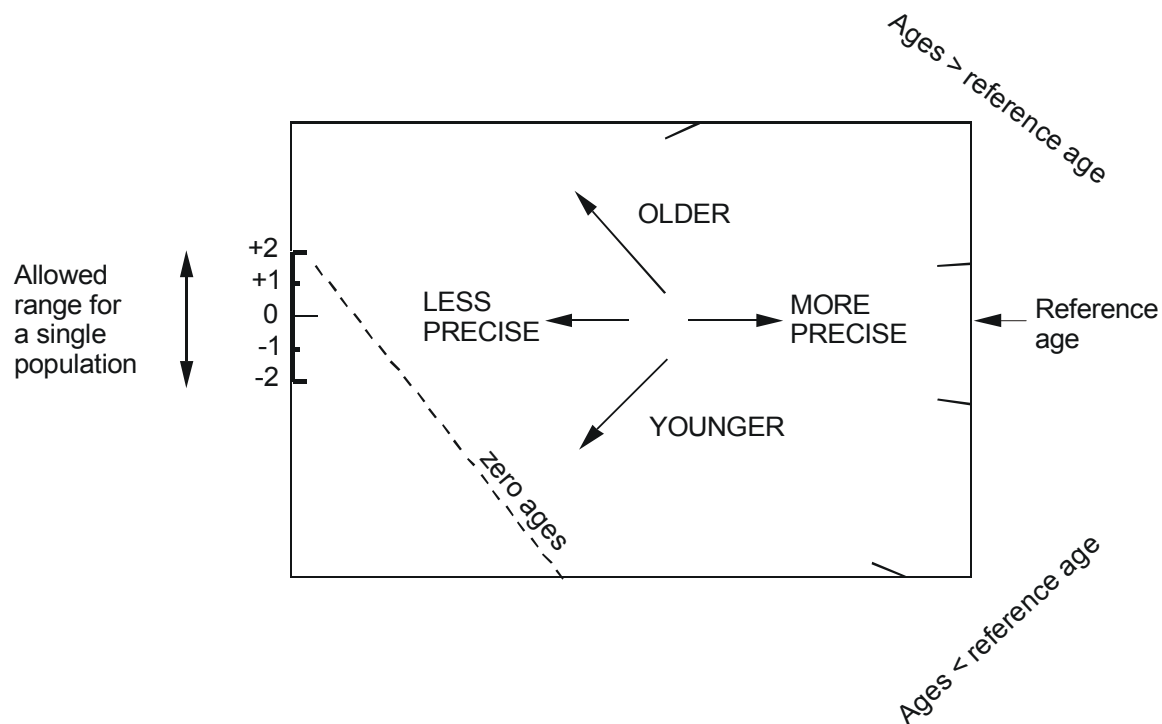


Figure B.2 Simplified structure of Normal and Arc-sin radial plots.



Fission Track Age Data Sheets - Glossary

N_s	=	Number of spontaneous tracks in N_a grid squares
N_i	=	Number of induced tracks in N_a grid squares
N_a	=	Number of grid squares counted in each grain
RATIO	=	N_s/N_i
U (ppm)	=	Uranium content of each grain (= U content of standard glass * ρ_i/ρ_D)
Cl (wt%)	=	Weight percent chlorine content of each grain
ρ_s	=	Spontaneous track density (ρ_s) = $N_s/(N_a \cdot \text{area of basic unit})$
ρ_i	=	Induced track density (ρ_i) = $N_i/(N_a \cdot \text{area of basic unit})$
F.T. AGE	=	Fission track age, calculated using equation B.1
Area of basic unit	=	Area of one grid square
Chi squared	=	χ^2 parameter, used to assess variation of single grain ages within the sample
P(chi squared)	=	Probability of obtaining observed χ^2 value for the relevant number of degrees of freedom, if all grains belong to a single population
Age Dispersion	=	% variation in single grain ages - see discussion in text re "Central age"
N_s/N_i	=	Pooled ratio, total spontaneous tracks divided by total induced tracks for all grains
Mean ratio	=	Mean of (N_s/N_i) for individual grains
Zeta	=	Calibration constant, determined empirically for each observer
ρ_D	=	Track density (ρ_D) from uranium standard glass (interpolated from values at each end of stack)
ND	=	Total number of tracks counted for determining ρ_D
POOLED AGE	=	Fission track age calculated from pooled ratio N_s/N_i . Valid only when $P(\chi^2) > 5\%$
CENTRAL AGE	=	Alternative to pooled age when $P(\chi^2) < 5\%$

Key to Figures:

A: Radial plot of single grain ages <i>(See Figures B.1 and B.2 for details of radial plot construction)</i>	B: Distribution of Cl contents in apatite grains
C: Single grain age vs weight % Cl for individual apatite grains.	D: Distribution of confined track lengths



GC813-1 Apatite
Counted by: MEM

Ontaratue H-34 100-850'

Slide ref	Current grain no	N _s	N _i	N _a	ρ _s	ρ _i	RATIO	U (ppm)	Cl (wt%)	F.T. AGE (Ma)
G887-1	4	2	17	16	1.986E+05	1.688E+06	0.118	14.7	0.16	30.3 ± 22.6
G887-1	5	13	9	18	1.148E+06	7.945E+05	1.444	6.9	0.06	361.9 ± 157.3
G887-1	6	62	39	60	1.642E+06	1.033E+06	1.590	9.0	0.20	397.2 ± 82.0
G887-1	7	1	4	12	1.324E+05	5.297E+05	0.250	4.6	0.00	64.1 ± 71.7
		78	69		1.169E+06	1.034E+06		9.0		

Area of basic unit = 6.293E-07 cm⁻²

$\chi^2 = 19.128$ with 3 degrees of freedom

P(χ^2) = 0.0%

Age Dispersion = 85.595%

Ns / Ni = 1.130 ± 0.187

Mean Ratio = 0.850 ± 0.387

Ages calculated using a zeta of 392.9 ± 7.4 for CN5 glass

ρ_D = 1.312E+06cm⁻² ND = 2017

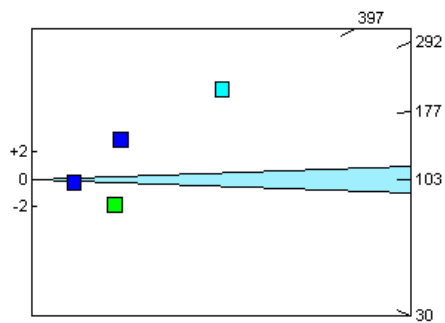
ρ_D interpolated between top of can; ρ_D = 1.312E+06cm⁻² ND = 1032

bottom of can; ρ_D = 1.252E+06cm⁻² ND = 985

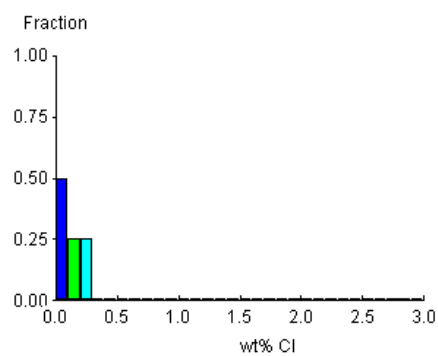
POOLED AGE = 285.0 ± 47.8 Ma

CENTRAL AGE = 174.5 ± 85.0 Ma

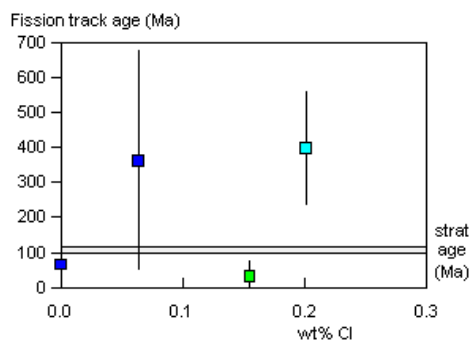
A:



B:



C:



D:

No confined tracks



GC813-2 Apatite
Counted by: MEM

Ontaratu H-34 1150-1900'

Slide ref	Current grain no	N _s	N _i	N _a	ρ _s	ρ _i	RATIO	U (ppm)	Cl (wt%)	F.T. AGE (Ma)
G887-2	4	8	57	20	6.356E+05	4.529E+06	0.140	39.5	0.05	35.9 ± 13.6
G887-2	6	3	8	24	1.986E+05	5.297E+05	0.375	4.6	0.32	95.6 ± 64.8
G887-2	12	0	4	16	0.000E+00	3.973E+05	0.000	3.5	0.93	0.0 ± 140.1
G887-2	14	0	5	20	0.000E+00	3.973E+05	0.000	3.5	0.46	0.0 ± 103.7
G887-2	16	21	52	25	1.335E+06	3.305E+06	0.404	28.8	0.39	102.9 ± 26.8
G887-2	17	0	11	40	0.000E+00	4.370E+05	0.000	3.8	0.00	0.0 ± 39.9
G887-2	18	0	4	12	0.000E+00	5.297E+05	0.000	4.6	0.30	0.0 ± 140.1
G887-2	19	3	16	12	3.973E+05	2.119E+06	0.188	18.5	0.38	48.0 ± 30.2
		35	157		3.291E+05	1.476E+06		12.9		

Area of basic unit = 6.293E-07 cm⁻²

$\chi^2 = 12.997$ with 7 degrees of freedom

$P(\chi^2) = 7.2\%$

Age Dispersion = 57.450%

Ns / Ni = 0.223 ± 0.042

Mean Ratio = 0.138 ± 0.061

Ages calculated using a zeta of 392.9 ± 7.4 for CN5 glass

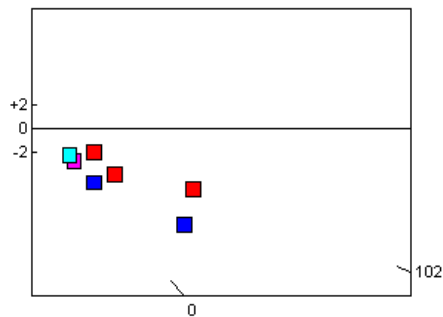
$\rho_D = 1.307E+06 \text{ cm}^{-2}$ ND = 2017

ρ_D interpolated between top of can; $\rho_D = 1.312E+06 \text{ cm}^{-2}$ ND = 1032
bottom of can; $\rho_D = 1.252E+06 \text{ cm}^{-2}$ ND = 985

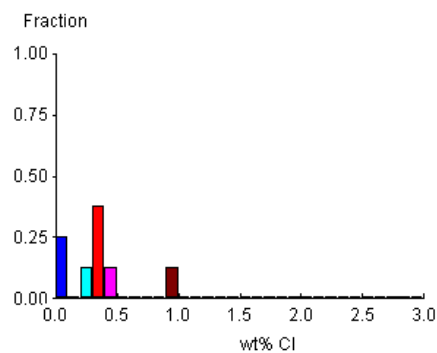
POOLED AGE = 57.0 ± 10.8 Ma

CENTRAL AGE = 46.0 ± 15.0 Ma

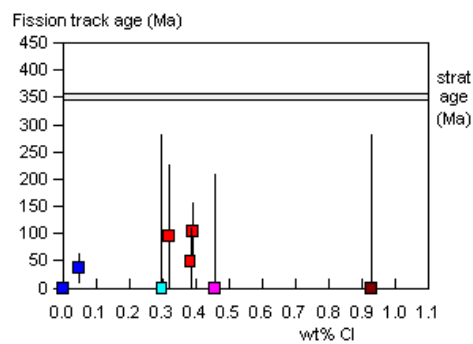
A:



B:



C:



D:

No confined tracks



GC813-3 Apatite
Counted by: MEM

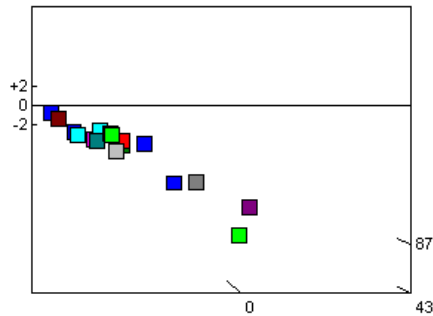
Ontaratie H-34 2300-2900'

Slide ref	Current grain no	N _s	N _i	N _a	ρ _s	ρ _i	RATIO	U (ppm)	Cl (wt%)	F.T. AGE (Ma)
G887-3	3	6	50	30	3.178E+05	2.648E+06	0.120	23.2	0.01	30.6 ± 13.3
G887-3	4	9	26	10	1.430E+06	4.132E+06	0.346	36.2	0.10	88.0 ± 34.1
G887-3	5	0	5	16	0.000E+00	4.966E+05	0.000	4.3	0.00	0.0 ± 103.3
G887-3	6	1	10	25	6.356E+04	6.356E+05	0.100	5.6	0.44	25.5 ± 26.8
G887-3	7	0	1	12	0.000E+00	1.324E+05	0.000	1.2	0.02	0.0 ± 1811.7
G887-3	8	3	10	21	2.270E+05	7.567E+05	0.300	6.6	0.28	76.3 ± 50.3
G887-3	9	12	63	25	7.628E+05	4.004E+06	0.190	35.0	1.71	48.6 ± 15.4
G887-3	11	4	19	25	2.543E+05	1.208E+06	0.211	10.6	0.76	53.7 ± 29.6
G887-3	13	5	18	8	9.932E+05	3.575E+06	0.278	31.3	0.40	70.7 ± 35.8
G887-3	14	0	2	3	0.000E+00	1.059E+06	0.000	9.3	0.93	0.0 ± 416.2
G887-3	16	8	112	50	2.543E+05	3.560E+06	0.071	31.1	0.15	18.3 ± 6.7
G887-3	17	0	6	14	0.000E+00	6.810E+05	0.000	6.0	0.30	0.0 ± 81.8
G887-3	18	22	111	15	2.331E+06	1.176E+07	0.198	102.9	1.00	50.5 ± 11.9
G887-3	19	1	11	16	9.932E+04	1.092E+06	0.091	9.6	0.86	23.2 ± 24.3
G887-3	20	4	13	20	3.178E+05	1.033E+06	0.308	9.0	0.00	78.3 ± 44.8
G887-3	21	4	14	40	1.589E+05	5.562E+05	0.286	4.9	0.17	72.7 ± 41.3
G887-3	22	2	18	48	6.621E+04	5.959E+05	0.111	5.2	1.24	28.4 ± 21.2
		81	489		3.405E+05	2.056E+06		18.0		

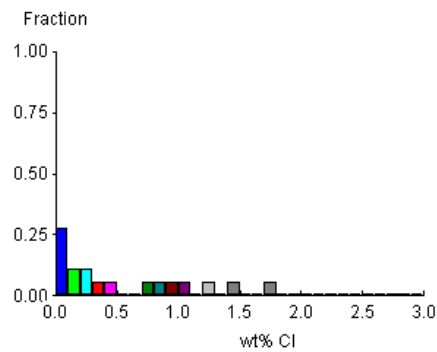
Area of basic unit = 6.293E-07 cm²
 $\chi^2 = 18.196$ with 16 degrees of freedom
 $P(\chi^2) = 31.3\%$
 Age Dispersion = 25.403%
 Ns / Ni = 0.166 ± 0.020
 Mean Ratio = 0.154 ± 0.029

Ages calculated using a zeta of 392.9 ± 7.4 for CN5 glass
 $\rho_D = 1.303E+06 \text{ cm}^{-2}$ ND=2017
 ρ_D interpolated between top of can; $\rho_D = 1.312E+06 \text{ cm}^{-2}$ ND=1032
 bottom of can; $\rho_D = 1.252E+06 \text{ cm}^{-2}$ ND=985
POOLED AGE = 42.3 ± 5.2 Ma
CENTRAL AGE = 43.7 ± 6.5 Ma

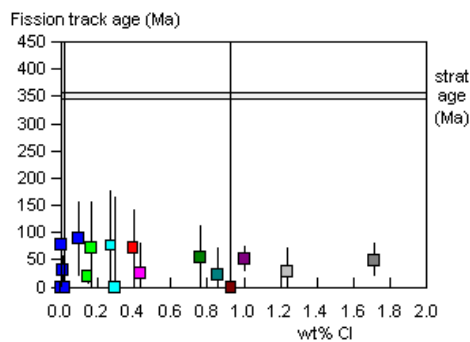
A:



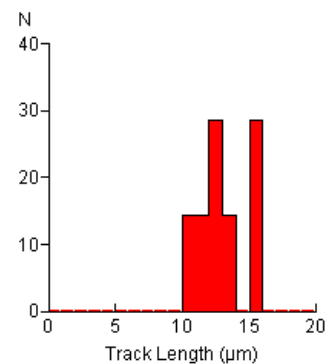
B:



C:



D:



Mean track length 12.94 ± 0.67 μm Std. Dev. 1.78 μm 7 tracks



GC813-4 Apatite
Counted by: MEM

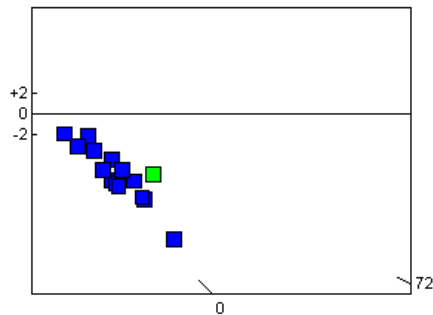
Ontaratue H-34 2910-3620'

Slide ref	Current grain no	N _s	N _i	N _a	ρ _s	ρ _i	RATIO	U (ppm)	Cl (wt%)	F.T. AGE (Ma)
G887-4	3	2	16	36	8.828E+04	7.063E+05	0.125	6.2	0.03	31.8 ± 23.9
G887-4	4	7	34	12	9.270E+05	4.502E+06	0.206	39.5	0.10	52.3 ± 21.8
G887-4	6	1	10	20	7.945E+04	7.945E+05	0.100	7.0	0.01	25.5 ± 26.7
G887-4	7	0	18	40	0.000E+00	7.151E+05	0.000	6.3	0.00	0.0 ± 23.0
G887-4	8	2	7	12	2.648E+05	9.270E+05	0.286	8.1	0.08	72.5 ± 58.1
G887-4	9	0	20	20	0.000E+00	1.589E+06	0.000	14.0	0.00	0.0 ± 20.5
G887-4	10	0	56	30	0.000E+00	2.966E+06	0.000	26.0	0.00	0.0 ± 7.0
G887-4	11	2	27	12	2.648E+05	3.575E+06	0.074	31.4	0.07	18.9 ± 13.8
G887-4	12	2	21	24	1.324E+05	1.390E+06	0.095	12.2	0.00	24.2 ± 18.0
G887-4	13	1	34	36	4.414E+04	1.501E+06	0.029	13.2	0.00	7.5 ± 7.6
G887-4	14	1	33	35	4.540E+04	1.498E+06	0.030	13.2	0.00	7.7 ± 7.8
G887-4	15	0	14	12	0.000E+00	1.854E+06	0.000	16.3	0.00	0.0 ± 30.3
G887-4	16	0	6	15	0.000E+00	6.356E+05	0.000	5.6	0.01	0.0 ± 81.5
G887-4	17	0	21	10	0.000E+00	3.337E+06	0.000	29.3	0.00	0.0 ± 19.5
G887-4	18	0	3	6	0.000E+00	7.945E+05	0.000	7.0	0.06	0.0 ± 211.5
		18	320		8.939E+04	1.589E+06		14.0		

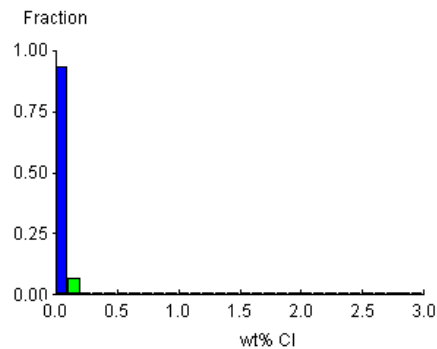
Area of basic unit = 6.293E-07 cm⁻²
 $\chi^2 = 27.053$ with 14 degrees of freedom
 $P(\chi^2) = 1.9\%$
 Age Dispersion = 83.297%
 Ns / Ni = 0.056 ± 0.014
 Mean Ratio = 0.063 ± 0.023

Ages calculated using a zeta of 392.9 ± 7.4 for CN5 glass
 $\rho_D = 1.298E+06 \text{ cm}^{-2}$ ND=2017
 ρ_D interpolated between top of can; $\rho_D = 1.312E+06 \text{ cm}^{-2}$ ND=1032
 bottom of can; $\rho_D = 1.252E+06 \text{ cm}^{-2}$ ND=985
 POOLED AGE = 14.3 ± 3.5 Ma
CENTRAL AGE = 14.7 ± 4.9 Ma

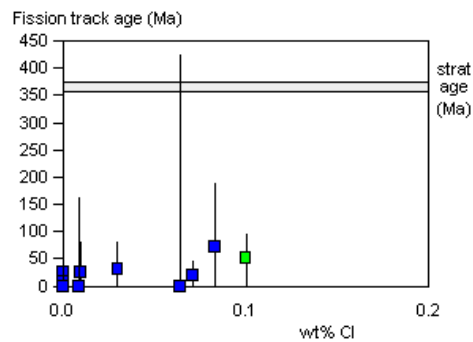
A:



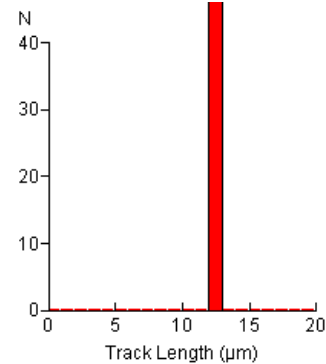
B:



C:



D:



Mean track length 12.85 ± 0.00 μm Std. Dev. μm 1 tracks



APPENDIX C

Principles of Interpretation of AFTA Data in Sedimentary Basins

C.1 Introduction

Detrital apatite grains are incorporated into sedimentary rocks from three dominant sources - crystalline basement rocks, older sediments and contemporaneous volcanism. Apatites derived from the first two sources will, in general, contain fission tracks when they are deposited, with AFTA parameters characteristic of the source regions. However, apatites derived from contemporaneous volcanism, or from rapidly uplifted basement, will contain no tracks when they are deposited. For now, we will restrict discussion to this situation, and generalise at a later point to cover the case of apatites which contain tracks that have been inherited from source regions.

C.2 Basic principles of Apatite Fission Track Analysis

Fission tracks are trails of radiation damage, which are produced within apatite grains at a more or less constant rate through geological time, as a result of the spontaneous fission of ^{238}U impurity atoms. Therefore, the number of fission events which occur within an apatite grain during a fixed time interval depends on the magnitude of the time interval and the uranium content of the grain. Each fission event leads to the formation of a single fission track, and the proportion of tracks which can intersect a polished surface of an apatite grain depends on the length of the tracks. Therefore, the number of tracks which are etched in unit area of the surface of an apatite grain (the "spontaneous track density") depends on three factors - (i) The time over which tracks have been accumulating; (ii) The uranium content of the apatite grain; and, (iii) The distribution of track lengths in the grain. In sedimentary rocks which have not been subjected to temperatures greater than $\sim 50^\circ\text{C}$ since deposition, spontaneous fission tracks have a characteristic distribution of confined track lengths, with a mean length in the range 14-15 μm and a standard deviation of $\sim 1 \mu\text{m}$. In such samples, by measuring the spontaneous track density and the uranium content of a collection of apatite grains, a "fission track age" can be calculated which will be equal to the time over which tracks have been accumulating. The technique is calibrated against other isotopic systems using age standards which also have this type of length distribution (see Appendix B).



In samples which have been subjected to temperatures greater than $\sim 50^{\circ}\text{C}$ after deposition, fission tracks are shortened because of the gradual repair of the radiation damage which constitutes the unetched tracks. In effect, the tracks shrink from each end, in a process which is known as fission track "annealing". The final length of each individual track is essentially determined by the maximum temperature which that track has experienced. A time difference of an order of magnitude produces a change in fission track parameters which is equivalent to a temperature change of only $\sim 10^{\circ}\text{C}$, so temperature is by far the dominant factor in determining the final fission track parameters. As temperature increases, all existing tracks shorten to a length determined by the prevailing temperature, regardless of when they were formed. After the temperature has subsequently decreased, all tracks formed prior to the thermal maximum are "frozen" at the degree of length reduction they attained at that time. Thus, the length of each track can be thought of as a maximum-reading thermometer, recording the maximum temperature to which it has been subjected.

Therefore, in samples for which the present temperature is maximum, all tracks have much the same length, resulting in a narrow, symmetric distribution. The degree of shortening will depend on the temperature, with the mean track length falling progressively from $\sim 14\text{ }\mu\text{m}$ at 50°C , to zero at around $110^{\circ}\text{--}120^{\circ}\text{C}$ - the precise temperature depending on the timescale of heating and the composition of the apatites present in the sample (see below). Values quoted here relate to times of the order of 10^7 years (heating rates around 1 to 10°C/Ma) and average apatite composition. If the effective timescale of heating is shorter than 10^7 years, the temperature responsible for a given degree of track shortening will be higher, depending in detail on the kinetics of the annealing process (Green et al., 1986; Laslett et al., 1987; Duddy et al., 1988; Green et al., 1989b). Shortening of tracks produces an accompanying reduction in the fission track age, because of the reduced proportion of tracks which can intersect the polished surface. Therefore, the fission track age is also highly temperature dependent, falling to zero at around 120°C due to total erasure of all tracks.

Samples which have been heated to a maximum paleotemperature less than $\sim 120^{\circ}\text{C}$ at some time in the past and subsequently cooled will contain two populations of tracks, and will show a more complex distribution of lengths and ages. If the maximum paleotemperature was less than $\sim 50^{\circ}\text{C}$ then the two components will not be resolvable, but for maximum paleotemperatures between $\sim 50^{\circ}$ and 120°C the presence of two components can readily be identified. Tracks formed prior to the thermal maximum will all be shortened to approximately the same degree (the precise value depending on the maximum paleotemperature), while those formed during and after cooling will be longer, due to the lower prevailing temperatures. The length distribution in such



samples will be broader than in the simple case, consisting of a shorter and a longer component, and the fission track age will reflect the amount of length reduction shown by the shorter component (determined by the maximum paleotemperature).

If the maximum paleotemperature was sufficient to shorten tracks to between 9 and 11 μm , and cooling to temperatures of $\sim 50^\circ\text{C}$ or less was sufficiently rapid, tracks formed after cooling will have lengths of 14-15 μm and the resulting track length distribution will show a characteristic bimodal form. If the maximum paleotemperature was greater than ~ 110 to 120°C , all pre-existing tracks will be erased, and all tracks now present will have formed after the onset of cooling. The fission track age in such samples relates directly to the time of cooling.

In thermal history scenarios in which a heating episode is followed by cooling and then temperature increases again, the tracks formed during the second heating phase will undergo progressive shortening. The tracks formed prior to the initial cooling, which were shortened in the first heating episode, will not undergo further shortening until the temperature exceeds the maximum temperature reached in the earlier heating episode. (In practice, differences in timescale of heating can complicate this simple description. In detail, it is the integrated time-temperature effect of the two heating episodes which should be considered.) If the maximum and peak paleotemperatures in the two episodes are sufficiently different ($>\sim 10^\circ\text{C}$), and the later peak paleotemperature is less than the earlier maximum value, then the AFTA parameters allow determination of both episodes. As the peak paleotemperature in the later episode approaches the earlier maximum, the two generations of tracks become increasingly more difficult to resolve, and when the two paleotemperatures are the same, both components are shortened to an identical degree and all information on the earlier heating phase will be lost.

No information is preserved on the approach to maximum paleotemperature because the great majority of tracks formed up to that time have the same mean track length. Only those tracks formed in the last few per cent of the history prior to the onset of cooling are not shortened to the same degree (because temperature dominates over time in the annealing kinetics). These form a very small proportion of the total number of tracks and therefore cannot be resolved within the length distribution because of the inherent spread of several μm in the length distribution.

To summarise, AFTA allows determination of the magnitude of the maximum temperature and the time at which cooling from that maximum began. In some circumstances, determination of a subsequent peak paleotemperature and the time of cooling is also possible.



C.3 Quantitative understanding of fission track annealing in apatite

Annealing kinetics and modelling the development of AFTA parameters

Our understanding of the behaviour of fission tracks in apatite during geological thermal histories is based on study of the response of fission tracks to elevated temperatures in the laboratory (Green et al., 1986; Laslett et al., 1987; Duddy et al., 1988; Green et al., 1989b), in geological situations (Green et al., 1989a), observations of the lengths of spontaneous tracks in apatites from a wide variety of geological environments (Gleadow et al., 1986), and the relationship between track length reduction and reduction in fission track age observed in controlled laboratory experiments (Green, 1988).

These studies resulted in the capability to simulate the development of AFTA parameters resulting from geological thermal histories for an apatite of average composition (Durango apatite, ~0.43 wt% Cl). Full details of this modelling procedure have been explained in Green et al. (1989b). The following discussion presents a brief explanation of the approach.

Geological thermal histories involving temperatures varying through time are broken down into a series of isothermal steps. The progressive shortening of track length through sequential intervals is calculated using the extrapolated predictions of an empirical kinetic model fitted to laboratory annealing data. Contributions from tracks generated throughout the history (remembering that new tracks are continuously generated through time as new fissions occur) are summed to produce the final distribution of track lengths expected to result from the input history. In summing these components, care is taken to allow for various biases which affect revelation of confined tracks (Laslett et al., 1982). The final length reduction of each component of tracks is converted to a contribution of fission track age, using the relationship between track length and density reduction determined by Green (1988). These age contributions are summed to generate the final predicted fission track age.

This approach depends critically on the assumption that extrapolation of the laboratory-based kinetic model to geological timescales, over many orders of magnitude in time, is valid. This was assessed critically by Green et al. (1989b), who showed that predictions from this approach agree well with observed AFTA parameters in apatites of the appropriate composition in samples from a series of reference wells in the Otway Basin of south-east Australia (Gleadow and Duddy, 1981; Gleadow et al., 1983; Green et al., 1989a). This point is illustrated in Figure C.1. Green et al. (1989b) also quantitatively assessed the errors associated with extrapolation of the Laslett et al. (1987) model from



laboratory to geological timescales (i.e. precision, as opposed to accuracy). Typical levels of precision are $\sim 0.5 \mu\text{m}$ for mean lengths $< \sim 10 \mu\text{m}$, and $\sim 0.3 \mu\text{m}$ for lengths $> \sim 10 \mu\text{m}$. These figures are equivalent to an uncertainty in estimates of maximum paleotemperature derived using this approach of $\sim 10^\circ\text{C}$. Precision is largely independent of thermal history for any reasonable geological history. Accuracy of prediction from this model is limited principally by the effect of apatite composition on annealing kinetics, as explained in the next section.

Compositional effects

Natural apatites essentially have the composition $\text{Ca}_5(\text{PO}_4)_3(\text{F}, \text{OH}, \text{Cl})$. Most common detrital and accessory apatites are predominantly Fluor-apatites, but may contain appreciable amounts of chlorine. The amount of chlorine in the apatite lattice exerts a subtle compositional control on the degree of annealing, with apatites richer in fluorine being more easily annealed than those richer in chlorine. The result of this effect is that in a single sample, individual apatite grains may show a spread in the degree of annealing (i.e. length reduction and fission track age reduction). This effect becomes most pronounced in the temperature range $90 - 120^\circ\text{C}$ (assuming a heating timescale of $\sim 10 \text{ Ma}$), and can be useful in identifying samples exposed to paleotemperatures in this range. At temperatures below $\sim 80^\circ\text{C}$, the difference in annealing sensitivity is less marked, and compositional effects can largely be ignored.

Our original quantitative understanding of the kinetics of fission track annealing, as described above, relates to a single apatite (Durango apatite) with $\sim 0.43 \text{ wt\% Cl}$, on which most of our original experimental studies were carried out. Recently, we have extended this quantitative understanding to apatites with Cl contents up to $\sim 3 \text{ wt\%}$. This new, multi-compositional kinetic model is based both on new laboratory annealing studies on a range of apatites with different F-Cl compositions (Figure C.2), and on observations of geological annealing in apatites from a series of samples from exploration wells in which the section is currently at maximum temperature since deposition. A composite model for Durango apatite composition was first created by fitting a common model to the old laboratory data (from Green et al., 1986) and the new geological data for a similar composition. This was then extended to other compositions on the basis of the multi-compositional laboratory and geological data sets. Details of the multi-compositional model are contained in a Technical Note, available from Geotrack in Melbourne.



The multi-compositional model allows prediction of AFTA parameters for any Cl content between 0 and 3 wt%, using a similar approach to that used in our original single composition modelling, as outlined above. Then, for an assumed or measured distribution of Cl contents within a sample, the composite parameters for the sample can be predicted. The range of Cl contents from 0 to 3 wt% spans the range of compositions commonly encountered, as discussed in the next section.

Predictions of the new multi-compositional model are in good agreement with the geological constraints on annealing rates provided by the Otway Basin reference wells, as shown in Figure C.3. However, note that the AFTA data from these Otway Basin wells were among those used in construction of the new model, so this should not be viewed as independent verification, but rather as a demonstration of the overall consistency of the model.

Distributions of Cl content in common AFTA samples

Figure C.4a shows a histogram of Cl contents, measured by electron microprobe, in apatite grains from more than 100 samples of various types. Most grains have Cl contents less than ~0.5 wt%. The majority of grains with Cl contents greater than this come from volcanic sources and basic intrusives, and contain up to ~2 wt% Cl. Figure C.4b shows the distribution of Cl contents measured in randomly selected apatite grains from 61 samples of "typical" quartzo-feldspathic sandstone. This distribution is similar to that in Figure C.4a, except for a more rapid fall-off as Cl content increases. Apatites from most common sandstones give distributions of Cl content which are very similar to that in Figure C.4b. Volcanogenic sandstones typically contain apatites with higher Cl contents, with a much flatter distribution for Cl contents up to ~1.5%, falling to zero at ~2.5 to 3 wt%, as shown in Figure C.4c. Cl contents in granitic basement samples and high-level intrusives are typically much more dominated by compositions close to end-member Fluorapatite, although many exceptions occur to this general rule.

Information about the spread of Cl contents in samples analysed in this report can be found in Appendix A.

Alternative kinetic models

Recently, both Carlson (1990) and Crowley et al. (1991) have published alternative kinetic models for fission track annealing in apatite. Carlson's model is based on our laboratory annealing data for Durango apatite (Green et al., 1986) and other (unpublished) data. In his abstract, Carlson claims that because his model is "based on explicit physical mechanisms, extrapolations of annealing rates to the lower temperatures and longer timescales required for the interpretation of natural fission track



length distributions can be made with greater confidence than is the case for purely empirical relationships fitted to the experimental annealing data". As explained in detail by Green et al. (1993), all aspects of Carlson's model are in fact purely empirical, and his model is inherently no "better" for the interpretation of data than any other. In fact, detailed inspection shows that Carlson's model does not fit the laboratory data set at all well. Therefore, we recommend against use of this model to interpret AFTA data.

The approach taken by Crowley et al. (1991) is very similar to that taken by Laslett et al., (1987). They have fitted models to new annealing data in two apatites of different composition - one close to end-member Fluorapatite (B-5) and one having a relatively high Sr content (113855). The model developed by Crowley et al. (1991) from their own annealing data for the B-5 apatite gives predictions in geological conditions which are consistently higher than measured values, as shown in Figure C.5. Corrigan (1992) reported a similar observation in volcanogenic apatites in samples from a series of West Texas wells. Since the B-5 apatite is close to end-member Fluor-apatite, while the Otway Group apatites contain apatites with Cl contents from zero up to ~3 wt% (and the West Texas apatites have up to 1 wt%), the fluorapatites should have mean lengths rather less than the measured values, which should represent a mean over the range of Cl contents present. Therefore, the predictions of the Crowley et al. (1991) B-5 model appear to be consistently high.

We attribute this to the rather restricted temperature-time conditions covered by the experiments of Crowley et al. (1991), with annealing times between one and 1000 hours, in contrast to times between 20 minutes and 500 days in the experiments of Green et al. (1986). In addition, few of the measured length values in Crowley et al.'s study fall below 11 μm (in only five out of 60 runs in which lengths were measured in apatite B-5) and their model is particularly poorly defined in this region.

Crowley et al. (1991) also fitted a new model to the annealing data for Durango apatite published by Green et al. (1986). Predictions of their fit to our data are not very much different to those from the Laslett et al. (1987) model (Figure C.6). We have not pursued the differences between their model and ours in detail because the advent of our multi-compositional model has rendered the single compositional approach obsolete.

C.4 Evidence for elevated paleotemperatures from AFTA

The basic principle involved in the interpretation of AFTA data in sedimentary basins is to determine whether the degree of annealing shown by tracks in apatite from a particular sample could have been produced if the sample has never been hotter than its present temperature at any time since deposition. To do this, the burial history derived



from the stratigraphy of the preserved sedimentary section is used to calculate a thermal history for each sample using the present geothermal gradient and surface temperature (i.e. assuming these have not changed through time). This is termed the "Default Thermal History". For each sample, the AFTA parameters predicted as a result of the Default Thermal History are then compared to the measured data. If the data show a greater degree of annealing than calculated on the basis of this history, the sample must have been hotter at some time in the past. In this case, the AFTA data are analysed to provide estimates of the magnitude of the maximum paleotemperature in that sample, and the time at which cooling commenced from the thermal maximum.

The degree of annealing is assessed in two ways - from fission track age and track length data. The stratigraphic age provides a basic reference point for the interpretation of fission track age, because reduction of the fission track age below the stratigraphic age unequivocally reveals that appreciable annealing has taken place after deposition of the host sediment. Large degrees of fission track age reduction, with the pooled or central fission track age very much less than the stratigraphic age, indicate severe annealing, which requires paleotemperatures of at least $\sim 100^{\circ}\text{C}$ for any reasonable geological time-scale of heating ($> \sim 1$ Ma). Note that this applies even when apatites contain tracks inherited from source areas. More moderate degrees of annealing can be detected by inspection of the single grain age data, as the most sensitive (fluorine-rich) grains will begin to give fission track ages significantly less than the stratigraphic age before the central or pooled age has been reduced sufficiently to give a noticeable signal. Note that this aspect of the single grain age data can also be used for apatites which have tracks inherited from source areas. If signs of moderate annealing (from single grain age reduction) or severe annealing (from the reduction in pooled or central age) are seen in samples in which the Default Thermal History predicts little or no effect, the sample must have been subjected to elevated paleotemperatures at some time in the past. Figure C.7 shows how increasing degrees of annealing are observable in radial plots of the single grain fission track age data.

Similarly, the present temperature from which a sample is taken, and the way in which this has been approached (as inferred from the preserved sedimentary section), forms a basic point of reference for track length data. The observed mean track length is compared with the mean length predicted from the Default Thermal History. If the observed degree of track shortening in a sample is greater than that expected from the Default Thermal History (i.e. the mean length is significantly less than the predicted value), either the sample must have been subjected to higher paleotemperatures at some time after deposition, or the sample contains shorter tracks which were inherited from sediment source areas at the time the sediment was deposited. If shorter tracks were



inherited from source areas, the sample should still contain a component of longer tracks corresponding to the tracks formed after deposition. In general, the fission track age should be greater than the stratigraphic age. This can be assessed quantitatively using the computer models for the development of AFTA parameters described in an earlier section. If the presence of shorter tracks cannot be explained by their inheritance from source areas, the sample must have been hotter in the past.

C.5 Quantitative determination of the magnitude of maximum paleotemperature and the timing of cooling using AFTA

Values of maximum paleotemperature and timing of cooling in each sample are determined using a forward modelling approach based on the quantitative description of fission track annealing described in earlier sections. The Default Thermal History described above is used as the basis for this forward modelling, but with the addition of episodes of elevated paleotemperatures as required to explain the data. AFTA parameters are modelled iteratively through successive thermal history scenarios in order to identify thermal histories that can account for observed parameters. The range of values of maximum paleotemperature and timing of cooling which can account for the measured AFTA parameters (fission track age and track length distribution) are defined using a maximum likelihood-based approach. In this way, best estimates ("maximum likelihood values") can be defined together with $\pm 95\%$ confidence limits.

In samples in which all tracks have been totally annealed at some time in the past, only a minimum estimate of maximum paleotemperature is possible. In such cases, AFTA data provide most control on the time at which the sample cooled to temperatures at which tracks could be retained. The time at which cooling began could be earlier than this time, and therefore the timing also constitutes a minimum estimate.

Comparison of the AFTA parameters predicted by the multi-compositional model with measured values in samples which are currently at their maximum temperatures since deposition shows a good degree of consistency, suggesting the uncertainty in application of the model should be less than $\pm 10^\circ\text{C}$. This constitutes a significant improvement over earlier approaches, since the kinetic models used are constrained in both laboratory and geological conditions. It should be appreciated that relative differences in maximum paleotemperature can be identified with greater precision than absolute paleotemperatures, and it is only the estimation of absolute paleotemperature values to which the $\pm 10^\circ\text{C}$ uncertainty relates.



Cooling history

If the data are of high quality and provided that cooling from maximum paleotemperatures began sufficiently long ago (so that the history after this time is represented by a significant proportion of the total tracks in the sample), determination of the magnitude of a subsequent peak paleotemperature and the timing of cooling from that peak may also be possible (as explained in Section C.2). A similar approach to that outlined above provides best estimates and corresponding $\pm 95\%$ confidence limits for this episode. Such estimates may simply represent part of a protracted cooling history, and evidence for a later discrete cooling episode can only be accepted if this scenario provides a significantly improved fit to the data. Geological evidence and consistency of estimates between a series of samples can also be used to verify evidence for a second episode.

In practise, most typical AFTA datasets are only sufficient to resolve two discrete episodes of heating and cooling. One notable exception to this is when a sample has been totally annealed in an early episode, and has then undergone two (or more) subsequent episodes with progressively lower peak paleotemperatures in each. But in general, complex cooling histories involving a series of episodes of heating and cooling will allow resolution of only two episodes, and the results will depend on which episodes dominate the data. Typically this will be the earliest and latest episodes, but if multiple cooling episodes occur within a narrow time interval the result will represent an approximation to the actual history.

C.6 Qualitative assessment of AFTA parameters

Various aspects of thermal history can often be assessed by qualitative assessment of AFTA parameters. For example, samples which have reached maximum paleotemperatures sufficient to produce total annealing, and which only contain tracks formed after the onset of cooling, can be identified from a number of lines of evidence. In a vertical sequence of samples showing increasing degrees of annealing, the transition from rapidly decreasing fission track age with increasing depth to more or less the same age over a range of depth denotes the transition from partial to total annealing of all tracks formed prior to the thermal maximum. In samples in which all tracks have been totally annealed, the single grain age data should show that none of the individual grain fission track ages are significantly older than the time of cooling, and grains in all compositional groups should give the same fission track age unless the sample has been further disturbed by a later episode. If the sample cooled rapidly to sufficiently low temperatures, little annealing will have taken place since cooling, and all grains will



give ages which are compatible with a single population around the time of cooling, as shown in Figure C.7.

Inspection of the distribution of single grain ages in partially annealed samples can often yield useful information on the time of cooling, as the most easily annealed grains (those richest in fluorine) may have been totally annealed prior to cooling, while more retentive (Cl-rich) compositions were only partially annealed (as in Figure C.7, centre). The form of the track length distribution can also provide information, from the relative proportions of tracks with different lengths. All of these aspects of the data can be used to reach a preliminary thermal history interpretation.

C.7 Allowing for tracks inherited from source areas

The effect of tracks inherited from source areas, and present at the time the apatite is deposited in the host sediment, is often posed as a potential problem for AFTA. However, this can readily be allowed for in analysing both the fission track age and length data.

In assessing fission track age data to determine the degree of annealing, the only criterion used is the comparison of fission track age with the value expected on the basis of the Default Thermal History. From this point of view, inherited tracks do not affect the conclusion: if a grain or a sample gives a fission track age which is significantly less than expected, the grain or sample has clearly undergone a higher degree of annealing than can be accounted for by the Default Thermal History, and therefore must have been hotter in the past, whether the sample contained tracks when it was deposited or not.

The presence of inherited tracks does impose a limit on our ability to detect post-depositional annealing from age data alone, as in samples which contain a fair proportion of inherited tracks, moderate degrees of annealing may reduce the fission track age from the original value, but not to a value which is significantly less than the stratigraphic age. This is particularly noticeable in the case of Tertiary samples containing apatites derived from Paleozoic basement. In such cases, although fission track age data may show no evidence of post-depositional annealing, track length data may well show such evidence quite clearly.

The influence of track lengths inherited from source areas can be allowed for by comparison of the fission track age with the value predicted by the Default Thermal History combined with inspection of the track length distribution. If the mean length is much less than the length predicted by the Default Thermal History, either the sample has been subjected to elevated paleotemperatures, sufficient to produce the observed degree of length reduction, or else the sample contains a large proportion of shorter



tracks inherited from source areas. However, in the latter case, the sample should give a pooled or central fission track age correspondingly older than the stratigraphic age, while the length distribution should contain a component of longer track lengths corresponding to the value predicted by the Default Thermal History. It is important in this regard that the length of a track depends primarily on the maximum temperature to which it has been subjected, whether in the source regions or after deposition in the sedimentary basin. Thus, any tracks retaining a provenance signature will have lengths towards the shorter end of the distribution where track lengths will not have "equilibrated" with the temperatures attained since deposition.

In general, it is only in extreme cases that inherited tracks render track length data insensitive to post-depositional annealing. For example, if practically all the tracks in a particular sample were formed prior to deposition, perhaps in a Pliocene sediment in which apatites were derived from a stable Paleozoic shield with fission track ages of ~300 Ma or more, the track length distribution will, in general, be dominated by inheritance, as only ~2% of tracks would have formed after deposition. Post-depositional heating will not be detectable as long as the maximum paleotemperature is insufficient to cause greater shortening than that which occurred in the source terrain. Even in such extreme cases, once a sample is exposed to temperatures sufficient to produce greater shortening than that inherited from source areas, the inherited tracks and those formed after deposition will all undergo the same degree of shortening, and the effects of post-depositional annealing can be recognised. In such cases, the presence of tracks inherited from source areas is actually very useful, because the number of tracks formed after deposition is so small that little or no information would be available without the inherited tracks.

C.8 Plots of fission track age and mean track length vs depth and temperature

AFTA data from well sequences are usually plotted as shown in Figure C.8. This figure shows AFTA data for two scenarios: one in which deposition has been essentially continuous from the Carboniferous to the present and all samples are presently at their maximum paleotemperature since deposition (Figure C.8a); and, one in which the section was exposed to elevated paleotemperatures prior to cooling in the Early Tertiary (Figure C.8b).

In both figures, fission track age and mean track length are plotted against depth and present temperature. Presentation of AFTA data in this way often provides insight into the thermal history interpretation, following principles outlined earlier in this Appendix.



In Figure C.8a, for samples at temperatures below $\sim 70^{\circ}\text{C}$, the fission track age is either greater than or close to the stratigraphic age, and little fission track age reduction has affected these samples. Track lengths in these samples are all greater than $\sim 13\ \mu\text{m}$. In progressively deeper samples, both the fission track age and mean track length are progressively reduced to zero at a present temperature of around 110°C , with the precise value depending on the spread of apatite compositions present in the sample. Track length distributions in the shallowest samples would be a mixture of tracks retaining information on the thermal history of source regions, while in deeper samples, all tracks would be shortened to a length determined by the prevailing temperature. This pattern of AFTA parameters is characteristic of a sequence which is currently at maximum temperatures.

The data in Figure C.8b show a very different pattern. The fission track age data show a rapid decrease in age, with values significantly less than the stratigraphic age at temperatures of ~ 40 to 50°C , at which such a degree of age reduction could not be produced in any geological timescale. Below this rapid fall, the fission track ages do not change much over $\sim 1\ \text{km}$ (30°C). This transition from rapid fall to consistent ages is diagnostic of the transition from partial to total annealing. Samples above the "break-in slope" contain two generations of tracks: those formed prior to the thermal maximum, which have been partially annealed (shortened) to a degree which depends on the maximum paleotemperature; and, those formed after cooling, which will be longer. Samples below the break-in slope contain only one generation of tracks, formed after cooling to lower temperatures at which tracks can be retained. At greater depths, where temperatures increase to $\sim 90^{\circ}\text{C}$ and above, the effect of present temperatures begins to reduce the fission track ages towards zero, as in the "maximum temperatures now" case.

The track length data also reflect the changes seen in the fission track age data. At shallow depths, the presence of the partially annealed tracks shortened prior to cooling causes the mean track length to decrease progressively as the fission track age decreases. However, at depths below the break in slope in the age profile, the track length increases again as the shorter component is totally annealed and so does not contribute to the measured distribution of track lengths. At greater depths, the mean track lengths decrease progressively to zero once more due to the effects of the present temperature regime.

Examples of such data have been presented, e.g. by Green (1989) and Kamp and Green (1990).



C.9 Determining paleogeothermal gradients and amount of section removed on unconformities

Estimates of maximum paleotemperatures in samples over a range of depths in a vertical sequence provides the capability of determining the paleogeothermal gradient immediately prior to the onset of cooling from those maximum paleotemperatures. The degree to which the paleogeothermal gradient can be constrained depends on a number of factors, particularly the depth range over which samples are analysed. If samples are only analysed over ~1 km, then the paleotemperature difference over that range may be only ~20 to 30°C. Since maximum paleotemperatures can often only be determined within a ~10°C range, this introduces considerable uncertainty into the final estimate of paleogeothermal gradient (see Figure C.9).

Another important factor is the difference between maximum paleotemperatures and present temperatures (“net cooling”). If this is only ~10°C, which is similar to the uncertainty in absolute paleotemperature determination, only broad limits can be established on the paleogeothermal gradient. In general, the control on the paleogeothermal gradient improves as the amount of net cooling increases. However, if the net cooling becomes so great that many samples were totally annealed prior to the onset of cooling - so that only minimum estimates of maximum paleotemperatures are possible - constraints on the paleogeothermal gradient from AFTA come only from that part of the section in which samples were not totally annealed. In this case, integration of AFTA data with VR measurements can be particularly useful in constraining the paleo-gradient.

Having constrained the paleogeothermal gradient at the time cooling from maximum paleotemperatures began, if we assume a value for surface temperature at that time, the amount of section subsequently removed by uplift and erosion can be calculated as shown in Figure C.10. The *net* amount of section removed is obtained by dividing the difference between the paleo-surface temperature (T_s) and the intercept of the paleotemperature profile at the present ground surface (T_i) by the estimated paleogeothermal gradient. The *total* amount of section removed is obtained by adding the thickness of section subsequently redeposited above the unconformity to the *net* amount estimated as in Figure C.10. If the analysis is performed using depths from the appropriate unconformity, then the analysis will directly yield the *total* amount of section removed.

Geotrack have developed a method of deriving estimates of both the paleogeothermal gradient and the net amount of section removed using estimated paleotemperatures



derived from AFTA and VR. Perhaps more importantly, this method also provides rigorous values for upper and lower 95% confidence limits on each parameter. The method is based on maximum likelihood estimation of the paleogeothermal gradient and the surface intercept, from a table of paleotemperature and depth values. The method is able to accept ranges for paleotemperature estimates (e.g. where the maximum paleotemperature can only be constrained to between, for example, 60 and 90°C), as well as upper and lower limits (e.g. <60°C for samples which show no detectable annealing; >110°C in samples which were totally annealed). Estimates of paleotemperature from AFTA and VR may be combined or analysed separately. Some results from this method have been reported by Bray et al. (1992). Full details of the methods employed are presented in a confidential, in-house, Geotrack research report, copies of which are available on request from the Melbourne office.

Results are presented in two forms. Likelihood profiles, plotting the log-likelihood as a function of either gradient or section removed, portray the probability of a given value of gradient or section removed. The best estimate is given by the value of gradient or section removed for which the log-likelihood is maximised. Ideally, the likelihood profiles should show a quadratic form, and values of gradient or section removed at which the log-likelihood has fallen by two from the maximum value define the upper and lower 95% confidence limits on the estimates. An alternative method of portraying this information is a crossplot of gradient against section removed, in which values which fall within 95% confidence limits (in two dimensions) are contoured. Note that the confidence limits defined by this method are rather tighter than those from the likelihood profiles, as the latter only reflect variation in one parameter, whereas the contoured crossplot takes variation of both parameters into account.

It must be emphasised that this method relies on the assumption that the paleotemperature profile was linear both throughout the section analysed and through the overlying section which has been removed. While the second part of this assumption can never be confirmed independently, visual inspection of the paleotemperature estimates as a function of depth should be sufficient to verify or deny the linearity of the paleotemperature profile through the preserved section.

Results of this procedure are shown in this report if the data allow sufficiently well-defined paleotemperature estimates to justify use of the method. Where the AFTA data suggest that the section is currently at maximum temperature since deposition, or that the paleotemperature profile was non-linear, or where data are of insufficient quality to allow rigorous paleotemperature estimation, the method is not used.



References

- Carlson, W.D. (1990) Mechanisms and kinetics of apatite fission-track annealing. *American Mineralogist*, 75, 1120 - 1139.
- Corrigan, J. (1992) Annealing models under the microscope, *On Track*, 2, 9-11.
- Crowley, K.D., Cameron, M. and Schaefer, R.L. (1991) Experimental studies of annealing of etched fission tracks in apatite. *Geochimica et Cosmochimica Acta*, 55, 1449-1465.
- Duddy, I.R., Green, P.F. and Laslett G.M. (1988) Thermal annealing of fission tracks in apatite 3. Variable temperature behaviour. *Chem. Geol. (Isot. Geosci. Sect.)*, 73, 25-38.
- Gleadow, A.J.W. and Duddy, I.R. (1981) A natural long-term track annealing experiment for apatite. *Nuclear Tracks*, 5, 169-174.
- Gleadow, A.J.W., Duddy, I.R. and Lovering, J.F. (1983) Fission track analysis; a new tool for the evaluation of thermal histories and hydrocarbon potential. *APEA J*, 23, 93-102.
- Gleadow, A.J.W., Duddy, I.R., Green, P.F. and Lovering, J.F. (1986) Confined fission track lengths in apatite - a diagnostic tool for thermal history analysis. *Contr. Min. Petr.*, 94, 405-415.
- Green, P.F. (1988) The relationship between track shortening and fission track age reduction in apatite: Combined influences of inherent instability, annealing anisotropy, length bias and system calibration. *Earth Planet. Sci. Lett.*, 89, 335-352.
- Green, P.F., Duddy, I.R., Gleadow, A.J.W., Tingate, P.R. and Laslett, G.M. (1986) Thermal annealing of fission tracks in apatite 1. A qualitative description. *Chem. Geol. (Isot. Geosci. Sect.)*, 59, 237-253.
- Green, P.F., Duddy, I.R., Gleadow, A.J.W. and Lovering, J.F. (1989a) Apatite Fission Track Analysis as a paleotemperature indicator for hydrocarbon exploration. In: Naeser, N.D. and McCulloh, T. (eds.) *Thermal history of sedimentary basins - methods and case histories*, Springer-Verlag, New York, 181-195.
- Green, P.F., Duddy, I.R., Laslett, G.M., Hegarty, K.A., Gleadow, A.J.W. and Lovering, J.F. (1989b) Thermal annealing of fission tracks in apatite 4. Quantitative modelling techniques and extension to geological timescales. *Chem. Geol. (Isot. Geosci. Sect.)*, 79, 155-182.
- Green, P.F., Laslett, G.M. and Duddy, I.R. (1993) Mechanisms and kinetics of apatite fission track annealing: Discussion. *American Mineralogist*, 78, 441-445.
- Laslett, G.M., Kendall, W.S., Gleadow, A.J.W. and Duddy, I.R. (1982) Bias in measurement of fission track length distributions. *Nuclear Tracks*, 6, 79-85.
- Laslett, G.M., Green, P.F., Duddy, I.R. and Gleadow, A.J.W. (1987) Thermal annealing of fission tracks in apatite 2. A quantitative analysis. *Chem. Geol. (Isot. Geosci. Sect.)*, 65, 1-13.



Otway data and Laslett et al. (1987) predictions

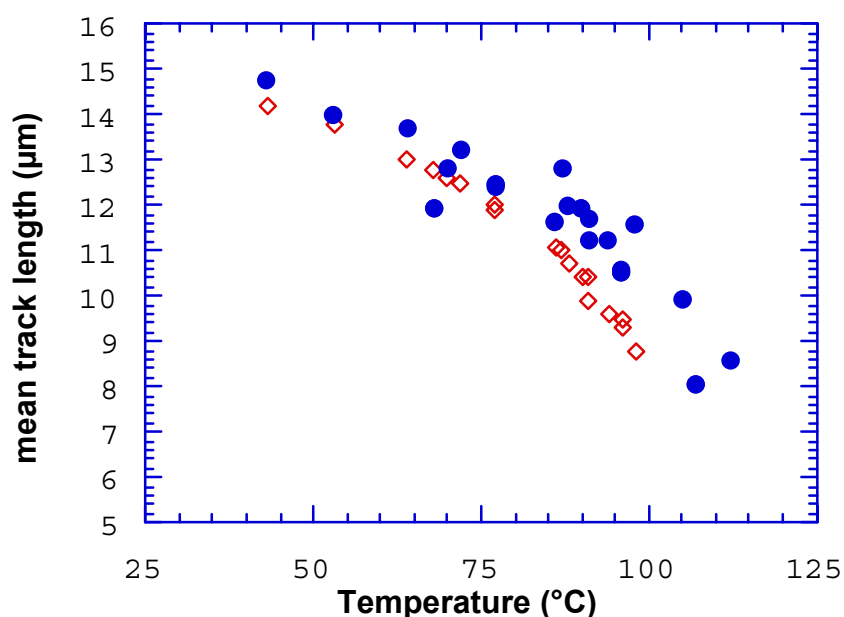


Figure C.1a Comparison of mean track length (solid circles) measured in samples from four Otway Basin reference wells (from Green et al, 1989a) and predicted mean track lengths (open diamonds) from the kinetic model of fission track annealing from Laslett et al. (1987). The predictions underestimate the measured values, but they refer to an apatite composition that is more easily annealed than the majority of apatites in these samples, so this is expected.

Otway Basin data (Durango composition) vs predictions of Laslett et al. (1987) model

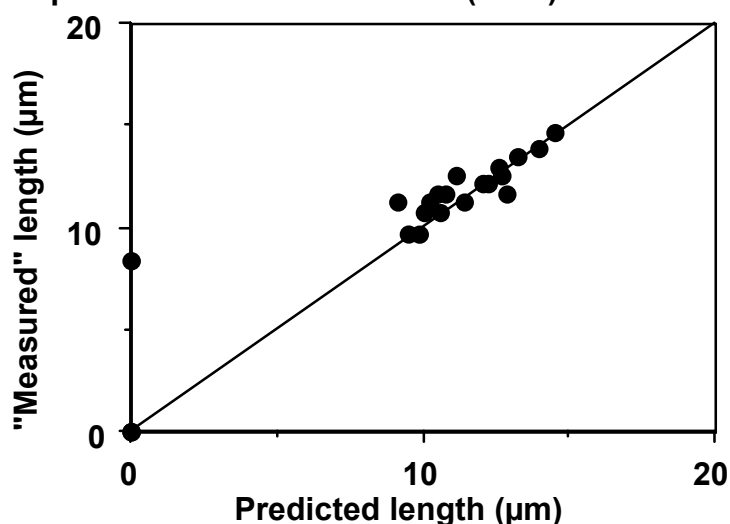


Figure C.1b Comparison of the mean track length in apatites of the same Cl content as Durango apatite from the Otway Group samples illustrated in figure C.1a, with values predicted for apatite of the same composition by the model of Laslett et al. (1987). The agreement is clearly very good except possibly at lengths below ~10 μm.

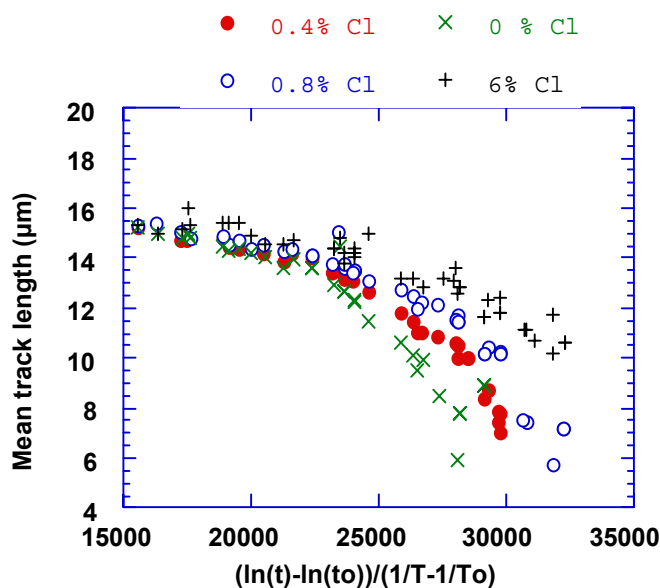


Figure C.2 Mean track length in apatites with four different chlorine contents, as a combined function of temperature and time, to reduce the data to a single scale. Fluorapatites are more easily annealed than chlorapatites, and the annealing kinetics show a progressive change with increasing Cl content.

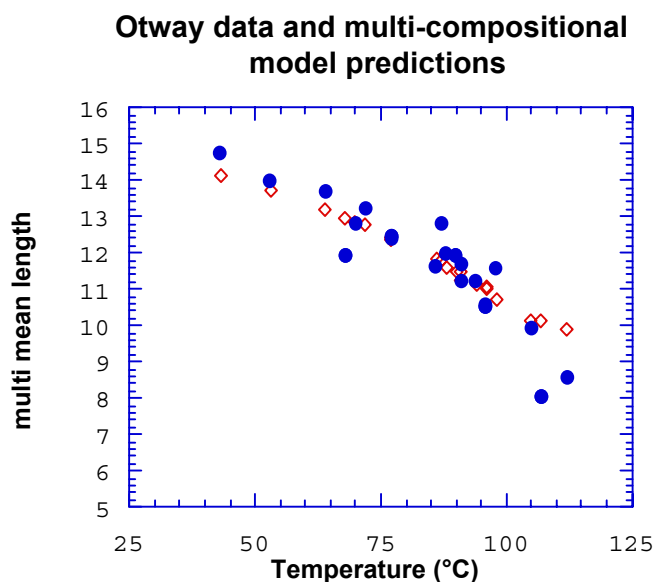
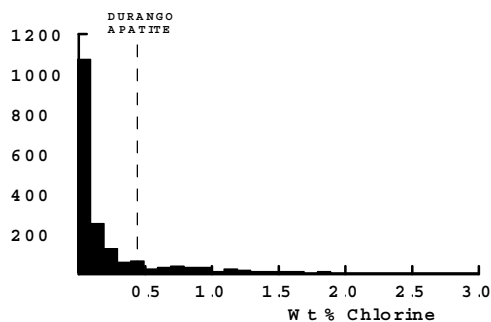


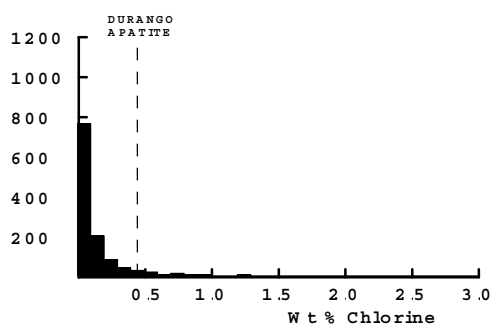
Figure C.3 Comparison of measured mean track length (solid circles) in samples from four Otway Basin reference wells (from Green et al, 1989a) and predicted mean track lengths (open diamonds) from the new multi-compositional kinetic model of fission track annealing described in Section C.3. This model takes into account the spread of Cl contents in apatites from the Otway Group samples and the influence of Cl content on annealing rate. The agreement is clearly very good over the range of the data.



All samples



"Normal sandstones"



Volcanogenic sandstones

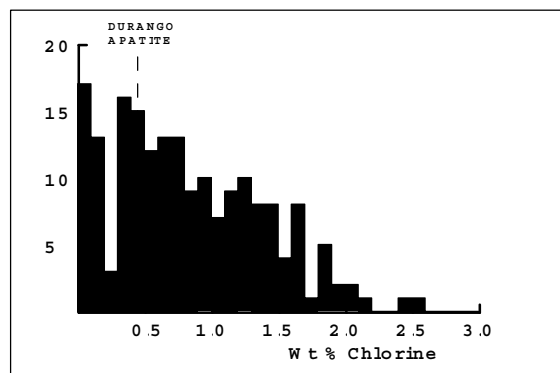


Figure C.4 **a:** Histogram of Cl contents (wt%) in over 1750 apatite grains from over 100 samples of various sedimentary and igneous rocks. Most samples give Cl contents below ~0.5 wt %, while those apatites giving higher Cl contents are characteristic of volcanogenic sandstones and basic igneous sources.

b: Histogram of Cl contents (wt%) in 1168 apatite grains from 61 samples which can loosely be characterised as "normal sandstone". The distribution is similar to that in the upper figure, except for a lower number of grains with Cl contents greater than ~1%.

c: Histogram of Cl contents (wt%) in 188 apatite grains from 15 samples of volcanogenic sandstone. The distribution is much flatter than the other two, with much higher proportion of Cl-rich grains.

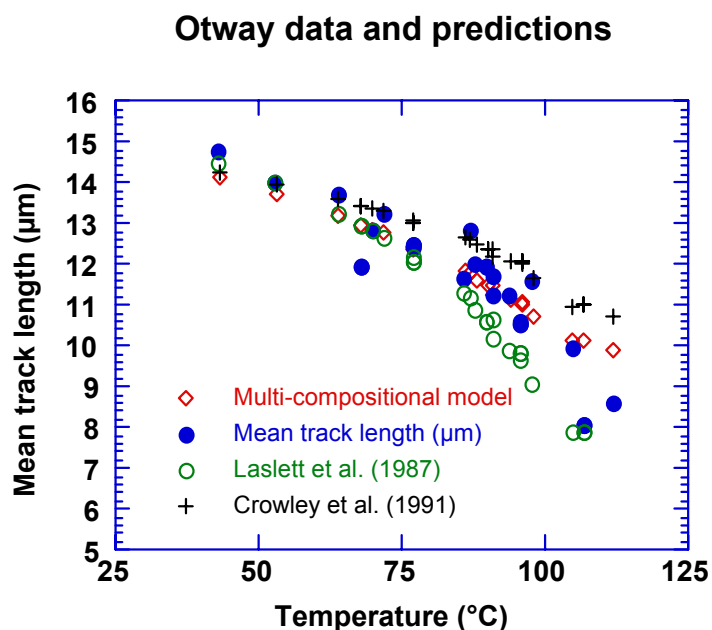


Figure C.5 Comparison of mean track length in samples from four Otway Basin reference wells (from Green et al, 1989a) and predicted mean track lengths from three kinetic models for fission track annealing. The Crowley et al. (1991) model relates to almost pure Fluorapatite (B-5), yet overpredicts mean lengths in the Otway Group samples which are dominated by Cl-rich apatites. The predictions of that model are therefore not reliable.

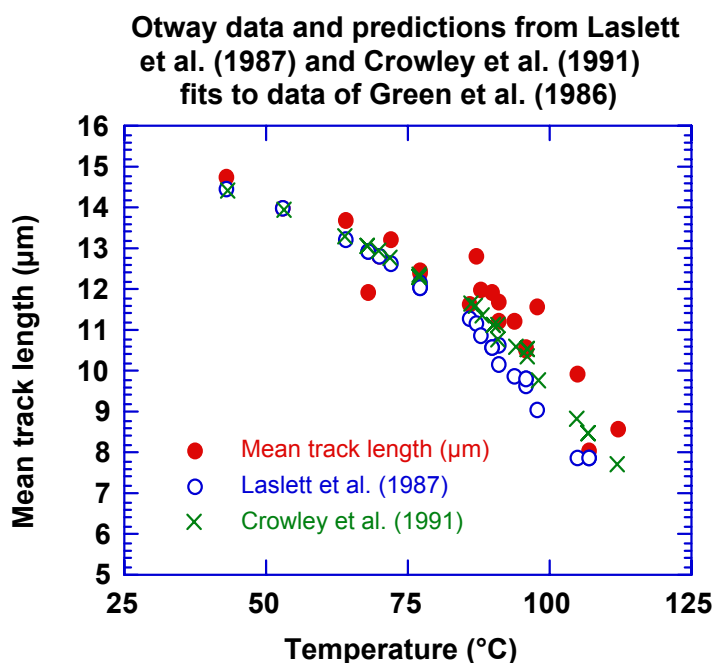
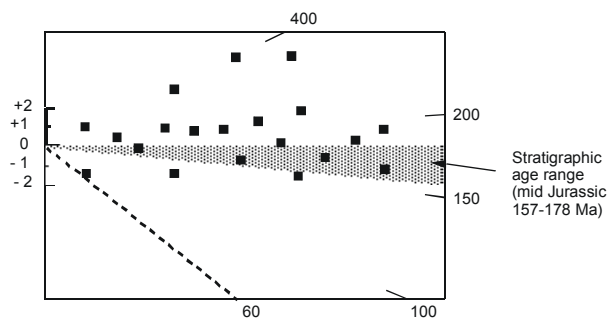


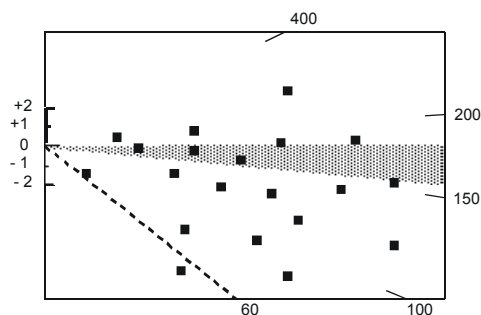
Figure C.6 Comparison of mean track length in samples from four Otway Basin reference wells with values predicted from Laslett et al. (1987) and the model fitted to the annealing data of Green et al. (1986) by Crowley et al. (1991). The predictions of the two models are not very different.



Little or no post-depositional annealing ($T < 60^\circ\text{C}$)



Moderate post-depositional annealing ($T \sim 90^\circ\text{C}$)



Total post-depositional annealing ($T > 110^\circ\text{C}$)

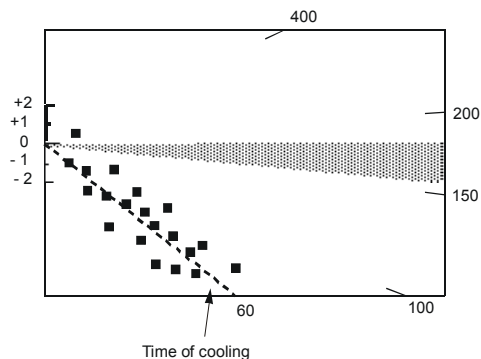


Figure C.7

Radial plots of single grain age data in three samples of mid-Jurassic sandstone that have been subjected to varying degrees of post-depositional annealing prior to cooling at ~ 60 Ma. The mid-point of the stratigraphic age range has been taken as the reference value (corresponding to the horizontal).

The upper diagram represents a sample which has remained at paleotemperatures less than $\sim 60^\circ\text{C}$, and has therefore undergone little or no post-depositional annealing. All single grain ages are either compatible with the stratigraphic age (within $y = \pm 2$ in the radial plot) or older than the stratigraphic age ($y_i > 2$).

The centre diagram represents a sample which has undergone a moderate degree of post-depositional annealing, having reached a maximum paleotemperature of around $\sim 90^\circ\text{C}$ prior to cooling. While some of the individual grain ages are compatible with the stratigraphic age ($-2 < y_i < +2$) and some may be significantly greater than the stratigraphic age ($y_i > 2$), a number of grains give ages which are significantly less than the stratigraphic age ($y < 2$).

The lower diagram represents a sample in which all apatite grains were totally annealed, at paleotemperatures greater than $\sim 110^\circ\text{C}$, prior to rapid cooling at ~ 60 Ma. All grains give fission track ages compatible with a fission track age of ~ 60 Ma (i.e., all data plot within ± 2 of the radial line corresponding to an age of ~ 60 Ma), and most are significantly younger than the stratigraphic age.



MAXIMUM TEMPERATURES NOW

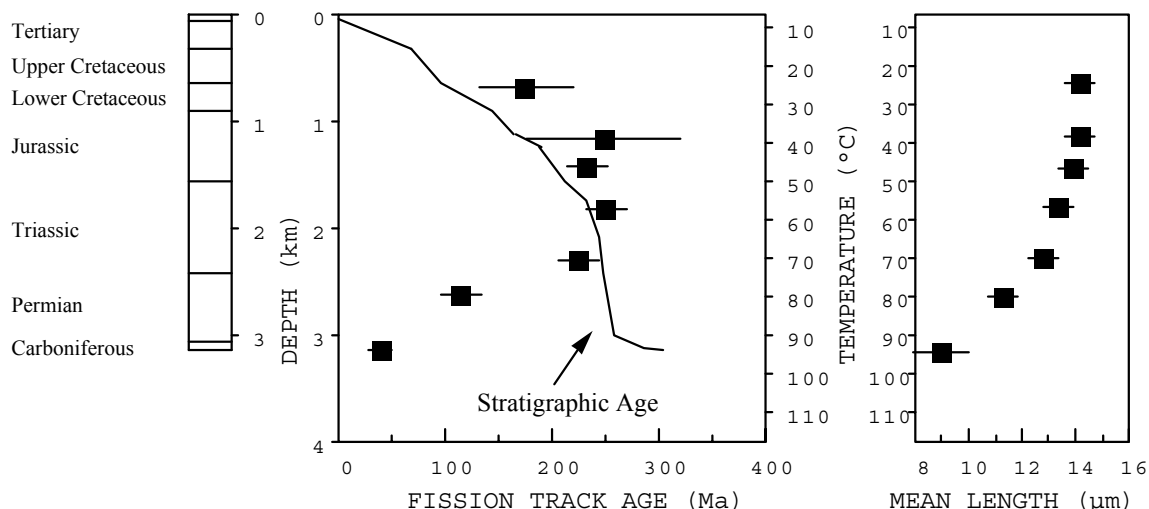


Figure C.8a

Typical pattern of AFTA parameters in a well in which samples throughout the entire section are currently at their maximum temperatures since deposition. Both the fission track age and mean track length undergo progressive reduction to zero at temperatures of $\sim 100 - 110^{\circ}\text{C}$, the actual value depending on the range of apatite compositions present.

HOTTER IN THE PAST

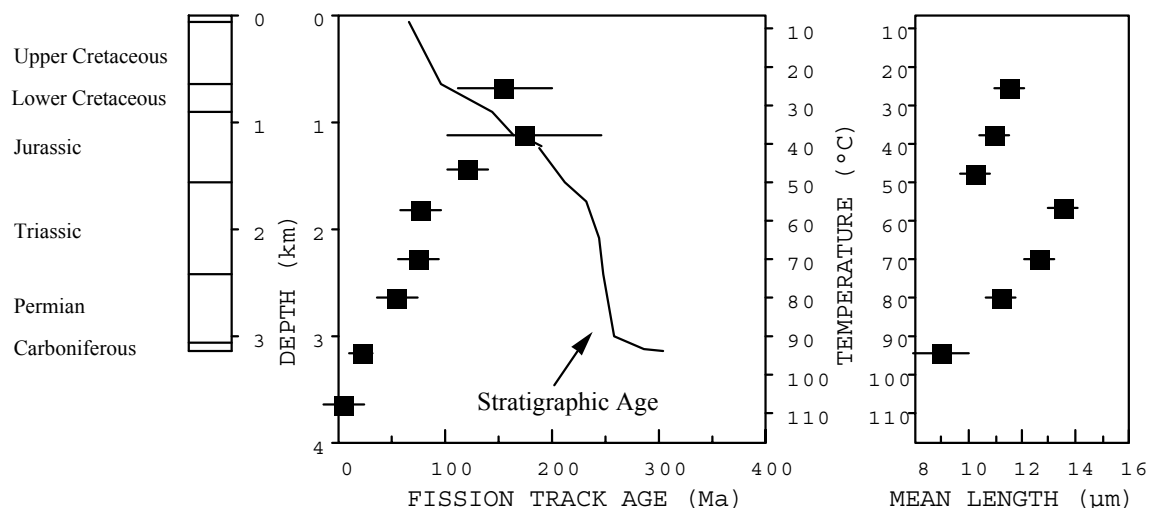
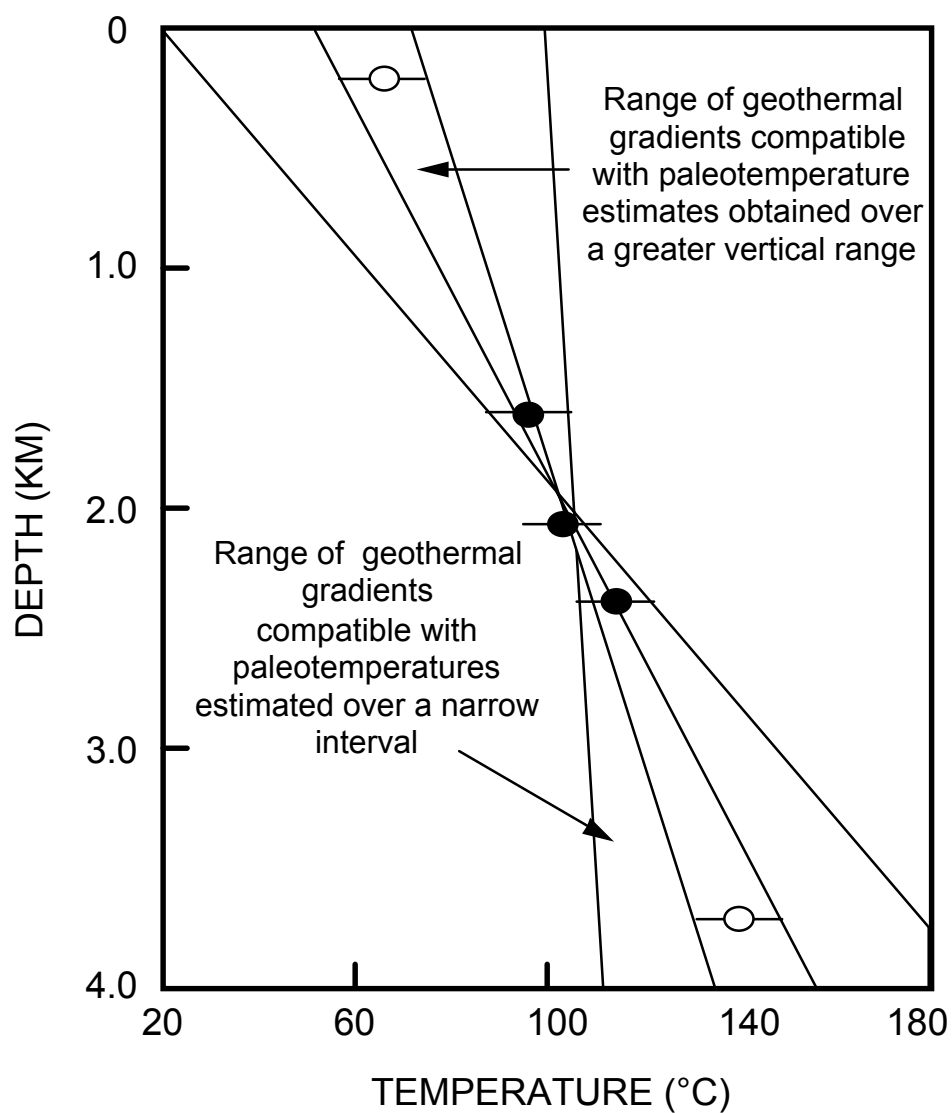


Figure C.8b

Typical pattern of AFTA parameters in a well in which samples throughout the section were exposed to elevated paleotemperatures after deposition (prior to cooling in the Early Tertiary, in this case). Both the fission track age and mean track length show more reduction at temperatures of ~ 40 to 50°C than would be expected at such temperatures. At greater depths (higher temperatures), the constancy of fission track age and the increase in track length are both diagnostic of exposure to elevated paleotemperatures. See Appendix C for further discussion

**Figure C.9**

It is important to obtain paleotemperature constraints over as great a range of depths as possible in order to provide a reliable estimate of paleogeothermal gradient. If paleotemperatures are only available over a narrow depth range, then the paleogeothermal gradient can only be very loosely constrained.

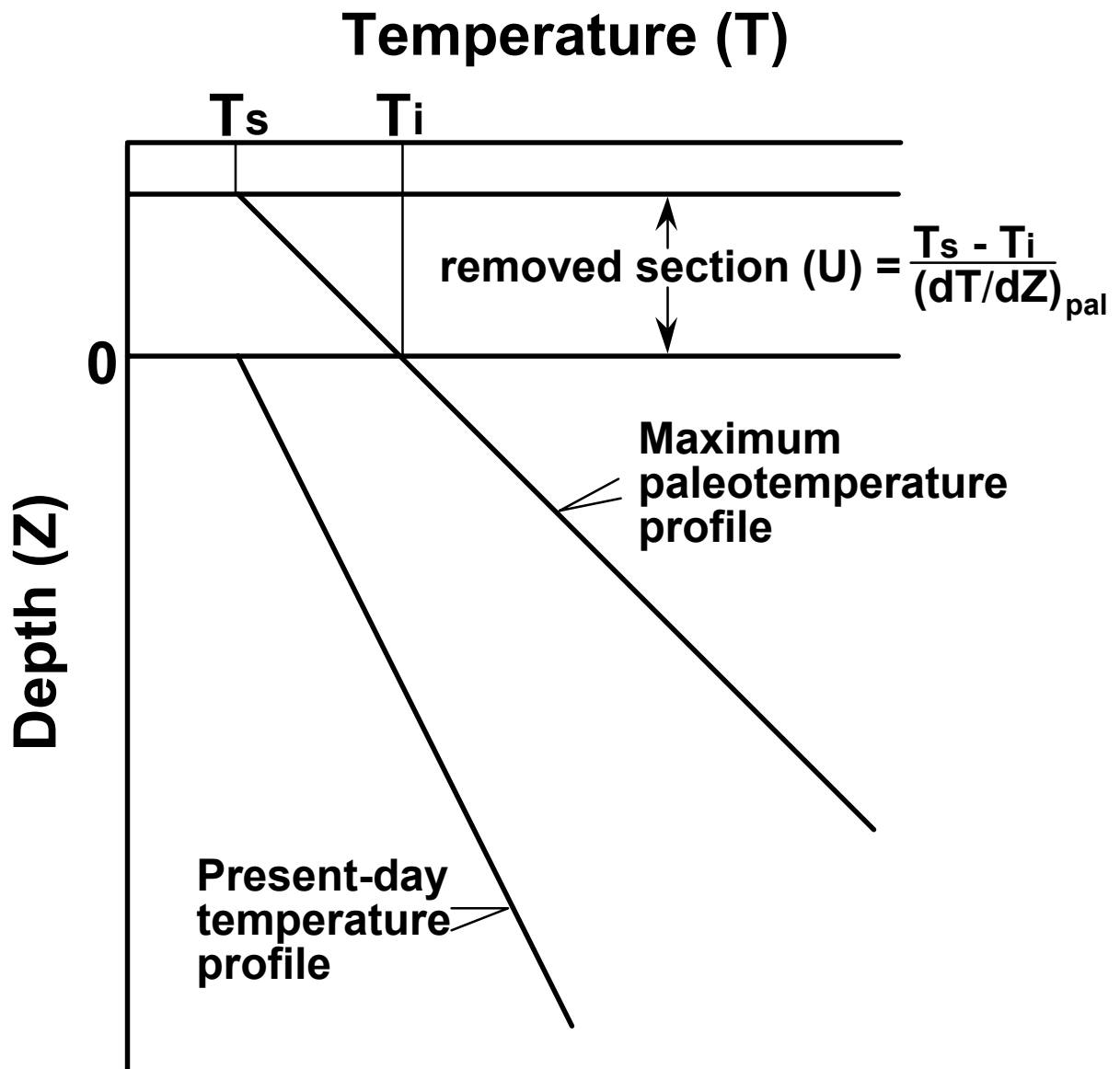


Figure C.10 If the paleogeothermal gradient can be constrained by AFTA and VR, as explained in the text, then for an assumed value of surface temperature, T_s , the amount of section removed can be estimated, as shown.



APPENDIX D

Vitrinite Reflectance Measurements

D.1 New vitrinite reflectance determinations

New vitrinite reflectance data were collected as part of this study, with details of determinations described in sections D.1 and D.2 below. In addition, further vitrinite reflectance data were supplied by the client, as summarised in section D.3.

Samples

Samples were submitted for vitrinite reflectance determination to Keiraville Konsultants, Australia. Results and sample details are summarised in Table D.2, while supporting data, including maceral descriptions and raw data sheets, are presented in the following pages.

Equipment

Leitz MPV1.1 photometer equipped with separate fluorescence illuminator, Swift point counter. Reflectance standards: spinel 0.42%, YAG 0.91%, GGG 1.72%, SiC standard for cokes and masked uranyl glass for measurement of intensity (I) in fluorescence mode. With the Keiraville Konsultants equipment, it is possible to alternate from reflectance to fluorescence mode to check for associated fluorescing liptinite, or importantly with some samples, to check for bitumen impregnation, or the presence, intensity, and source of oil-cut.

Sample preparation

Samples are normally mounted in cold setting polyester resin and polished using Cr₂O₃ and MgO polishing powders. Epoxy resins or araldite can be used if required. "Whole rock" samples are normally used but demineralisation can be undertaken. Large samples of coals and cokes can be mounted and examined.

Vitrinite Reflectance measurement

The procedure used generally follows Australian Standard (AS) 2486, but has been slightly modified for use with dispersed organic matter (DOM). For each sample, a minimum of 25 fields is measured (the number may be less if vitrinite is rare or if a limited number of particles of vitrinite is supplied, as may be the case with hand-picked



samples). If wide dispersal of vitrinite reflectances is found, the number of readings (N) is increased until a stable mean is obtained.

Vitrinite identification is made primarily on textural grounds, and this allows an independent assessment to be made of cavings and re-worked vitrinite populations. Histograms are only used for population definition when a cavings population significantly overlaps the range of the indigenous population. Where such data provides additional information, the mean maximum reflectance of inertinite and/or the mean maximum reflectance of liptinite (exinite) is reported. For each field, the maximum reflectance position is located and the reading recorded. The stage is then rotated by 180° which should give the same reading. In practice, the readings are seldom identical because of stage run-out and slight surface irregularities. If the readings are within $\pm 5\%$ relative, they are accepted. If not, the cause of the difference is sought and the results rejected. The usual source of differences is surface relief. The measurement of both maxima results in a total of 50 measurements being taken for the 25 fields reported. Thus, the 50 readings consist of 25 pairs of closely spaced readings which provide a check on the levelling of the surface and hence additional precision.

As the vitrinite reflectance measurements are being made, the various features of the samples are noted on a check sheet to allow a sample description to be compiled. When the reflectance measurements are complete, a thorough check is made of liptinite fluorescence characteristics. At the same time, organic matter abundance is estimated using a global estimate, a grain count method or point count method as required.

Data presentation

Individual sample results are reported in the following format:

KK No.	Depth (ft)	\overline{R}_{Vmax}^{*1}	Range ^{*2}	N ^{*3}
x10324	3106	0.79	0.64 - 0.91	25
<hr/>				
*1 Mean of all the maximum reflectance readings obtained.				
*2 Lowest Rmax and highest Rmax of the population considered to represent the first generation vitrinite population.				
*3 Number of fields measured (Number of measurements = 2N because 2 maximum values are recorded for each field)				

***Methods - Organic matter abundance and type.***

After completion of vitrinite reflectance readings, the microscope is switched to fluorescence-mode and an estimate made of the abundance of each liptinite maceral. Fluorescence colours are also noted (BG 3 long UV excitation, TK400 dichroic mirror and a K490 barrier filter). The abundances are estimated using comparison charts. The categories used for liptinite (and other components) are:

Descriptor	%	Source potential
Absent	0	None
Rare	<0.1	Very poor
Sparse	$0.1 < x < 0.5$	Poor to fair
Common	$0.5 < x < 2.0$	Fair to good
Abundant	$2.0 < x < 10.0$	Good to very good
Major	$10.0 < x < 40.0$	Very good (excellent if algal)
Dominant	>40.0	Excellent

Dispersed Organic Matter (DOM) composition

At the same time as liptinite abundances are estimated, total DOM, vitrinite and inertinite abundances are estimated and reported in the categories listed above. Liptinite (exinite) fluorescence intensity and colour, lithology and a brief description of organic matter type and abundance are also recorded in a further column. Coal is described separately from dispersed organic matter (DOM). These data can be used to estimate the specific yield of the DOM and form a valuable adjunct to TOC data.

Lithological composition

The lithological abundances are ranked. For cuttings, these data can be useful in conjunction with geophysical logs in assessing the abundance and nature of cavings. For cores, it provides a record of the lithology examined and of the lithological associations of the organic matter.

Coal abundance and composition

Where coals are present, their abundance is recorded and their composition is reported as microlithotypes thus:

Coal major, Vitrinite>Inertinite>Exinite, Clarodurite>vitrite>clarite>inertite.



These data give an approximate maceral composition and information about the organic facies of the coal. Where coal is a major or dominant component, and more precise maceral composition data are required, point count analyses should be requested. However, the precision of the original sampling is commonly a limiting factor in obtaining better quality data.

Abundance factor analysis

Especially where cuttings samples are used, abundance factor analyses are used to obtain an assessment of the maceral assemblages in the various lithologies. This can be done by a combination analysis using a point counter, but a large number of categories is required, and the precision is low if DOM is less than about 10%. For an abundance factor analysis (for core, 50 microscope fields of view) we assess the abundance of DOM, coal and shaly coal in 50 grains. The data can be used to plot DOM and coal abundance profiles.

Analyst/Advisor: Professor A.C. Cook

Prior to transmittal of final results, all samples are examined and checked by A.C. Cook who has more than 30 years' experience of work on coals, cokes, source rocks and source rock maturation.

D.2 Integration of vitrinite reflectance data with AFTA

Vitrinite reflectance is a time-temperature indicator governed by a kinetic response in a similar manner to the annealing of fission tracks in apatite as described in Appendix C. In this study, vitrinite reflectance data are interpreted on the basis of the distributed activation energy model describing the evolution of VR with temperature and time described by Burnham and Sweeney (1989), as implemented in the BasinMod™ software package of Platte River Associates. In a considerable number of wells from around the world, in which AFTA has been used to constrain the thermal history, we have found that the Burnham and Sweeney (1989) model gives good agreement between predicted and observed VR data, in a variety of settings.

As in the case of fission track annealing, it is clear from the chemical kinetic description embodied in equation 2 of Burnham and Sweeney (1989) that temperature is more important than time in controlling the increase of vitrinite reflectance. If the Burnham and Sweeney (1989) distributed activation energy model is expressed in the form of an Arrhenius plot (a plot of the logarithm of time versus inverse absolute temperature),



then the slopes of lines defining contours of equal vitrinite reflectance in such a plot are very similar to those describing the kinetic description of annealing of fission tracks in Durango apatite developed by Laslett et al. (1987), which is used to interpret the AFTA data in this report. This feature of the two quite independent approaches to thermal history analysis means that for a particular sample, a given degree of fission track annealing in apatite of Durango composition will be associated with the same value of vitrinite reflectance regardless of the heating rate experienced by a sample. Thus paleotemperature estimates based on either AFTA or VR data sets should be equivalent, regardless of the duration of heating. As a guide, Table D.1 gives paleotemperature estimates for various values of VR for two different heating times.

One practical consequence of this relationship between AFTA and VR is, for example, that a VR value of 0.7% is associated with total annealing of all fission tracks in apatite of Durango composition, and that total annealing of all fission tracks in apatites of more Chlorine-rich composition is accomplished between VR values of 0.7 and ~0.9%.

Furthermore, because vitrinite reflectance continues to increase progressively with increasing temperature, VR data allow direct estimation of maximum paleotemperatures in the range where fission tracks in apatite are totally annealed (generally above ~110°C) and where therefore AFTA only provides minimum estimates. Maximum paleotemperature estimates based on vitrinite reflectance data from a well in which most AFTA samples were totally annealed will allow constraints on the paleogeothermal gradient that would not be possible from AFTA alone. In such cases the AFTA data should allow tight constraints to be placed on the time of cooling and also the cooling history, since AFTA parameters will be dominated by the effects of tracks formed after cooling from maximum paleotemperatures. Even in situations where AFTA samples were not totally annealed, integration of AFTA and VR can allow paleotemperature control over a greater range of depth, e.g. by combining AFTA from sand-dominated units with VR from other parts of the section, thereby providing tighter constraint on the paleogeothermal gradient.

D.3 Client-supplied vitrinite reflectance

Vitrinite reflectance and other data (if applicable) supplied by the client is summarised in Table D.3. Unless specified, this vitrinite reflectance data has been treated at face value, as if it were collected in the same manner as described for the new data, because detailed information is usually not available.



References

- Burnham, A.K. and Sweeney, J.J. (1989). A chemical kinetic model of vitrinite reflectance maturation. *Geochim. et Cosmochim. Acta*, 53, 2649-2657.
- Laslett, G.M., Green, P.F., Duddy, I.R. and Gleadow, A.J.W. (1987). Thermal annealing of fission tracks in apatite 2. A quantitative analysis. *Chem. Geol. (Isot. Geosci.Sect.)*, 65, 1-13.



Table D.1: Paleotemperature - vitrinite reflectance nomogram based on Equation 2 of Burnham and Sweeney (1989)

Paleotemperature (°C / °F)	Vitrinite Reflectance (%)	
	1 Ma Duration of heating	10 Ma Duration of heating
40 / 104	0.29	0.32
50 / 122	0.31	0.35
60 / 140	0.35	0.40
70 / 158	0.39	0.45
80 / 176	0.43	0.52
90 / 194	0.49	0.58
100 / 212	0.55	0.64
110 / 230	0.61	0.70
120 / 248	0.66	0.78
130 / 266	0.72	0.89
140 / 284	0.81	1.04
150 / 302	0.92	1.20
160 / 320	1.07	1.35
170 / 338	1.23	1.55
180 / 356	1.42	1.80
190 / 374	1.63	2.05
200 / 392	1.86	2.33
210 / 410	2.13	2.65
220 / 428	2.40	2.94
230 / 446	2.70	3.23



Table D.2: Vitrinite reflectance sample details and results - well samples from North West Territories (Geotrack Report #813A)

Sample number	Depth (m)	Sample type	Stratigraphic Subdivision	Stratigraphic age (Ma)	Present temperature ^{*1} (°C)	VR (Range) %	N
Ontaratue H-34							
GC813-1	30-259 (100-850')	cuttings	Martin House Fm - Arctic Red Fm	115-98	5	0.66 (0.54-0.78)	8
						1.73 ^{*2} (1.06-2.64)	25
GC813-2	351-579 (1150-1900')	cuttings	Imperial	356-346	18	0.75 (0.61-0.90)	14
						1.70 ^{*2} (1.22-2.24)	20
GC813-3.1	732-792 (2400-2600')	cuttings	Imperial	356-346	30	0.95 (0.87-1.09)	5
						1.77 ^{*2} (1.30-3.14)	25
GC813-4.1	887-985 (2910-3230')	cuttings	Hume - Canol / Hare Indian	369-356	36	1.11 (0.94-1.33)	12
						1.85 ^{*2} (1.44-2.72)	20
GC813-4.2	1006-1103 (3300-3620')	cuttings	Bear Rock Ist - Hume	373-363	41	1.15 (0.99-1.36)	9
						1.96 ^{*2} (1.42-2.64)	20
GC813-5	1370-1388 (4495-4555')	core	Bear Rock Ist	373-369	54	-	
						2.15 ^{*3} (1.89-2.45)	25
GC813-6.1	1585-1603 (5200-5260')	cuttings	Bear Rock Ist	373-369	62	1.14 (1.05-1.23)	3
						2.63 ^{*2} (2.08-3.46)	10
GC813-6.2	1670-1716 (5480-5630')	cuttings	Silurian - Ordovician	490-470	66	-	
GC813-7	2347-2469 (7700-8100')	cuttings	Silurian - Ordovician	490-470	94	-	
						2.95 ^{*3} (2.29-3.22)	4
GC813-8	2890-2895 (9480-9499')	core	Cambrian	540-490	113	-	

**Table D.2: Continued**

Sample number	Depth (m)	Sample type	Stratigraphic Subdivision	Stratigraphic age (Ma)	Present temperature ^{*1} (°C)	VR (Range) %	N
GC813-10	3049-3055 (10004-10023')	core	Cambrian	540-490	119	3.57	1
						6.93 ^{*4} (5.62-8.37)	5
GC813-9	3018-3109 (9900-10200')	cuttings	Cambrian	540-490	119	10.53 (10.17-10.89)	2
GC813-11	3231-3241 (10602-10632')	core	Cambrian	540-490	126	-	

Note: Some samples may contain both vitrinite and inertinite. Only vitrinite data is shown.

^{*1} See Appendix A for discussion of present temperature data.

^{*2} Inertinite.

^{*3} bitumen.

^{*4} ?Graphitic C.



Table D.3: Vitrinite reflectance sample details and results supplied by client - North West Territories (Geotrack Report #813A)

Source number	Depth (m)	Sample type	Stratigraphic Subdivision	Stratigraphic age (Ma)	Present temperature *1 (°C)	VR (Range) %	N	Tmax
Ontaratue H-34								
	40 (130')		Arctic Red Fm	110-98	1	0.59 (0.57-0.61)	3	438
	110 (360')		Arctic Red Fm	110-98	4	0.55 (0.55-0.60)	2	442
	213 (700')		Arctic Red Fm	110-98	8	0.65 (0.63-0.67)	5	449
	305 (1000')		Imperial	356-346	12	0.66 (0.61-0.71)	10	446
	396 (1300')		Imperial	356-346	15	0.69 (0.66-0.70)	5	451
	488 (1600')		Imperial	356-346	19	1.04 (0.89-1.24)	50	455
	597 (1960')		Imperial	356-346	23	0.71 (0.66-0.74)	5	453
	668 (2190')		Imperial	356-346	26			463
	756 (2480')		Imperial	356-346	29	0.81 (0.77-0.83)	9	457
	841 (2760')		Imperial	356-346	33	0.92 (0.89-0.94)	3	474


Table D.3: Continued

Source number	Depth (m)	Sample type	Stratigraphic Subdivision	Stratigraphic age (Ma)	Present temperature *1 (°C)	VR (Range) %	N	Tmax
	902 (2960')		Canol / Hare Indian	363-356	35	0.98 (0.85-1.07)	5	464
	917 (3010')		Canol / Hare Indian	363-356	36			459
	933 (3060')		Canol / Hare Indian	363-356	36			457
	948 (3110')		Canol / Hare Indian	363-356	37			457
	963 (3160')		Canol / Hare Indian	363-356	37			469
	969 (3180')		Canol / Hare Indian	363-356	38			469
	978 (3210')		Canol / Hare Indian	363-356	38	1.17 (1.07-1.30)	18	461
	981 (3220')		Canol / Hare Indian	363-356	38			468
	994 (3260')		Hume	369-363	39	1.11 (1.06-1.18)	4	
	1042 (3420')		Hume	369-363	40			463
	1103 (3620')		Bear Rock lst	373-369	43			444
	1152 (3780')		Bear Rock lst	373-369	45			462
	1158 (3800')		Bear Rock lst	373-369	45	1.07 (1.00-1.14)	11	
	1216 (3990')		Bear Rock lst	373-369	47	1.18 (1.09-1.25)	4	448
	1981 (6500')		Silurian - Ordovician	490-470	77			352
	3051 (10009')		Cambrian	540-490	119			567
	3053 (10015')		Cambrian	540-490	119			565
	3054 (10020')		Cambrian	540-490	119			564

**Table D.3: Continued**

Source number	Depth (m)	Sample type	Stratigraphic Subdivision	Stratigraphic age (Ma)	Present temperature * ¹ (°C)	VR (Range) %	N	Tmax
	3170 (10400')		Cambrian	540-490	123			313
	3232 (10603')		Cambrian	540-490	126			465
	3235 (10612')		Cambrian	540-490	126			405
	3237 (10619')		Cambrian	540-490	126			442
	3310 (10860')		Cambrian	540-490	129			427
	3383 (11100')		Cambrian	540-490	132	2.45 (3.09-3.55)	4	367
	3459 (11348')		Cambrian	540-490	135			389
	3533 (11590')		Cambrian	540-490	138			418
	3627 (11900')		Cambrian	540-490	141			411
	3719 (12200')		Cambrian	540-490	145			376
	4054 (13300')		Cambrian	540-490	158			436

Note: Some samples may contain both vitrinite and inertinite. Only vitrinite data is shown.

*¹ See Appendix A for discussion of present temperature data.


GC813

KK # Ref #.	Depth (ft) /Type	\bar{R}_{vmax}	Range	N
----------------	---------------------	------------------	-------	---

ONTARATUE H-34, p1

Sample description including liptinite fluorescence, maceral abundances, mineral fluorescence

CRETACEOUS					
T7824 1 Ctgs	100-850 \bar{R}_{lmax}	0.66 1.73	0.54-0.78 1.06-2.64	8 25	Common sporinite and sparse liptodetrinite, orange to dull orange, common lamalginite, dull orange. (Claystone> argillaceous siltstone>carbonate>sandstone. Dom abundant, I>L>V. Inertinite abundant, liptinite common, vitrinite rare. Rare dull orange fluorescing bitumen in claystone. Mineral fluorescence weak dull orange, brighter in carbonate. Glauconite sparse. Iron oxides rare. Pyrite sparse, locally abundant.)
DEVONIAN					
IMPERIAL FORMATION					
T7825 2 Ctgs	1150-1900 \bar{R}_{lmax}	0.75 1.70	0.61-0.90 1.22-2.24	14 20	Rare sporinite, dull orange. (Siltstone>sandstone>claystone> carbonate. Dom common, I>V>L. Inertinite common, vitrinite and liptinite rare. Rare dull orange fluorescing bitumen in claystone. Mineral fluorescence patchy bright orange. Glauconite rare. Iron oxides rare. Pyrite sparse.)
T7826 3.1 Ctgs	2400-2600 \bar{R}_{lmax}	0.95 1.77	0.87-1.09 1.30-3.14	5 25	Rare lamalginite and liptodetrinite, dull orange. (Argillaceous siltstone>sandstone>claystone>carbonate. Dom sparse, I>L>V. Inertinite sparse, liptinite and vitrinite rare. Diffuse organic matter common. Mineral fluorescence patchy orange. Glauconite rare. Iron oxides rare. Pyrite sparse.)
CANOL/HARE INDIAN FORMATION					
T7827 4.1 Ctgs	2910-3230 \bar{R}_{lmax}	1.11 1.85	0.94-1.33 1.44-2.72	12 20	Rare lamalginite and liptodetrinite, dull orange. (Artificial composites>claystone>siltstone>carbonate>sandstone. Dom sparse, I>V>L. Inertinite sparse, vitrinite and liptinite rare. Rare dull orange fluorescing bitumen in claystone. Diffuse organic matter common. Mineral fluorescence patchy moderate orange. Iron oxides rare. Pyrite abundant.)
HUME FORMATION					
T7828 4.2 Ctgs	3300-3620 \bar{R}_{lmax}	1.15 1.96	0.99-1.36 1.42-2.64	9 20	Rare sporinite and liptodetrinite, dull orange. (Siltstone> carbonate>artificial composites>sandstone>claystone. Dom sparse, I>V>L. Inertinite sparse, vitrinite and liptinite rare. Diffuse organic matter common. Mineral fluorescence patchy moderate orange. Iron oxides rare. Pyrite common, locally abundant.)
BEAR ROCK FORMATION					
T7829 5 Core	4495-4555 \bar{R}_{Bmax}	- 2.15	- 1.89-2.45	- 25	Fluorescing liptinite absent. (Carbonate with minor sandstone. Dom absent. Abundant non-fluorescing bitumen. The bitumen population reported appears to be isotropic, bitumen cokes are also present and range up to 3.4% in reflectance. Carbonate is sparry. Mineral fluorescence none. Iron oxides common, occur as recrystallised masses along the carbonate grain boundaries. Pyrite rare.)
T7830 6.1 Ctgs	5200-5260 \bar{R}_{lmax}	1.14 2.63	1.05-1.23 2.08-3.46	3 10	Rare lamalginite and liptodetrinite, orange to dull orange. (Carbonate>siltstone>claystone>artificial composites. Dom sparse, I>L>V. Inertinite sparse, liptinite and vitrinite rare. Organic matter absent in carbonates. Organic matter populations are cavings and indigenous organic matter is probably absent on contaminant free basis. Mineral fluorescence variable, bright orange to dull orange to none. Pyrite abundant.)


GC813

KK #	Depth (ft)					
Ref #.	/Type	\bar{R}_{vmax}	Range	N		ONTARATUE H-34, p2 Sample description including liptinite fluorescence, maceral abundances, mineral fluorescence
T7831 6.2 Ctgs	5480-5630	-	-	-		?Silurian Ronning Fluorescing liptinite absent. (Carbonate>siltstone, siltstone is a cavings population. Dom absent except in cavings where dom sparse, I>V, L absent. Vitrinite in cavings with reflectance of 1.16% (1.00%-1.32%). Rare bitumen is present in some grains rare and appears to be cavings from the Bear Rock Formation with a reflectance of 2.07% (2.06-2.08%). Organic matter absent on cavings-free basis. Mineral fluorescence weak dull orange to none. Pyrite common to abundant.)
T7832 7 Ctgs	7700-8100	-	-	-		Cambrian Franklin Mtn Fluorescing liptinite absent. (Carbonate>>sandstone. Dom from both lithologies. Rare bitumen that is higher in reflectance than the Bear Rock bitumen and is assumed to be an in situ bitumen population. Mineral fluorescence variable, very weak dull orange to none. Pyrite abundant.)
T7833 8 Core	9480-9499	-	-	-		Cambrian Saline River Formation Fluorescing liptinite absent. (Carbonate, argillaceous. Dom absent. Rare diffuse humic organic matter possibly derived from graptolites but this has not taken a polish and does not yield reflectances data. Mineral fluorescence absent except from weak dull orange from dolomite crystals. Pyrite abundant.)
T7834 9 Ctgs	9900-10200	10.53	10.17-1-.89	2		Cambrian Mt Clark Formation Fluorescing liptinite absent. (Siltstone>sandstone>argillaceous siltstone. ?Dom rare, ? V only. Mineral fluorescence absent. Iron oxides abundant probably derived from iron sulphides during sample drying and storage. Pyrite abundant.)
T7835 10 Core	10004-10023	3.57	-	1		Fluorescing liptinite absent. (Siltstone with strongly sutured grain boundaries. Dom rare, two reflectance populations. A lower reflectance population with strong bireflectance and a higher reflecting population occurring as short thin needles with bireflectance weak relative to the maximum values. Mineral fluorescence absent. A number of mineral phases present typical of high temperature settings. Pyrite abundant.)
T7836 11 Core	10602-10632	-	-	-		Proterozoic Fluorescing liptinite absent. (Claystone> fine-grained siltstone. Dom appears to be absent, but some very small needles of graphitic material may be present but these are too small to measure. Mineral fluorescence absent. Pyrite abundant.)

The Cretaceous section is mid-mature for oil generation indicating the strength of post-Cretaceous coalification. The underlying Devonian is only marginally higher in the level of maturation and it is possible that no break in coalification occurs between these units. However, the maturation gradient down to the Hume Formation at 3230 is relatively high. The bitumens in the Bear Rock Formation suggest and even higher gradient and the lower values found below 4555 are probably all caving from about the Imperial to Canol interval. Bitumens from the Franklin Formation from 8100 suggest a continuation of the trend seen in the shallower section. Below that depth, organic matter is rare and the nature of the high reflectance components is uncertain, possibly the high reflectance populations from 9900 and 10004 should be ignored. The mineralogy of the deeper samples and the degree of suturing in the siltstone from the Mt Clark Formation suggest high temperature alteration.

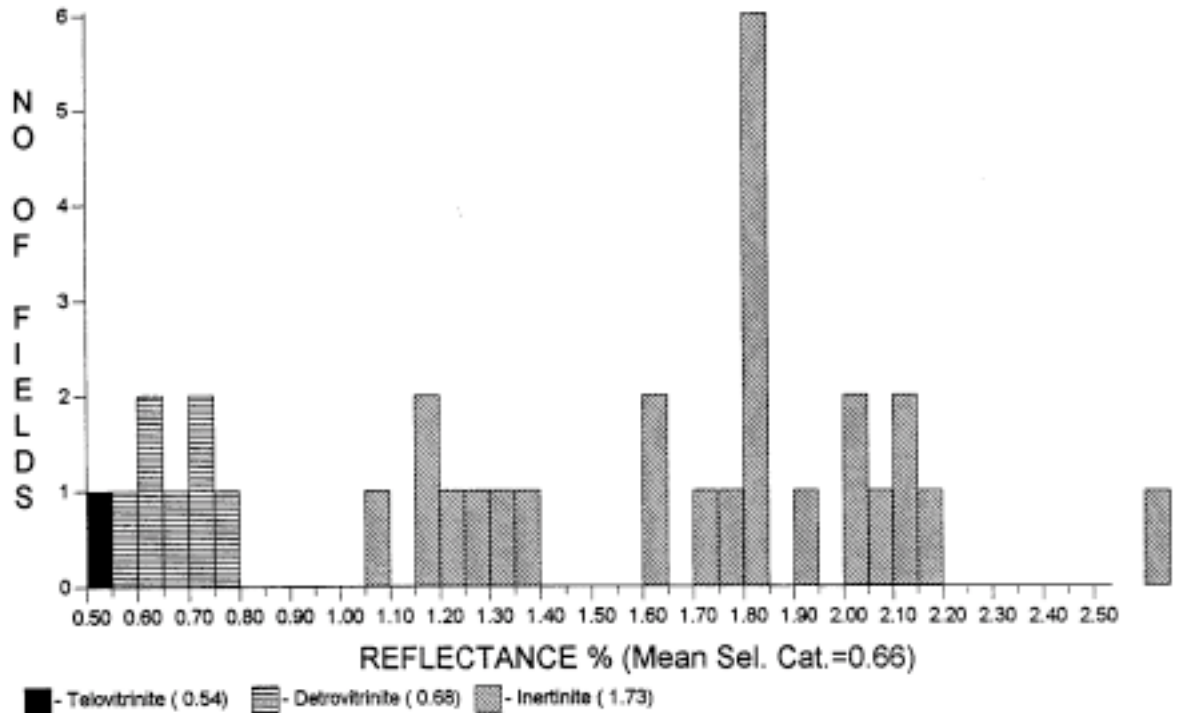
Source potential is good within the Cretaceous and the Imperial Formation. Initial source potential may have been better within the Canol than is currently apparent. The Bear Rock Formation has been an oil reservoir at an earlier stage in its history and some evidence of reservoiring within the Franklin Mtn Formation is also evident.



Keiraville Konsultants Pty. Ltd.
7 Dallas Street,
Keiraville, NSW 2500
Australia.

Telephone: (02) 42 299843
International: +61-2-42 299843
Fax: +61-(0)2-42 299624
Email: acc@ozemail.com.au

813-1 ONTARATUE H-34, 100-850', Ctgs (T7824)



<u>Category</u>	<u>No. of Readings</u>	<u>Mean</u>	<u>Standard Deviation</u>
Telovitrinite	1	0.54	0.000
Detrovitrinite	7	0.68	0.067
Inertinite	25	1.73	0.378
Total:	33	1.47	0.566

Selected categories: Telovitrinite, Detrovitrinite,

No. of readings:	8
Mean of selected categories:	0.66
Standard deviation of selected categories:	0.077

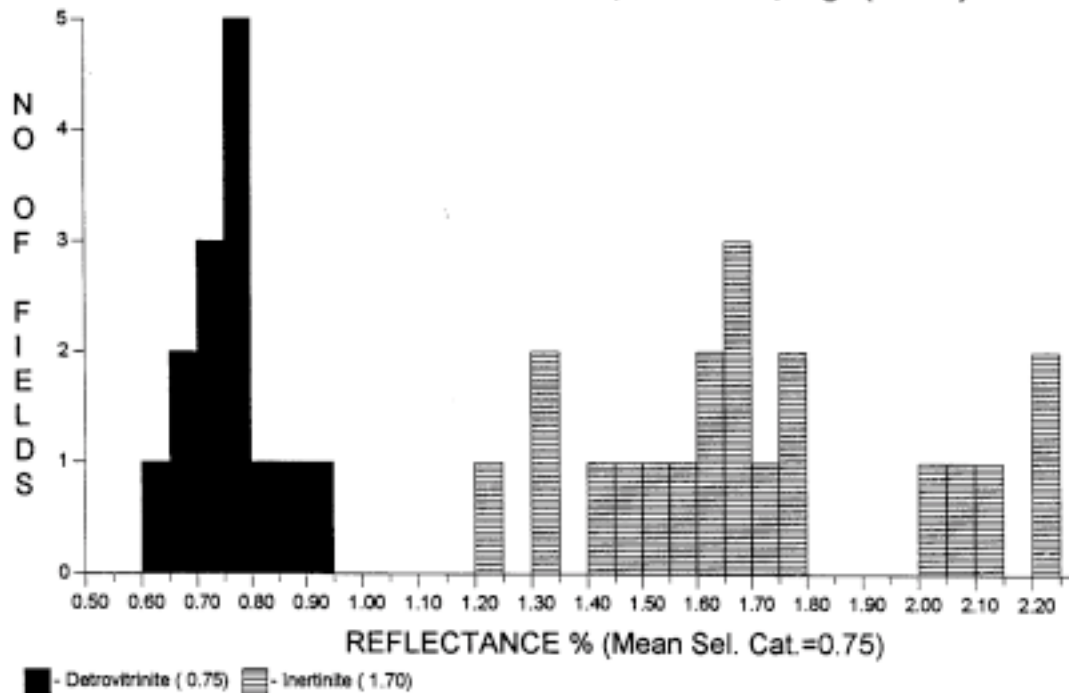
**Keiraville Consultants Pty. Ltd.**7 Dallas Street,
Keiraville, NSW 2500
Australia.

Telephone: (02) 42 299843

International: +61-2-42 299843

Fax: +61-(0)2-42 299624

Email: acc@ozemail.com.au

813-2 ONTARATUE H-34, 1150-1900', Ctgs (T7825)

<u>Category</u>	<u>No. of Readings</u>	<u>Mean</u>	<u>Standard Deviation</u>
Detrovitrinite	14	0.75	0.078
Inertinite	20	1.70	0.288
Total:	34	1.31	0.516

Selected categories: Detrovitrinite,

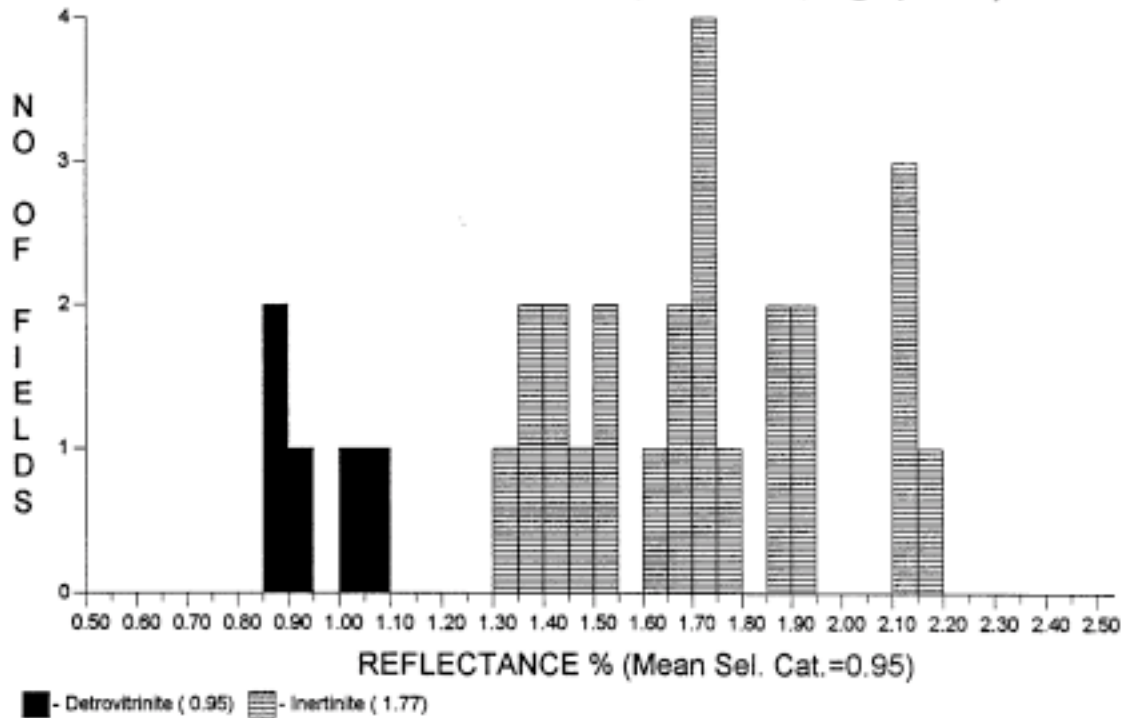
No. of readings:	14
Mean of selected categories:	0.75
Standard deviation of selected categories:	0.078



Keiraville Konsultants Pty. Ltd.
7 Dallas Street,
Keiraville, NSW 2500
Australia.

Telephone: (02) 42 299843
International: +61-2-42 299843
Fax: +61-(0)2-42 299624
Email: acc@ozemail.com.au

813-3.1 ONTARATUE H-34, 2400-2600', Ctgs (T7826)



<u>Category</u>	<u>No. of Readings</u>	<u>Mean</u>	<u>Standard Deviation</u>
Detrovitrinite	5	0.95	0.085
Inertinite	25	1.77	0.375
Total:	30	1.63	0.460

Selected categories: Detrovitrinite,

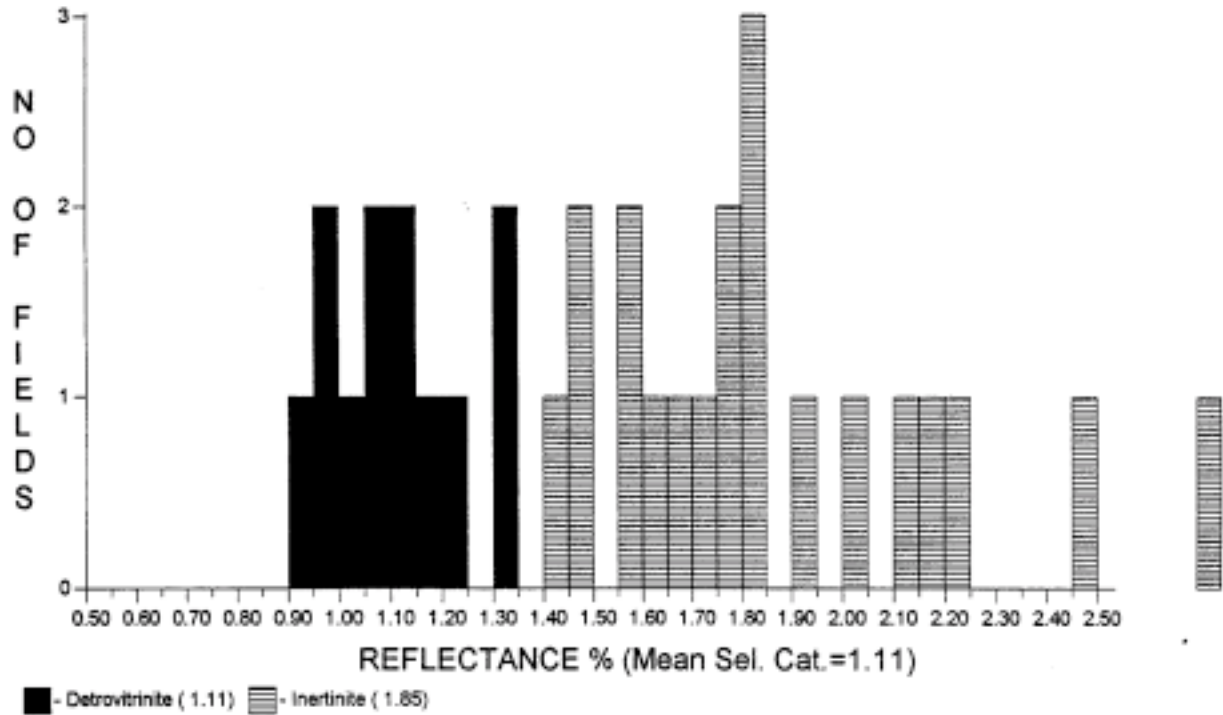
No. of readings: 5
Mean of selected categories: 0.95
Standard deviation of selected categories: 0.085



Keiraville Konsultants Pty. Ltd.
7 Dallas Street,
Keiraville, NSW 2500
Australia.

Telephone: (02) 42 299843
International: +61-2-42 299843
Fax: +61-(0)2-42 299624
Email: acc@ozemail.com.au

GC813-4.1, Ontaratue H-34, 2910-3230,Ctg (T7827)



<u>Category</u>	<u>No. of Readings</u>	<u>Mean</u>	<u>Standard Deviation</u>
Detrovitrinite	12	1.11	0.126
Inertinite	20	1.85	0.336
<u>Total:</u>	32	1.57	0.455

Selected categories: Detrovitrinite,

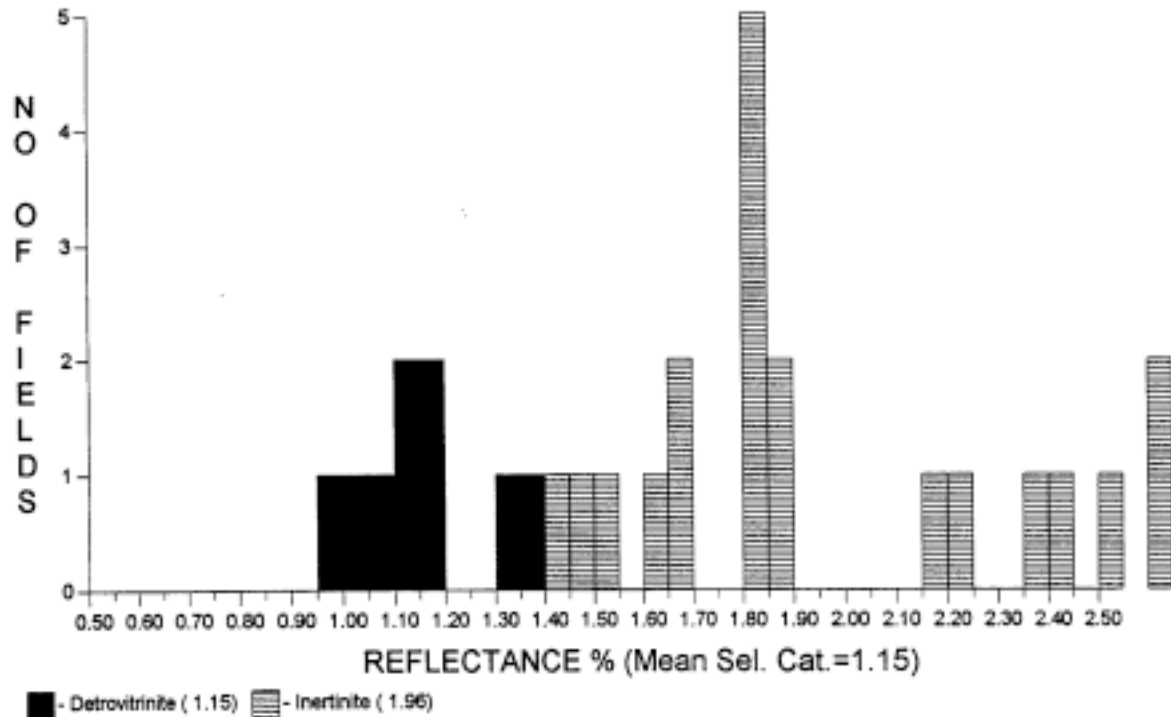
No. of readings: 12
 Mean of selected categories: 1.11
 Standard deviation of selected categories: 0.126



Keiraville Konsultants Pty. Ltd.
7 Dallas Street,
Keiraville, NSW 2500
Australia.

Telephone: (02) 42 299843
International: +61-2-42 299843
Fax: +61-(0)2-42 299624
Email: acc@ozemail.com.au

GC813-4.2, Ontaratue H-34, 3300-3620', Ctgs (T7828)



<u>Category</u>	<u>No. of Readings</u>	<u>Mean</u>	<u>Standard Deviation</u>
Detrovitrinite	9	1.15	0.125
Inertinite	20	1.96	0.383
Total:	29	1.71	0.496

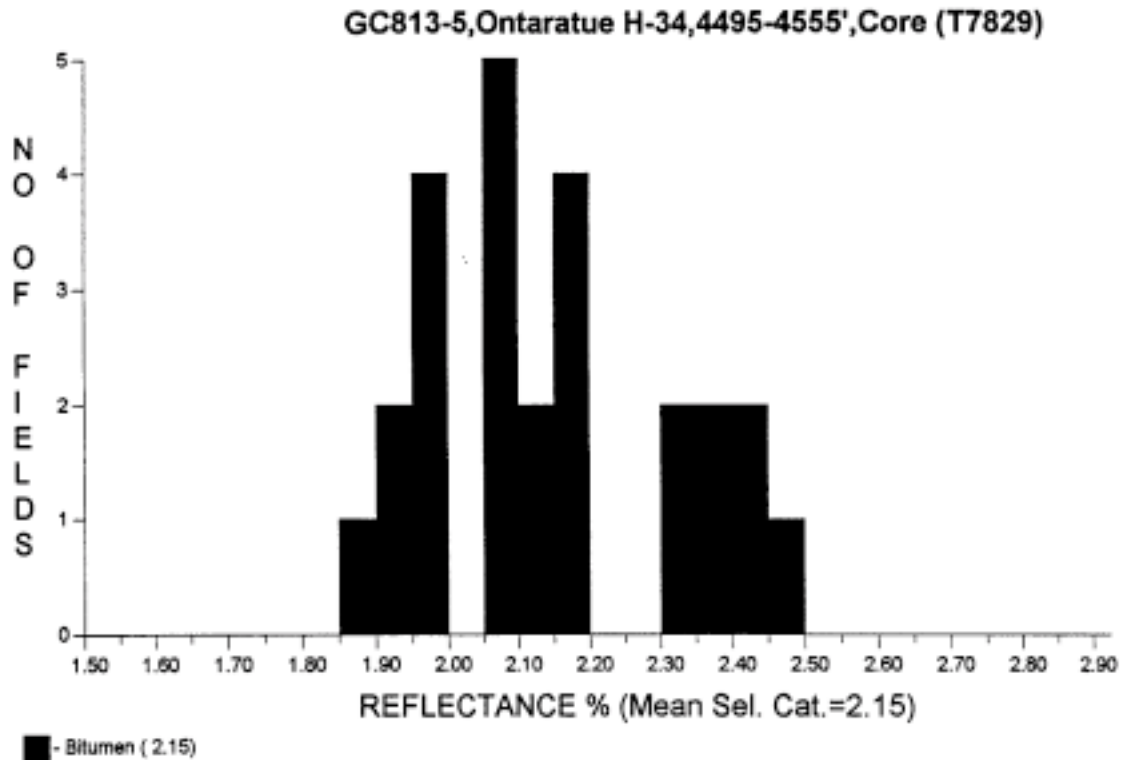
Selected categories: Detrovitrinite,

No. of readings:	9
Mean of selected categories:	1.15
Standard deviation of selected categories:	0.125



Keiraville Konsultants Pty. Ltd.
7 Dallas Street,
Keiraville, NSW 2500
Australia.

Telephone: (02) 42 299843
International: +61-2-42 299843
Fax: +61-(0)2-42 299624
Email: acc@ozemail.com.au



<u>Category</u>	<u>No. of Readings</u>	<u>Mean</u>	<u>Standard Deviation</u>
Bitumen	25	2.15	0.171
<u>Total:</u>	25	2.15	0.171

Selected categories: Bitumen.

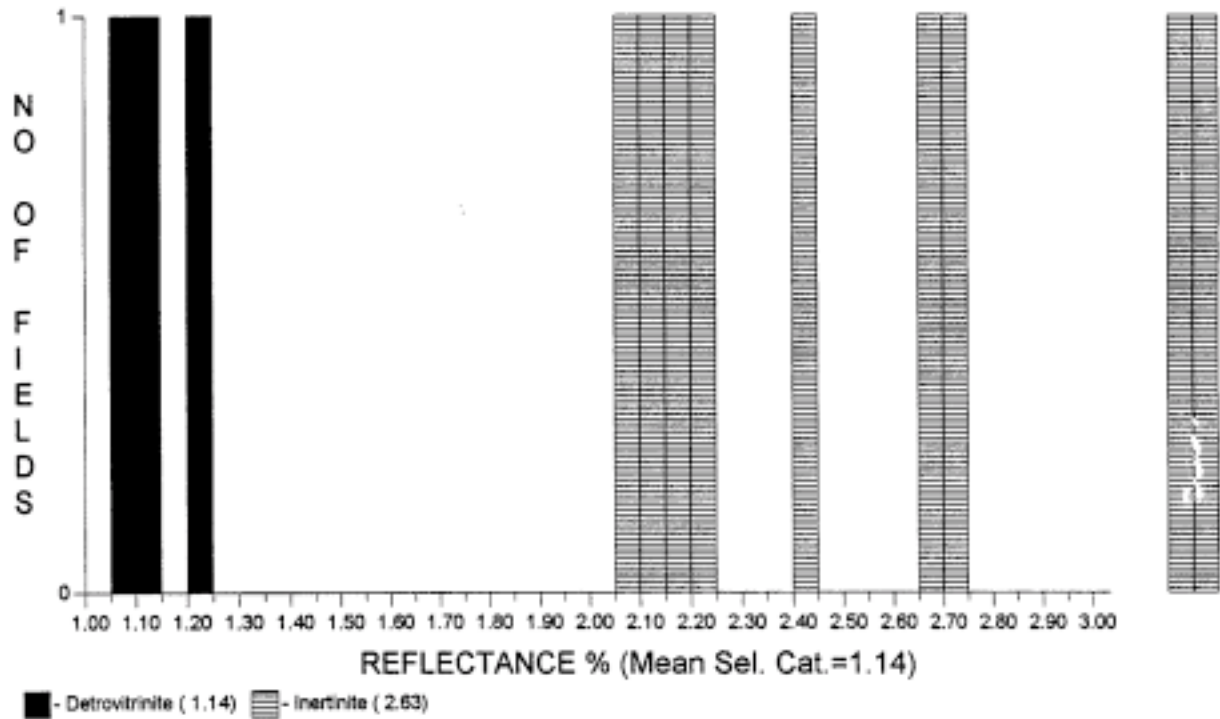
No. of readings:	25
Mean of selected categories:	2.15
Standard deviation of selected categories:	0.171



Keiraville Konsultants Pty. Ltd.
 7 Dallas Street,
 Keiraville, NSW 2500
 Australia.

Telephone: (02) 42 299843
 International: +61-2-42 299843
 Fax: +61-(0)2-42 299624
 Email: acc@ozemail.com.au

GC813-6.1, Ontaratue H-34, 5200-5260', Ctgs (T7830)



<u>Category</u>	<u>No. of Readings</u>	<u>Mean</u>	<u>Standard Deviation</u>
Detrovitrinite	3	1.14	0.074
Inertinite	10	2.63	0.481
Total:	13	2.29	0.758

Selected categories: Detrovitrinite,

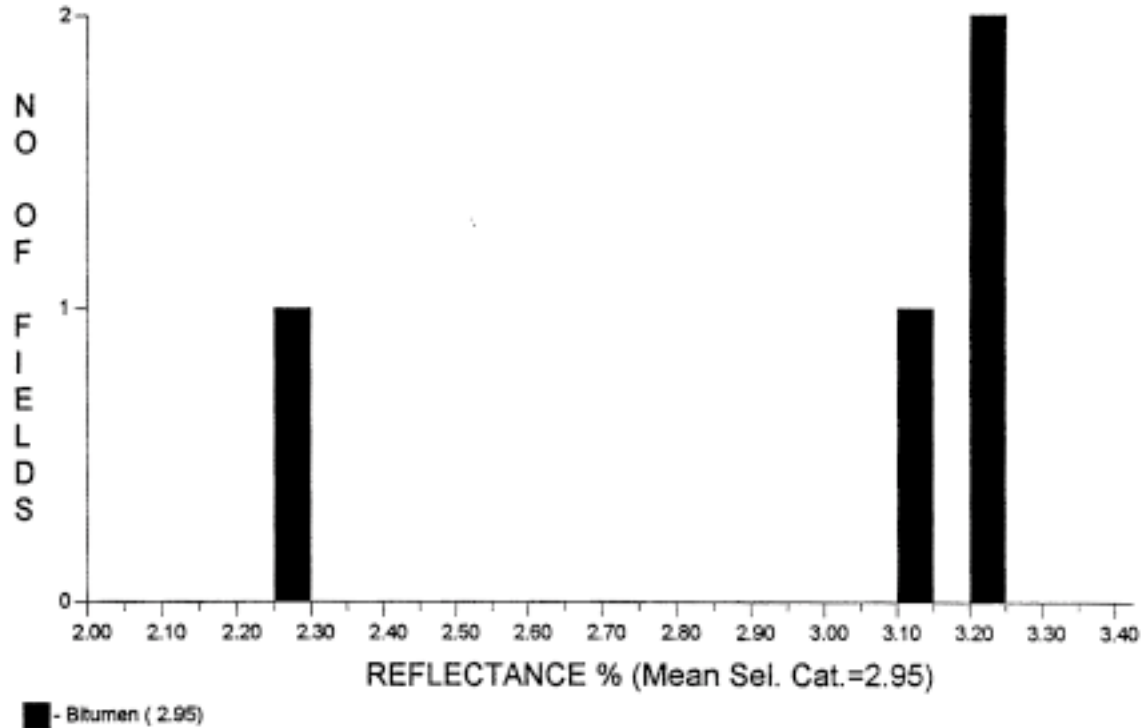
No. of readings: 3
 Mean of selected categories: 1.14
 Standard deviation of selected categories: 0.074



Keiraville Konsultants Pty. Ltd.
7 Dallas Street,
Keiraville, NSW 2500
Australia.

Telephone: (02) 42 299843
International: +61-2-42 299843
Fax: +61-(0)2-42 299624
Email: acc@ozemail.com.au

GC813-7 Ontaratue H-34, 7710-8100' Mt Fr Ctgs (T7832)



<u>Category</u>	<u>No. of Readings</u>	<u>Mean</u>	<u>Standard Deviation</u>
Bitumen	4	2.95	0.385
<u>Total:</u>	4	2.95	0.385

Selected categories: Bitumen.

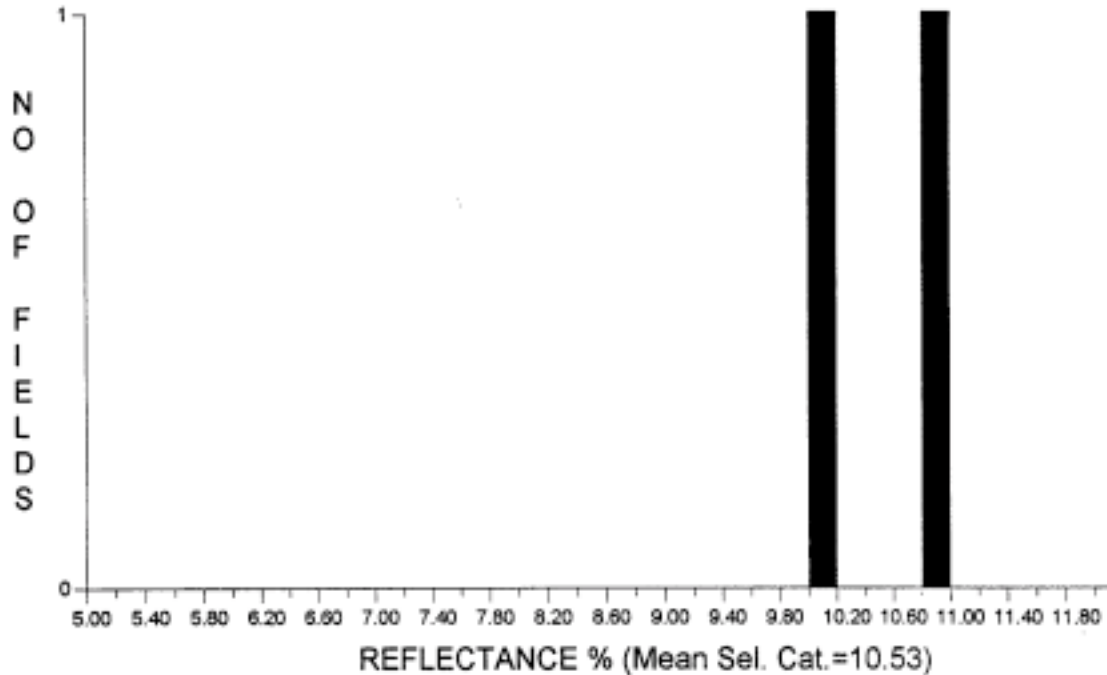
No. of readings:	4
Mean of selected categories:	2.95
Standard deviation of selected categories:	0.385



Keiraville Konsultants Pty. Ltd.
 7 Dallas Street,
 Keiraville, NSW 2500
 Australia.

Telephone: (02) 42 299843
 International: +61-2-42 299843
 Fax: +61-(0)2-42 299624
 Email: acc@ozemail.com.au

GC813-9 Ontaratue H-34, Mt CI, 9900-10200' Ctgs (T7834)



■ - ?"Vitrinite" (10.53)

<u>Category</u>	<u>No. of Readings</u>	<u>Mean</u>	<u>Standard Deviation</u>
? "Vitrinite"	2	10.53	0.360
<u>Total:</u>	2	10.53	0.360

Selected categories: ? "Vitrinite".

No. of readings:	2
Mean of selected categories:	10.53
Standard deviation of selected categories:	0.360

**Keiraville Consultants Pty. Ltd.**

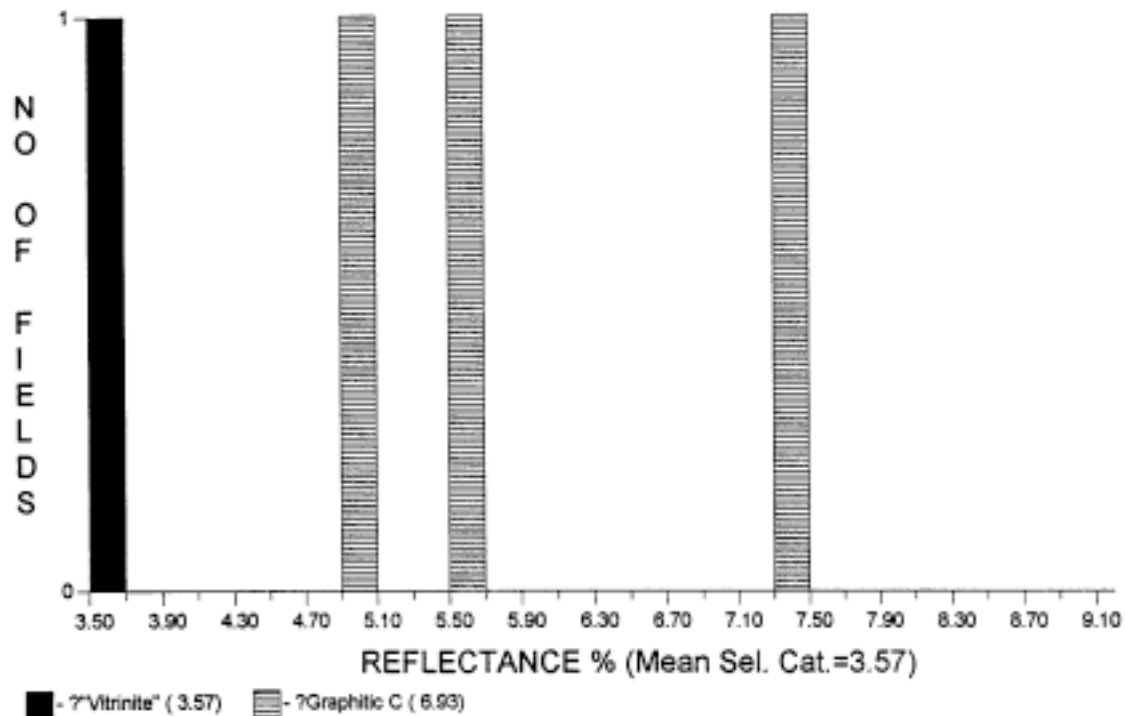
7 Dallas Street,
Keiraville, NSW 2500
Australia.

Telephone: (02) 42 299843

International: +61-2-42 299843

Fax: +61-(0)2-42 299624

Email: acc@ozemail.com.au

GC813-10 Ontaratue H-34, Mt Cl 10004--23' Ctgs (T7835)

<u>Category</u>	<u>No. of Readings</u>	<u>Mean</u>	<u>Standard Deviation</u>
?Vitrinite"	1	3.57	0.000
?Graphitic C	5	6.93	1.367
Total:	6	6.37	1.767

Selected categories: ?Vitrinite",

No. of readings:	1
Mean of selected categories:	3.57
Standard deviation of selected categories:	0.000



R	VITRINITE			INERTINITE			LIPTINITE			OIL DROPS			BITUMEN		
	No Read	Pop Range	R	No Read	Pop Range	R	No Read	Pop Range	R	No Read	Pop Range	R	No Read	Pop Range	R
0.10			0.40			0.70			1.00			1.30			1.60
0.11			0.41			0.71			1.01			1.31			1.61
0.12			0.42			0.72			1.02			1.32			1.62
0.13			0.43			0.73			1.03			1.33			1.63
0.14			0.44			0.74			1.04			1.34			1.64
0.15			0.45			0.75			1.05			1.35			1.65
0.16			0.46			0.76			1.06			1.36			1.66
0.17			0.47			0.77			1.07			1.37			1.67
0.18			0.48			0.78			1.08			1.38			1.68
0.19			0.49			0.79			1.09			1.39			1.69
0.20			0.50			0.80			1.10			1.40			1.70
0.21			0.51			0.81			1.11			1.41			1.71
0.22			0.52			0.82			1.12			1.42			1.72
0.23			0.53			0.83			1.13			1.43			1.73
0.24			0.54			0.84			1.14			1.44			1.74
0.25			0.55			0.85			1.15			1.45			1.75
0.26			0.56			0.86			1.16			1.46			1.76
0.27			0.57			0.87			1.17			1.47			1.77
0.28			0.58			0.88			1.18			1.48			1.78
0.29			0.59			0.89			1.19			1.49			1.79
0.30			0.60			0.90			1.20			1.50			1.80
0.31			0.61			0.91			1.21			1.51			1.81
0.32			0.62			0.92			1.22			1.52			1.82
0.33			0.63			0.93			1.23			1.53			1.83
0.34			0.64			0.94			1.24			1.54			1.84
0.35			0.65			0.95			1.25			1.55			1.85
0.36			0.66			0.96			1.26			1.56			1.86
0.37			0.67			0.97			1.27			1.57			1.87
0.38			0.68			0.98			1.28			1.58			1.88
0.39			0.69			0.99			1.29			1.59			1.89
TV	VITRINITE			INERTINITE			LIPTINITE			OIL DROPS			BITUMEN		
	<0.1 %			2.5 %			1.5 %			0.8			Oil cut		
TV	DV	Sfus	Scler	Fus	Macr	ID	Micr	Spor	Cut	Sub	Res	Ld	Bituminite	Telalginite	Lamalginitite
								0.6				0.1			0.8

Sample Number..T7824....Well Name...GEOTRACK, GC 813-1 Ontaratu H-34...Cretaceous..... Depth..100-850 SampleType....Ctgs....
Date ..07/09/ 2001.. Op..SPR..... FGV - First Generation Vitrinite, RV - Reworked Vitrinite, BTT - Bituminite, B - Bitumen, Inert - Inertinite, Cav - Cavings, DA - Drilling
Mud Additives Copyright Keiraville Consultants MICR D:\RWORK.ms6813VRW.doc



VITRINITE ≤0.1 %										INERTINITE 0.8 %										LIPTINITE ≤0.1 %										OIL DROPS				BITUMEN	
TV	DV	Sfus	Scler	Fus	Macr	ID	Micr	Spor ≤0.1	Cut	Sub	Res	Ld	Bituminite	Telalginite	Lamalginite	Oil	cut																		
R	No Read	R	No Read	Pop Range	R	No Read	Pop Range	R	No Read	R	Pop Range	R	No Read	Pop Range	R	No Read	Pop Range	R	No Read	Pop Range	R	No Read	Pop Range												
0.10		0.40			0.70		1.00			1.30			1.60	1	1.90		2.20	1		2.50															
0.11		0.41			0.71	2	1.01			1.31			1.61		1.91		2.21			2.51															
0.12		0.42			0.72		1.02			1.32	1		1.62	1	1.92		2.22			2.52															
0.13		0.43			0.73	1	1.03			1.33			1.63		1.93		2.23		Inert	2.53															
0.14		0.44			0.74		1.04			1.34	1		1.64		1.94		2.24	1	↓	2.54															
0.15		0.45			0.75		1.05			1.35			1.65		1.95		2.25			2.55															
0.16		0.46			0.76	1	1.06			1.36			1.66	3	Inert	1.96	2.26			2.56															
0.17		0.47			0.77	1	1.07			1.37			1.67		1.97		2.27			2.57															
0.18		0.48			0.78	1	1.08			1.38			1.68		1.98		2.28			2.58															
0.19		0.49			0.79	2	1.09			1.39			1.69		1.99		2.29			2.59															
0.20		0.50			0.80		1.10			1.40			1.70	1	2.00		2.30			2.60															
0.21		0.51			0.81		1.11			1.41			1.71		2.01		2.31			2.61															
0.22		0.52			0.82		1.12			1.42	1	Inert	1.72		2.02	1	Inert	2.32		2.62															
0.23		0.53			0.83	1	1.13			1.43			1.73		2.03		2.33			2.63															
0.24		0.54			0.84		1.14			1.44			1.74		2.04		2.34			2.64															
0.25		0.55			0.85		1.15			1.45			1.75		2.05		2.35			2.65															
0.26		0.56			0.86	1	1.16			1.46	1		1.76	2	2.06		2.36			2.66															
0.27		0.57			0.87		1.17			1.47			1.77		2.07		2.37			2.67															
0.28		0.58			0.88		1.18			1.48			1.78		2.08	1	2.38			2.68															
0.29		0.59			0.89		FGV			1.49			1.79		2.09		2.39			2.69															
0.30		0.60			0.90	1	1.20			1.50			1.80		2.10	1	2.40			2.70															
0.31		0.61	1	↑	0.91		1.21			1.51			1.81		2.11		2.41			2.71															
0.32		0.62		FGV	0.92		1.22	1	↑	1.52			1.82		2.12		2.42			2.72															
0.33		0.63			0.93		1.23			Inert	1.53		1.83		2.13		2.43			2.73															
0.34		0.64			0.94		1.24			1.54	1		1.84		2.14		2.44			2.74															
0.35		0.65	1		0.95		1.25			1.55			1.85		2.15		2.45			2.75															
0.36		0.66			0.96		1.26			1.56			1.86		2.16		2.46			2.76															
0.37		0.67	1		0.97		1.27			1.57			1.87		2.17		2.47			2.77															
0.38		0.68			0.98		1.28			1.58	1		1.88		2.18		2.48			2.78															
0.39		0.69			0.99		1.29			1.59			1.89		2.19		2.49			2.79															

Sample Number..T7825..... Well Name...GEOTRACK, GC 813-2 Ontaratué H-34...Devonian Imperial Formation Depth..1150-1900 SampleType....Ctgs....
Date. ..07/09/ 2001.. Op..SPR..... FGV - First Generation Vitrinite, RV - Reworked Vitrinite, BTT - Bituminite, B - Bitumen, Inert - Inertinite, Cav - Cavings, DA - Drilling
Mud Additives Copyright Keiraville Consultants MICR D:\R\WORK.ms6\813VRW.doc



VITRINITE				INERTINITE										LIPTINITE										OIL DROPS				BITUMEN	
<0.1 %				0.3 %										<0.1 %															
TV	DV	Sfus	Scfer	Fus	Macr	ID	Micr	Spor	Cut	Sub	Res	Ld	Bituminite	Telalginit	Lamalginit	Oil	cut												
R	No Read	Pop Range	R	No Read	Pop Range	R	No Read	Pop Range	R	No Read	Pop Range	R	No Read	Pop Range	R	No Read	Pop Range	R	No Read	Pop Range									
0.10		0.40	0.70		1.00	1	1.30	1	1.60	1.90	1	2.20		2.50															
0.11		0.41	0.71		1.01		1.31		Inert	1.61		2.21		2.51															
0.12		0.42	0.72		1.02		1.32			1.62	1	Inert	2.22	2.52															
0.13		0.43	0.73		1.03		1.33			1.63		2.23		2.53															
0.14		0.44	0.74		1.04		1.34			1.64	1	2.24		2.54															
0.15		0.45	0.75		1.05		1.35			1.65		2.25		2.55															
0.16		0.46	0.76		1.06	1	1.36	1		1.66	2	Inert	2.26	2.56															
0.17		0.47	0.77		1.07		1.37			1.67		2.27		2.57															
0.18		0.48	0.78		1.08		FGV	1		1.68		2.28		2.58															
0.19		0.49	0.79		1.09	1	1.39		1	1.69		2.29		2.59															
0.20		0.50	0.80		1.10	2	1.40	2		1.70	1	2.30		2.60															
0.21		0.51	0.81		1.11		1.41			1.71		2.31		2.61															
0.22		0.52	0.82		1.12		1.42			1.72	1	2.32		2.62															
0.23		0.53	0.83		1.13		1.43			1.73		2.33		2.63															
0.24		0.54	0.84		1.14		1.44			1.74	2	2.34		2.64															
0.25		0.55	0.85		1.15		1.45			1.75		2.35		Inert	2.65														
0.26		0.56	0.86		1.16		1.46			1.76		2.36		2.66															
0.27		0.57	0.87	1	1.17		1.47			1.77		2.37		2.67															
0.28		0.58	0.88	1	FGV		1.48	1		1.78	1	2.38		2.68															
0.29		0.59	0.89		1.19		1.49			1.79		2.39		2.69															
0.30		0.60	0.90	1	1.20		1.50			1.80		2.40	1	2.70															
0.31		0.61	0.91		1.21		1.51			1.81		2.41		2.71															
0.32		0.62	0.92		1.22	1	1.52	1		1.82	1	2.42		2.72															
0.33		0.63	0.93		1.23		1.53			1.83		2.43		2.73															
0.34		0.64	0.94		1.24		1.54	1		1.84	1	2.44		2.74															
0.35		0.65	0.95		1.25		1.55			1.85		2.45		2.75															
0.36		0.66	0.96		1.26		1.56			1.86	2	2.46	1	2.76															
0.37		0.67	0.97		1.27		1.57			1.87		2.47																	
0.38		0.68	0.98		1.28		1.58			1.88		2.48							Inert										
0.39		0.69	0.99		1.29		1.59			1.89		2.49		3.14	1														

Sample Number..T7826...Well Name...GEOTRACK, GC 813-3.1 Ontaratu H-34...Devonian Imperial Formation Depth..2400-2600 SampleType.....Ctgs....
Date. ..07/09/ 2001.. Op..SPR..... FGV - First Generation Vitrinite, RV - Reworked Vitrinite, BTT - Bituminite, B - Bitumen, Inert - Inertinite, Cav - Cavings, DA - Drilling
Mud Additives Copyright Keiraville Consultants MICR D:\R\WORK.ms6\813VRW.doc

[illegible]

Sample Number..T7827... Well Name...GEOTRACK, GC 813-4.1 Ontaratie H-34...DevonianCanol/Hare Indian Formation Depth..2910-3230 SampleType.... Ctgs....
Date. ..08/09/ 2001.. Op..SPR..... FGV - First Generation Vitrinite, RV - Reworked Vitrinite, BTT - Bituminite, B - Bitumen, Inert - Inertinite, Cav - Cavings, DA - Drilling
Mud Additives Copyright Keiraville Consultants MICR D:\R\WORK.ms6\813VRW.doc



VITRINITE <0.1 %				INERTINITE 0.4 %										LIPTONITE <0.1 %										OIL DROPS				BITUMEN	
TV	DV	Sfus	Scler	Fus	Macr	ID	Micr	Spor <0.1	Cut	Sub	Res	Ld <0.1	Bituminite	Telalginite	Lamalginitite	Oil cut													
R	No Read	Pop Range	R	No Read	Pop Range	R	No Read	Pop Range	R	No Read	Pop Range	R	No Read	Pop Range	R	No Read	Pop Range	R	No Read	Pop Range	R	No Read	Pop Range	R	No Read	Pop Range			
0.10			0.40			0.70			1.00	1		1.30			1.60	1		1.90			2.20			2.50					
0.11			0.41			0.71			1.01			1.31			1.61			1.91			2.21			2.51					
0.12			0.42			0.72			1.02			1.32			1.62			1.92			2.22			2.52					
0.13			0.43			0.73			1.03			1.33			1.63			1.93			2.23			2.53					
0.14			0.44			0.74			1.04		1	1.34			1.64			1.94		1	2.24			2.54	1				
0.15			0.45			0.75		1	1.05			1.35		FGV	1.65			1.95			2.25			2.55					
0.16			0.46			0.76			1.06		1	1.36		↓	1.66	2		1.96			2.26			2.56					
0.17			0.47			0.77			1.07			1.37			1.67			1.97			2.27			2.57					
0.18			0.48			0.78			1.08			1.38			1.68			1.98			2.28			2.58					
0.19			0.49			0.79			1.09			1.39			1.69			1.99			2.29			2.59					
0.20			0.50			0.80			1.10			1.40			1.70			2.00			2.30			2.60					
0.21			0.51			0.81			1.11			1.41			1.71			2.01			2.31			2.61					
0.22			0.52			0.82		1	1.12		1	1.42		↑	1.72			2.02			2.32			2.62	1				
0.23			0.53			0.83			1.13			1.43		Inert	1.73			2.03			2.33			2.63		Inert			
0.24			0.54			0.84		1	1.14			1.44			1.74			2.04			2.34			2.64	1	↓			
0.25			0.55			0.85			1.15			1.45			1.75			2.05			2.35			2.65					
0.26			0.56			0.86		1	1.16			1.46			1.76			2.06			2.36			2.66					
0.27			0.57			0.87		1	1.17			1.47			1.77			2.07			2.37			2.67					
0.28			0.58			0.88			1.18		1	1.48			1.78			2.08			2.38	1		2.68					
0.29			0.59			0.89			1.19			1.49			1.79			2.09			2.39			2.69					
0.30			0.60			0.90			1.20		1	1.50		Inert	1.80	3		2.10			2.40			2.70					
0.31			0.61			0.91			1.21			1.51			1.81			2.11			2.41			2.71					
0.32			0.62			0.92			1.22			1.52			1.82	2		2.12			2.42			2.72					
0.33			0.63			0.93			1.23			1.53			1.83			2.13			2.43			2.73					
0.34			0.64			0.94			1.24			1.54			1.84			2.14			2.44	1	Inert	2.74					
0.35			0.65			0.95			1.25			1.55			1.85			2.15			2.45			2.75					
0.36			0.66			0.96			1.26			1.56			1.86	1	1	2.16	Inert		2.46			2.76					
0.37			0.67			0.97			1.27			1.57			1.87			2.17			2.47			2.77					
0.38			0.68			0.98			1.28			1.58			1.88	1		2.18			2.48			2.78					
0.39			0.69			0.99			1.29			1.59			1.89			2.19			2.49			2.79					

Sample Number..T7828...Well Name...GEOTRACK, GC 813-4.2 Ontaratu H-34...Devonian Hume Formation Depth...3300-3620 SampleType....Ctgs....
Date. ..08/09/ 2001.. Op..SPR..... FGV - First Generation Vitrinite, RV - Reworked Vitrinite, BTT - Bituminite, B - Bitumen, Inert - Inertinite, Cav - Cavings, DA - Drilling
Mud Additives Copyright Keiraville Consultants MICR D:\RWORK.ms6\813VRW.doc



VITRINITE - %				INERTINITE - %								LIPTINITE - %										OIL DROPS				BITUMEN 2.0						
TV	DV	Sfus	Scler	Fus	Macr	ID	Micr	Spor	Cut	Sub	Res	Ld	Bituminite	Telalginitite	Lamalginite	Oil	cut															
R	No Read	Pop Range	R	No Read	Pop Range	R	No Read	Pop Range	R	No Read	Pop Range	R	No Read	Pop Range	R	No Read	Pop Range	R	No Read	Pop Range	R	No Read	Pop Range	R	No Read	Pop Range	R	No Read	Pop Range	R	No Read	Pop Range
0.10			0.40			0.70			1.00			1.30			1.60			1.90			2.20			2.50								
0.11			0.41			0.71			1.01			1.31			1.61			1.91			2.21			2.51								
0.12			0.42			0.72			1.02			1.32			1.62			1.92			2.22			2.52								
0.13			0.43			0.73			1.03			1.33			1.63		2	1.93			2.23			2.53								
0.14			0.44			0.74			1.04			1.34			1.64			1.94			2.24			2.54								
0.15			0.45			0.75			1.05			1.35			1.65			1.95			2.25			2.55								
0.16			0.46			0.76			1.06			1.36			1.66			1.96			2.26			2.56								
0.17			0.47			0.77			1.07			1.37			1.67		3	1.97			2.27			2.57								
0.18			0.48			0.78			1.08			1.38			1.68			1.98			2.28			2.58								
0.19			0.49			0.79			1.09			1.39			1.69		1	1.99			2.29			2.59								
0.20			0.50			0.80			1.10			1.40			1.70			2.00			2.30			2.60								
0.21			0.51			0.81			1.11			1.41			1.71			2.01			2.31			2.61								
0.22			0.52			0.82			1.12			1.42			1.72			2.02			2.32	1		2.62								
0.23			0.53			0.83			1.13			1.43			1.73			2.03			2.33	1		2.63								
0.24			0.54			0.84			1.14			1.44			1.74			2.04			2.34			2.64								
0.25			0.55			0.85			1.15			1.45			1.75			2.05			2.35	1		2.65								
0.26			0.56			0.86			1.16			1.46			1.76		2	2.06			2.36			2.66								
0.27			0.57			0.87			1.17			1.47			1.77		2	2.07			2.37			2.67								
0.28			0.58			0.88			1.18			1.48			1.78			2.08			2.38			2.68								
0.29			0.59			0.89			1.19			1.49			1.79		1	2.09			2.39	1		2.69								
0.30			0.60			0.90			1.20			1.50			1.80			2.10			2.40			2.70								
0.31			0.61			0.91			1.21			1.51			1.81			2.11			2.41			2.71								
0.32			0.62			0.92			1.22			1.52			1.82			2.12			2.42			2.72								
0.33			0.63			0.93			1.23			1.53			1.83		2	2.13			2.43	1		2.73								
0.34			0.64			0.94			1.24			1.54			1.84			2.14			2.44	1	B	2.74								
0.35			0.65			0.95			1.25			1.55			1.85			2.15			2.45	1	↓	2.75								
0.36			0.66			0.96			1.26			1.56			1.86		1	2.16			2.46			2.76								
0.37			0.67			0.97			1.27			1.57			1.87		2	2.17			2.47			2.77								
0.38			0.68			0.98			1.28			1.58			1.88		1	2.18			2.48			2.78								
0.39			0.69			0.99			1.29			1.59			1.89	1	↑	2.19			2.49			2.79								

Sample Number..T7829...Well Name...GEOTRACK, GC 813-5 Ontaratu H-34...Devonian Bear Rock Formation Depth..4495-4555 SampleType...Core...
Date...08/09/ 2001.. Op..SPR..... FGV - First Generation Vitrinite, RV - Reworked Vitrinite, BTT - Bituminite, B - Bitumen, Inert - Inertinite, Cav - Cavings, DA - Drilling
Mud Additives Copyright Keiraville Consultants MICR D:\RWORK.ms6\813VRW.doc



VITRINITE ≤0.1 %										INERTINITE 0.2 %										LIPTINITE ≤0.1 %										OIL DROPS				BITUMEN	
TV	DV	Sfus	Scler	Fus	Macr	ID	Micr	Spor	Cut	Sub	Res	Ld	Bituminite	Telalginit	Lamalginit	Oil	cut																		
R	No Read	Pop Range	R	No Read	Pop Range	R	No Read	Pop Range	R	No Read	Pop Range	R	No Read	Pop Range	R	No Read	Pop Range	R	No Read	Pop Range	R	No Read	Pop Range	R	No Read	Pop Range	R	No Read	Pop Range						
0.10			0.40			0.70			1.00			1.30			1.60			1.90			2.20			2.50											
0.11			0.41			0.71			1.01			1.31			1.61			1.91			2.21			2.51											
0.12			0.42			0.72			1.02			1.32			1.62			1.92			2.22			2.52											
0.13			0.43			0.73			1.03			1.33			1.63			1.93			2.23			2.53											
0.14			0.44			0.74			1.04			1.34			1.64			1.94			2.24	1		2.54											
0.15			0.45			0.75		1	↑	1.35		1.65			1.95			2.25			2.55														
0.16			0.46			0.76			1.06			1.36		?Cav	1.66			1.96			2.26			2.56											
0.17			0.47			0.77			1.07			1.37			1.67			1.97			2.27			2.57											
0.18			0.48			0.78			1.08			1.38			1.68			1.98			2.28			2.58											
0.19			0.49			0.79			1.09			1.39			1.69			1.99			2.29			2.59											
0.20			0.50			0.80			1.10			1.40			1.70			2.00			2.30			2.60											
0.21			0.51			0.81			1.11			1.41			1.71			2.01			2.31			2.61											
0.22			0.52			0.82			1.12			1.42		Cav	1.72			2.02			2.32			2.62											
0.23			0.53			0.83		1	1.13		Vit	1.43			1.73			2.03			2.33			2.63											
0.24			0.54			0.84			1.14			1.44			1.74			2.04			2.34			2.64											
0.25			0.55			0.85			1.15			1.45			1.75			2.05			2.35			2.65											
0.26			0.56			0.86			1.16			1.46			1.76			2.06			2.36			2.66	1										
0.27			0.57			0.87			1.17			1.47			1.77			2.07			2.37			2.67											
0.28			0.58			0.88			1.18			1.48			1.78		1	2.08		↑	2.38			2.68											
0.29			0.59			0.89			1.19			1.49			1.79			2.09		?Cav	2.39			2.69											
0.30			0.60			0.90			1.20			1.50			1.80			2.10			2.40			2.70											
0.31			0.61			0.91			1.21			1.51			1.81			2.11			2.41			2.71											
0.32			0.62			0.92			1.22			1.52		Cav	1.82		1	2.12		1	2.42	1	Inert	2.72											
0.33			0.63			0.93		1	1.23		↓	1.53			1.83			2.13			2.43			2.73											
0.34			0.64			0.94			1.24			1.54			1.84			2.14		Inert	2.44			2.74	1										
0.35			0.65			0.95			1.25			1.55			1.85			2.15			2.45														
0.36			0.66			0.96			1.26			1.56			1.86			2.16			2.46			3.18		Inert									
0.37			0.67			0.97			1.27			1.57			1.87			2.17			2.47			3.22	1	?Cav									
0.38			0.68			0.98			1.28			1.58			1.88		1	2.18			2.48			3.46	1	↓									
0.39			0.69			0.99			1.29			1.59			1.89			2.19			2.49														

Sample Number..T7830...Well Name...GEOTRACK, GC 813-6.1 Ontaratie H-34...Devonian Bear Roack..... Depth..5200-5260 SampleType....Ctgs....
Date. ..08/09/ 2001.. Op..SPR..... FGV - First Generation Vitritine, RV - Reworked Vitritine, BTT - Bituminite, B - Bitumen, Inert - Inertinite, Cav - Cavings, DA - Drilling
Mud Additives Copyright Keiraville Consultants MICR D:\R\WORK.ms6\813VRW.doc



VITRINITE										INERTINITE										LIPTINITE										OIL DROPS		BITUMEN	
[<0.1] %										[<0.1] %										- %												[<0.1]	
R	No Read	Pop Range	R	No Read	Pop Range	R	No Read	Pop Range	R	No Read	Pop Range	R	No Read	Pop Range	R	No Read	Pop Range	R	No Read	Pop Range	R	No Read	Pop Range	R	No Read	Pop Range	R	No Read	Pop Range				
TV	DV																												Oil cut				
0.10			0.40			0.70			1.00	1	↑	1.30			1.60			1.90			2.20			2.50									
0.11			0.41			0.71			1.01		Cav vt	1.31			1.61			1.91			2.21			2.51									
0.12			0.42			0.72			1.02			1.32	1	↓	1.62			1.92			2.22			2.52									
0.13			0.43			0.73			1.03			1.33			1.63			1.93			2.23			2.53									
0.14			0.44			0.74			1.04			1.34			1.64			1.94			2.24			2.54									
0.15			0.45			0.75			1.05			1.35			1.65			1.95			2.25			2.55									
0.16			0.46			0.76			1.06			1.36			1.66			1.96			2.26			2.56									
0.17			0.47			0.77			1.07			1.37			1.67			1.97			2.27			2.57									
0.18			0.48			0.78			1.08			1.38			1.68			1.98			2.28			2.58									
0.19			0.49			0.79			1.09			1.39			1.69			1.99			2.29			2.59									
0.20			0.50			0.80			1.10			1.40			1.70			2.00			2.30			2.60									
0.21			0.51			0.81			1.11			1.41			1.71			2.01			2.31			2.61									
0.22			0.52			0.82			1.12			1.42			1.72			2.02			2.32			2.62									
0.23			0.53			0.83			1.13			1.43			1.73			2.03			2.33			2.63									
0.24			0.54			0.84			1.14			1.44			1.74			2.04			2.34			2.64									
0.25			0.55			0.85			1.15			1.45			1.75			2.05			2.35			2.65									
0.26			0.56			0.86			1.16			1.46			1.76		1	↑	2.06			2.36			2.66								
0.27			0.57			0.87			1.17			1.47			1.77			2.07			Cav B	2.37			2.67								
0.28			0.58			0.88			1.18			1.48			1.78		1	↓	2.08			2.38			2.68								
0.29			0.59			0.89			1.19			1.49			1.79			2.09			2.39			2.69									
0.30			0.60			0.90			1.20			1.50			1.80			2.10			2.40			2.70									
0.31			0.61			0.91			1.21			1.51			1.81			2.11			2.41			2.71									
0.32			0.62			0.92			1.22			1.52			1.82			2.12			2.42			2.72									
0.33			0.63			0.93			1.23			1.53			1.83			2.13			2.43			2.73									
0.34			0.64			0.94			1.24			1.54			1.84			2.14			2.44			2.74									
0.35			0.65			0.95			1.25			1.55			1.85			2.15			2.45			2.75									
0.36			0.66			0.96			1.26			1.56			1.86			2.16			2.46			2.76									
0.37			0.67			0.97			1.27			1.57			1.87			2.17			2.47			2.77									
0.38			0.68			0.98			1.28			1.58			1.88			2.18			2.48			2.78									
0.39			0.69			0.99			1.29			1.59			1.89			2.19			2.49			2.79									

Sample Number..T7831... Well Name...GEOTRACK, GC 813-6-2 Ontaratu H-34...?Silurian Ronning Formation Depth..5480-5630 SampleType....Ctgs....
Date. ..09/09/ 2001.. Op..ACC..... FGV - First Generation Vitrinite, RV - Reworked Vitrinite, BTT - Bituminite, B - Bitumen, Inert - Inertinite, Cav - Cavings, DA - Drilling
Mud Additives Copyright Keiraville Consultants MICR D:\R\WORK.ms6\813VRW.doc



VITRINITE - %										INERTINITE - %										LIPTINITE - %										OIL DROPS		BITUMEN <0.1%	
TV	DV	Sfus	Scler	Fus	Macr	ID	Micr	Spor	Cut	Sub	Res	Ld	Bituminite	Telalginite	Lamalginite	Oil	cut																
R	No Read	Pop Range	R	No Read	Pop Range	R	No Read	Pop Range	R	No Read	Pop Range	R	No Read	Pop Range	R	No Read	Pop Range	R	No Read	Pop Range	R	No Read	Pop Range	R	No Read	Pop Range	R	No Read	Pop Range				
2.20			2.50			2.80			3.10	1		3.40			3.70			4.00			4.30			4.60									
2.21			2.51			2.81			3.11			3.41			3.71			4.01			4.31			4.61									
2.22			2.52			2.82			3.12			3.42			3.72			4.02			4.32			4.62									
2.23			2.53			2.83			3.13			3.43			3.73			4.03			4.33			4.63									
2.24			2.54			2.84			3.14			3.44			3.74			4.04			4.34			4.64									
2.25			2.55			2.85			3.15			3.45			3.75			4.05			4.35			4.65									
2.26			2.56			2.86			3.16			3.46			3.76			4.06			4.36			4.66									
2.27			2.57			2.87			3.17			3.47			3.77			4.07			4.37			4.67									
2.28			2.58			2.88			3.18			3.48			3.78			4.08			4.38			4.68									
2.29	1	↑	2.59			2.89			3.19			3.49			3.79			4.09			4.39			4.69									
2.30		B	2.60		B	2.90		1	3.20			3.50			3.80			4.10			4.40			4.70									
2.31			2.61			2.91			3.21		B	3.51			3.81			4.11			4.41			4.71									
2.32			2.62			2.92		1	3.22	↓		3.52			3.82			4.12			4.42			4.72									
2.33			2.63			2.93			3.23			3.53			3.83			4.13			4.43			4.73									
2.34			2.64			2.94			3.24			3.54			3.84			4.14			4.44			4.74									
2.35			2.65			2.95			3.25			3.55			3.85			4.15			4.45			4.75									
2.36			2.66			2.96			3.26			3.56			3.86			4.16			4.46			4.76									
2.37			2.67			2.97			3.27			3.57			3.87			4.17			4.47			4.77									
2.38			2.68			2.98			3.28			3.58			3.88			4.18			4.48			4.78									
2.39			2.69			2.99			3.29			3.59			3.89			4.19			4.49			4.79									
2.40			2.70			3.00			3.30			3.60			3.90			4.20			4.50			4.80									
2.41			2.71			3.01			3.31			3.61			3.91			4.21			4.51			4.81									
2.42			2.72			3.02			3.32			3.62			3.92			4.22			4.52			4.82									
2.43			2.73			3.03			3.33			3.63			3.93			4.23			4.53			4.83									
2.44			2.74			3.04			3.34			3.64			3.94			4.24			4.54			4.84									
2.45			2.75			3.05			3.35			3.65			3.95			4.25			4.55			4.85									
2.46			2.76			3.06			3.36			3.66			3.96			4.26			4.56			4.86									
2.47			2.77			3.07			3.37			3.67			3.97			4.27			4.57			4.87									
2.48			2.78			3.08			3.38			3.68			3.98			4.28			4.58			4.88									
2.49			2.79			3.09			3.39			3.69			3.99			4.29			4.59			4.89									

Sample Number..T7832...Well Name...GEOTRACK, GC 813-7 Ontaratu H-34... Cambrian Franklin Mtn Formation Depth..7700-8100 SampleType....Ctgs....
 Date...09/09/ 2001.. Op..ACC..... FGV - First Generation Vitrinite, RV - Reworked Vitrinite, BTT - Bituminite, B - Bitumen, Inert - Inertinite, Cav - Cavings, DA - Drilling
 Mud Additives Copyright Keiraville Consultants MICR D:\RWORK.ms\813VRW.doc



VITRINITE - %			INERTINITE - %										LIPTINITE - %										OIL DROPS				BITUMEN	
TV	DV		Sfus	Scler	Fus	Macr	ID	Micr	Spor	Cut	Sub	Res	Ld	Bituminite	Telalginite	Lamalginite		Oil cut										
2.20			2.50			2.80			3.10			3.40			3.70		4.00		4.30		4.60							
2.21			2.51			2.81			3.11			3.41			3.71		4.01		4.31		4.61							
2.22			2.52			2.82			3.12			3.42			3.72		4.02		4.32		4.62							
2.23			2.53			2.83			3.13			3.43			3.73		4.03		4.33		4.63							
2.24			2.54			2.84			3.14			3.44			3.74		4.04		4.34		4.64							
2.25			2.55			2.85			3.15			3.45			3.75		4.05		4.35		4.65							
2.26			2.56			2.86			3.16			3.46			3.76		4.06		4.36		4.66							
2.27			2.57			2.87			3.17			3.47			3.77		4.07		4.37		4.67							
2.28			2.58			2.88			3.18			3.48			3.78		4.08		4.38		4.68							
2.29			2.59			2.89			3.19			3.49			3.79		4.09		4.39		4.69							
2.30			2.60			2.90			3.20			3.50			3.80		4.10		4.40		4.70							
2.31			2.61			2.91			3.21			3.51			3.81		4.11		4.41		4.71							
2.32			2.62			2.92			3.22			3.52			3.82		4.12		4.42		4.72							
2.33			2.63			2.93			3.23			3.53			3.83		4.13		4.43		4.73							
2.34			2.64			2.94			3.24			3.54			3.84		4.14		4.44		4.74							
2.35			2.65	Dom	absent	2.95			3.25			3.55			3.85		4.15		4.45		4.75							
2.36			2.66			2.96			3.26			3.56			3.86		4.16		4.46		4.76							
2.37			2.67			2.97			3.27			3.57			3.87		4.17		4.47		4.77							
2.38			2.68			2.98			3.28			3.58			3.88		4.18		4.48		4.78							
2.39			2.69			2.99			3.29			3.59			3.89		4.19		4.49		4.79							
2.40			2.70			3.00			3.30			3.60			3.90		4.20		4.50		4.80							
2.41			2.71			3.01			3.31			3.61			3.91		4.21		4.51		4.81							
2.42			2.72			3.02			3.32			3.62			3.92		4.22		4.52		4.82							
2.43			2.73			3.03			3.33			3.63			3.93		4.23		4.53		4.83							
2.44			2.74			3.04			3.34			3.64			3.94		4.24		4.54		4.84							
2.45			2.75			3.05			3.35			3.65			3.95		4.25		4.55		4.85							
2.46			2.76			3.06			3.36			3.66			3.96		4.26		4.56		4.86							
2.47			2.77			3.07			3.37			3.67			3.97		4.27		4.57		4.87							
2.48			2.78			3.08			3.38			3.68			3.98		4.28		4.58		4.88							
2.49			2.79			3.09			3.39			3.69			3.99		4.29		4.59		4.89							

Sample Number..T7833...Well Name...GEOTRACK, GC 813-8 Ontaratu H-34...Cambrian Saline River Formation Depth..9480-9499 SampleType....Core....
 Date...10/09/ 2001.. Op..ACC..... FGV - First Generation Vitrinite, RV - Reworked Vitrinite, BTT - Bituminite, B - Bitumen, Inert - Inertinite, Cav - Cavings, DA - Drilling
 Mud Additives Copyright Keiraville Consultants MICR D:\RWORK.ms\813VRW.doc



VITRINITE ? %			INERTINITE - %										LIPTINITE - %										OIL DROPS		BITUMEN	
TV	DV		Sfus	Scler	Fus	Macr	ID	Micr	Spor	Cut	Sub	Res	Ld	Bituminite	Telalginite	Lamalginite	Oil	cut								

Sample Number..T7834...Well Name...GEOTRACK, GC 813-9 Ontaratue H-34...Cambrian Mt Clark Formation Depth..9900-10200 SampleType....Ctgs....
 Date..10/09/ 2001.. Op..ACC..... FGV - First Generation Vitrinite, RV - Reworked Vitrinite, BTT - Bituminite, B - Bitumen, Inert - Inertinite, Cav - Cavings, DA - Drilling
 Mud Additives Copyright Keiraville Consultants MICR D:\RWORK.ms\813VRW.doc



VITRINITE ? 0.1 %				INERTINITE - %								LIPTINITE - %								OIL DROPS		BITUMEN			
TV	DV	Sfus	Scler	Fus	Macr	ID	Micr	Spor	Cut	Sub	Res	Ld	Bituminite	Tetraginite	Lamalginites	No Read	Pop Range	R	No Read	Pop Range	R	No Read	Pop Range	No Read	Pop Range

Sample Number..T7835...	Well Name...GEOTRACK, GC 813-10	Ontaratu H-34...Cambrian	Mt Clark Formation	Depth..10004-10023	SampleType....Core....
Date. ..10/09/2001..	Op..ACC.....	FGV - First Generation Vitrinite,	BTT - Bituminite, B - Bitumen, Inert - Inertinite, Gr - ?graphitic carbon of uncertain origin.	Cav - Cavings, DA - Drilling Mud Additives	MICR D:\RWORK.ms6\813VRW.doc	



R	VITRINITE										INERTINITE										LIPTINITE										OIL DROPS										BITUMEN	
	No Read	Pop Range	R	No Read	Pop Range	R	No Read	Pop Range	R	No Read	Pop Range	R	No Read	Pop Range	R	No Read	Pop Range	R	No Read	Pop Range	R	No Read	Pop Range	R	No Read	Pop Range	R	No Read	Pop Range	R	No Read	Pop Range	R	No Read	Pop Range	R	No Read	Pop Range	R	No Read	Pop Range	Oil cut
2.20			2.50			2.80			3.10			3.40			3.70			4.00			4.30			4.60																		
2.21			2.51			2.81			3.11			3.41			3.71			4.01			4.31			4.61																		
2.22			2.52			2.82			3.12			3.42			3.72			4.02			4.32			4.62																		
2.23			2.53			2.83			3.13			3.43			3.73			4.03			4.33			4.63																		
2.24			2.54			2.84			3.14			3.44			3.74			4.04			4.34			4.64																		
2.25			2.55			2.85			3.15			3.45			3.75			4.05			4.35			4.65																		
2.26			2.56			2.86			3.16			3.46			3.76			4.06			4.36			4.66																		
2.27			2.57			2.87			3.17			3.47			3.77			4.07			4.37			4.67																		
2.28			2.58			2.88			3.18			3.48			3.78			4.08			4.38			4.68																		
2.29			2.59			2.89			3.19			3.49			3.79			4.09			4.39			4.69																		
2.30			2.60			2.90			3.20			3.50			3.80			4.10			4.40			4.70																		
2.31			2.61			2.91			3.21			3.51			3.81			4.11			4.41			4.71																		
2.32			2.62	Dom		2.92			3.22			3.52			3.82			4.12			4.42			4.72																		
2.33			2.63			2.93			3.23			3.53			3.83			4.13			4.43			4.73																		
2.34			2.64			2.94			3.24			3.54			3.84			4.14			4.44			4.74																		
2.35			2.65			2.95			3.25			3.55			3.85			4.15			4.45			4.75																		
2.36			2.66			2.96			3.26			3.56			3.86			4.16			4.46			4.76																		
2.37			2.67			2.97			3.27			3.57			3.87			4.17			4.47			4.77																		
2.38			2.68			2.98			3.28			3.58			3.88			4.18			4.48			4.78																		
2.39			2.69			2.99			3.29			3.59			3.89			4.19			4.49			4.79																		
2.40			2.70			3.00			3.30			3.60			3.90			4.20			4.50			4.80																		
2.41			2.71			3.01			3.31			3.61			3.91			4.21			4.51			4.81																		
2.42			2.72			3.02			3.32			3.62			3.92			4.22			4.52			4.82																		
2.43			2.73			3.03			3.33			3.63			3.93			4.23			4.53			4.83																		
2.44			2.74			3.04			3.34			3.64			3.94			4.24			4.54			4.84																		
2.45			2.75			3.05			3.35			3.65			3.95			4.25			4.55			4.85																		
2.46			2.76			3.06			3.36			3.66			3.96			4.26			4.56			4.86																		
2.47			2.77			3.07			3.37			3.67			3.97			4.27			4.57			4.87																		
2.48			2.78			3.08			3.38			3.68			3.98			4.28			4.58			4.88																		
2.49			2.79			3.09			3.39			3.69			3.99			4.29			4.59			4.89																		

Sample Number..T7836...Well Name...GEOTRACK, GC 813-11 Ontaratie H-34...Proterozoic..... Depth..10602-10632 SampleType....Core....
 Date...10/09/ 2001.. Op..ACC..... FGV - First Generation Vitrinite, RV - Reworked Vitrinite, BTT - Bituminite, B - Bitumen, Inert - Inertinite, Cav - Cavings, DA - Drilling
 Mud Additives Copyright Keiraville Consultants MICR D:\RWORK.ms\813VRW.doc